NASA CR-
144468

S192 MULTISPECTRAL SCANNER
CHANNEL 13 ELECTROMECHANICAL NOISE INVESTIGATION
ECP-166

HONEYWELL
Radiation Center
2 Forbes Road
Lexington, Massachusetts 02173

S192 MULTISPECTRAL SCANNER
CHANNEL 13 ELECTROMECHANICAL NOISE INVESTIGATION
ECP-166

Contract No. NAS 9-11196

Prepared for

NASA Lyndon B. Johnson Spacecraft Center

Houston, Texas 77058

By

Honeywell Radiation Center

2 Forbes Road

Lexington, Massachusetts 02173

Prepared by H. Koumjian

H. Koumjian
Systems Engineer

Approved by K. Livermore

K. Livermore
Technical Director

Approved by R. G. Blades

R. G. Blades
Program Manager

INTRODUCTION

This report is in response to ECP 166 and ECP 166R1 paragraphs 5, 6 and 7. It contains a review of all data on the S192 Multispectral Scanner having to do with low frequency noise. The noise is component induced, i.e., either mechanical or electrical or a combination of both, and, as such is observed as discrete frequencies as well as excessive low frequency noise. To assist in understanding the source of the noise, several dynamic analyses both structural and electrical were made and are reported herein.

A review of S192 structural resonance test data obtained with the use of accelerometer and strain gage sensors is made in Section 1. In addition, a series of tests on the cooler/dewar/preamplifier assembly as supported on a foam pad are reported together with test data showing the vibration output from the External Scanner Motor as a source of vibration energy. Finally, test results on lead resonance in the S192 Dewar are reported.

The results of an analysis of the natural frequencies of the Dewar leads is given in Section 2.

An analysis of the S192 Cooler and its supporting structure was performed with the results summarized in Section 3.

Section 4 gives an analysis of the electronic stability of the forward signal both of the thermal channel (band 13). This includes an analysis of the automatic gain control and the offset control feedback loops as well as the preamplifier which utilizes on integrator feedback circuit.

Section 5 contains a chronological review of low frequency noise investigations using S192 output data: preamplifier, video processor, or digital data outputs. The period covered is from September 1971 through April 1973.

TABLE OF CONTENTS

SECTION 1
STRUCTURAL RESONANCE DATA REVIEW

1.1 SUMMARY

Accelerometer and strain gage response data has been examined from prequalification tests on System Number 1 (August, 1971); acceptance test data, System Number 2 (April, 1972); Vehicle Dynamic and Random Vibration Elements of the Qualification Tests (December, 1972); and various development and follow-on qualification tests. The development tests include Fixture Verification Tests, Telescope Tests, Encoder Tests, and Dewqr Tests (October, 1971). Follow-on Qualification Tests include the Qualification Retest of the External Scanner (January, 1973) and the Cooler/Dewar/Preamplifier Qualfification Test (February, 1973).

In addition to examining the above data for evidence of structural natural frequencies in the 5 to 40-Hz range, the 16 August, 1973 Cooler Vibration Analysis Tests (Cooler Serial Number 329, Runs 1 through 13) were examined for frequency forcing functions. During the examinations, careful recognition was given to physical design and design changes.

The above data indicates there are significant natural frequencies between the Cooler/Dewar/Preamplifier Assembly and its cantilever mount of 12, 17, and 27 Hz; there are significant oscillatory forcing couples of 20 and 40 Hz (proportional to drive motor voltage) within the Malaker Cooler; and there are lead natural frequencies within the Dewar of 18 and 38 Hz, visually observed during the development testing in October, 1971.

It has been further observed that the auxiliary support for the Cooler, designed to snub (or limit) oscillatory motion during ascent may not be adequate to prevent induction of microphonics.

1.2 DEWAR MICROPHONICS AND DETECTOR MOVEMENT AS NOISE SOURCES

The following possible causes of noise signals have been suggested:

(1) Dewar leads moving at a forced or natural frequency, interacting with a magnetic field (Earth or that generated by the S-192 or adjacent equipment) to produce a spurious signal.

(2) Dewar leads moving at a forced or natural frequency. The alternating strain causes an alternating resistance which in turn modulates the voltage drop along that section of lead.

(3) Dewar leads moving at a forced or natural frequency and inducing a change of contact resistance at points of attachment between leads and between leads and detectors.

(4) Movement of detectors along focal centerlines or lateral to it, causing modulation of the signal which is proportional to signal intensity.

(5) Magnetic flux interaction between the dc brush type torque motor in the Cooler, the Cold Finger and the Detectors within the Dewar.

(6) Excessive low frequency noise due to the 1/f corner in detector.

Item 1 above has been eliminated by tests run with the Dewar subjected to strong magnetic fields which has no effect upon the noise signal intensity.

Item 2, 3, and 4 would normally produce noise signals proportional to signal intensity, but not in the case of strong light or voltage bias. The HRC experiment in which the signal level (incoming radiation) was reduced to zero without changing the noise intensity level would eliminate Item 4 for all channels and Items 2 and 3 for the visual channels. The voltage bias and high amplification of Channel 13 would suggest Items 2 and 3 as possible contenders, in that channel.

1.3 DATA INDICATIONS FOR STRUCTURAL NATURAL FREQUENCIES IN THE 5-40 HERTZ RANGE

Both sinusoidal (search and Vehicle Dynamics) and random data were examined for evidence of resonant frequencies. The sinusoidal inputs, however, much more accurately identify the natural frequencies. Supporting data for this report, therefore, are accelerometer and strain gage responses to sinusoidal inputs. This data is shown in Figures 1 through 27 and summarized in Table I.

Two sets of data are summarized in Table I, that obtained from System 1 in August, 1971 and Qualification Test data from December 1972. There are two major physical differences to be noted in connection with this data: one, the auxiliary Cooler

support was inadvertently omitted for the August 1971 tests; and two, the Spare Cooler/Dewar/Preamplifier dummy weight was significantly higher for the Qualification tests. The following interpretations are suggested by the data:

I. The Cooler/Dewar/Preamplifier Assembly cantilevered off its flange mounting has natural frequencies of approximately 12, 17 and 27 Hz.

These frequencies are clearly shown in Figures 4 through 1.12. This data, however, suggests the source may be the C/D/P or interactions between the internal adapter plate and the Spare Mount or other assemblies. But Figures 1.21, 22, 25, 26 and 27 clearly indicate these frequencies are not present when the auxiliary Cooler mount is properly used. The conclusion is further supported by Figure 13, wherein the 27-Hz frequency is indicated, but neither the 12-Hz nor the 17-Hz is indicated.

II. The Internal Scanner Optical Bench may transmit structural frequencies below 30 Hertz. This is indicated by the data referenced above.

Table I

S-192 RESONANT FREQUENCY VS LOCATION

FIGURE	GAGE NO.	LOCATION
	AUGUST 1971 SYS. NO. 1 DATA	
1	S1	EXT. ADAPTER PLATE
2	S7	EXT. ADAPTER PLATE
3	S9	EXT. SCANNER
4	S11	INT. SCANNER
5	S15	INT. SPARE
6	A1X	INT. THER. CHANNEL
7	A3X	OPT. BENCH
8	A4Z	OPT. BENCH
9	A5Y	OPT. BENCH
10	A6Z	SPARE DMY. WT.
11	A7X	SPARE DMY. WT.
12	A8Y	SPARE DMY. WT.
13	A9Z	ANALOG ELEC.
14	A13Y	BAFFLE SEC. MRR.
15	A15Y	MTOOR HSNG.
16	A17Y	RELAY HSNG.
17	A23Z	ADAPT. FLANGE
18	A24X	ADAPT. FLANGE
19	A26Z	ADAPT. FLANGE
20	A29X	ADAPT. CORNER
	DECEMBER 1972 QUAL. DATA	
21	A2Y	OPT. BENCH
22	A3Z	OPT. BENCH
23	A7Y	THER. CHANNEL
24	A9Z	THER. CHANNEL
25	A4X	SPARE DMY. WT.
26	A5Y	SPARE DMY. WT.
27	A6Z	SPARE DMY. WT.

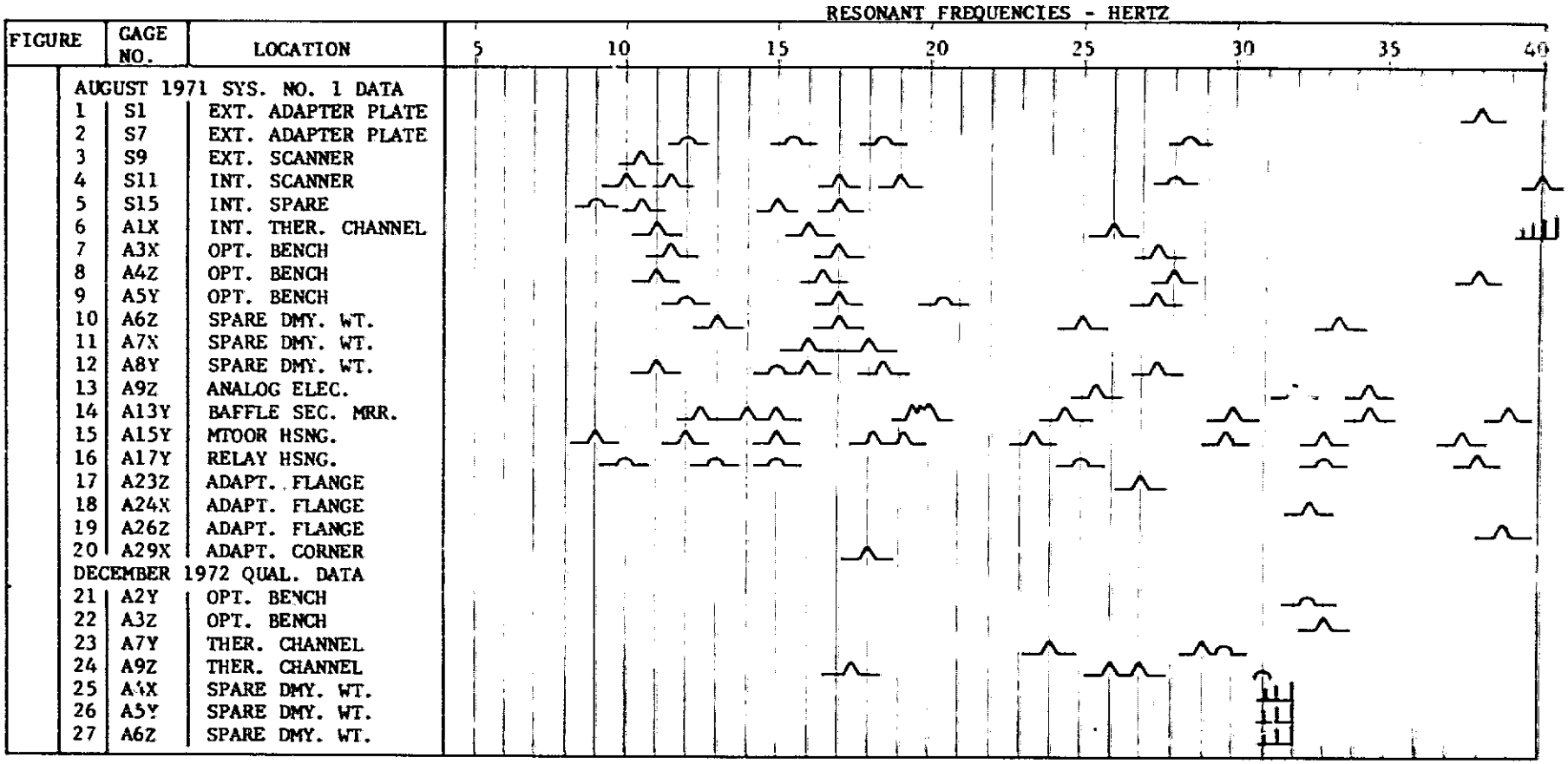

Very strong

Strong

Weak

III. There are a significant number of natural frequencies associated with the motor housing as a support, ranging from 8 through 40 Hertz. These are shown by Figures 14 and 15. There is no strong evidence, however, in Figures 21 through 27 that these disturbances are transmitted into the Dewar. The attenuation, however, is evident in moving only six inches from the Motor Housing to the Relay Housing, as shown by Figures 15 and 16.

1.4 THE COOLER/DEWAR/PREAMPLIFIER ASSEMBLY AS AN ENERGY SOURCE

Malaker Cooler, Serial Number 329, was subjected to a series of tests on 16 March, 1973. Runs 7 through 13 were made with an accelerometer located close to the tip of the cold finger, with the sensitive axis perpendicular to a plane established by the centerlines of the large and small tubes leading to the tip. Runs 1 through 6 were made with the accelerometer located on the body of the Cooler, close to the mounting flange, with the sensitive axis perpendicular to that of the cold finger mounting, that is, in line with the plane connecting the centerlines of the large and small tubes. Runs 1 through 6 are included herein as Figures 28 through 33; Runs 7 through 13 are included as Figures 34 through 40.

The Cooler was supported on foam in order to measure inertial response to internal forcing functions. The motor in the Cooler was energized at various voltages from 20.0 through 27.49. Accelerometer outputs were run through a wave analyzer and the results plotted as output in "g" peak vs Frequency, Hz. These are the results shown in Figures 34 through 40.

Examination of the data indicates there is a basic forcing function with frequency ranging from 15 Hz to 22.5 Hz, with a corresponding first harmonic ranging from 30 Hz to 45 Hz. The comparison between the magnitude of outputs of the two accelerometers for the same drive voltage indicates a rocking or coning motion response of the Cooler.

1.5 OTHER ENERGY SOURCES

The External Scanner Motor and associated drive must be considered as a subharmonic source of energy (it has a synchronous speed of approximately 100 Hz). This is shown in Figure 15, response data from a Y-sensitive accelerometer mounted on the motor housing.

Natural frequencies of 9, 13, 15, 18, 19, 23.5, 30, 33 and 37.5 exist at this point, but their amplitudes are sharply attenuated by the structure and interfaces between the Motor Housing measuring point and that of the Relay Housing (Figure 16). From these data, the attenuation as a function of frequency is as follows:

Frequency, Hz	9	13	15	18	19	24	30	33	38
Attenuation	1.11	1.08	1.76	2.25	1.89	7.58	6.51	6.50	6.09

There are at least 10 equivalent interfaces between the motor housing and the dewar. In addition, it is estimated that energy output in frequencies below 40 Hz from the External Scanner Motor is at least an order of magnitude below that produced by the Malaker Cooler drive. It is unlikely, therefore, that the External Scanner Drive is generating the subject noise signals.

1.6 LEAD RESONANCES IN S-192 DEWAR (OCTOBER, 1971 DEVELOPMENT TEST)

A development vibration test was performed on 19 October, 1971. A resonance search was made, starting at 3 Hertz, 0.2-inch double amplitude, and proceeding to 2000 Hertz at 3 octaves/minute, limiting input to 1.0 "g". This was the S-192 Prototype Dewar with a 79-V detector array.

Resonances were noted visually by looking through the visual channel. Frequencies at which resonances occurred were recorded as follows:

Axis of Vibration Along Mounting Flange Centerline:

36, 391, 694, 1100, 1770 Hertz

Axis of Vibration Perpendicular to Mounting Flange Centerline:

18, 38, 283, 503, 708, and 1000 Hertz

6-2478
7-68

TWO 37128	CUSTOMER HONEYWELL
ITEM S 192 SCANNER (SYS 1)	
SINE ☒ RANDOM ☐ ANALYSIS ☐	AXIS X-Y; SYST. NO. 8
REF. 200 Hz/in; SHAKER 4-TAND	
OPERATOR RMIDDLETON	DATE 8-20-71

PRE ACCEPTANCE SINE
1.0 OCT/MIN

REF

SCALE – 1.0 DB/DIV.

STRAIN GAGE NO 1
AC COMPONENT

STRAIN - μin/in

FREQUENCY IN CPS.

FIGURE 1

SEMI-LOGARITHMIC
4 CYCLES X 10 DIVISIONS PER INCH

6-2478
7-68

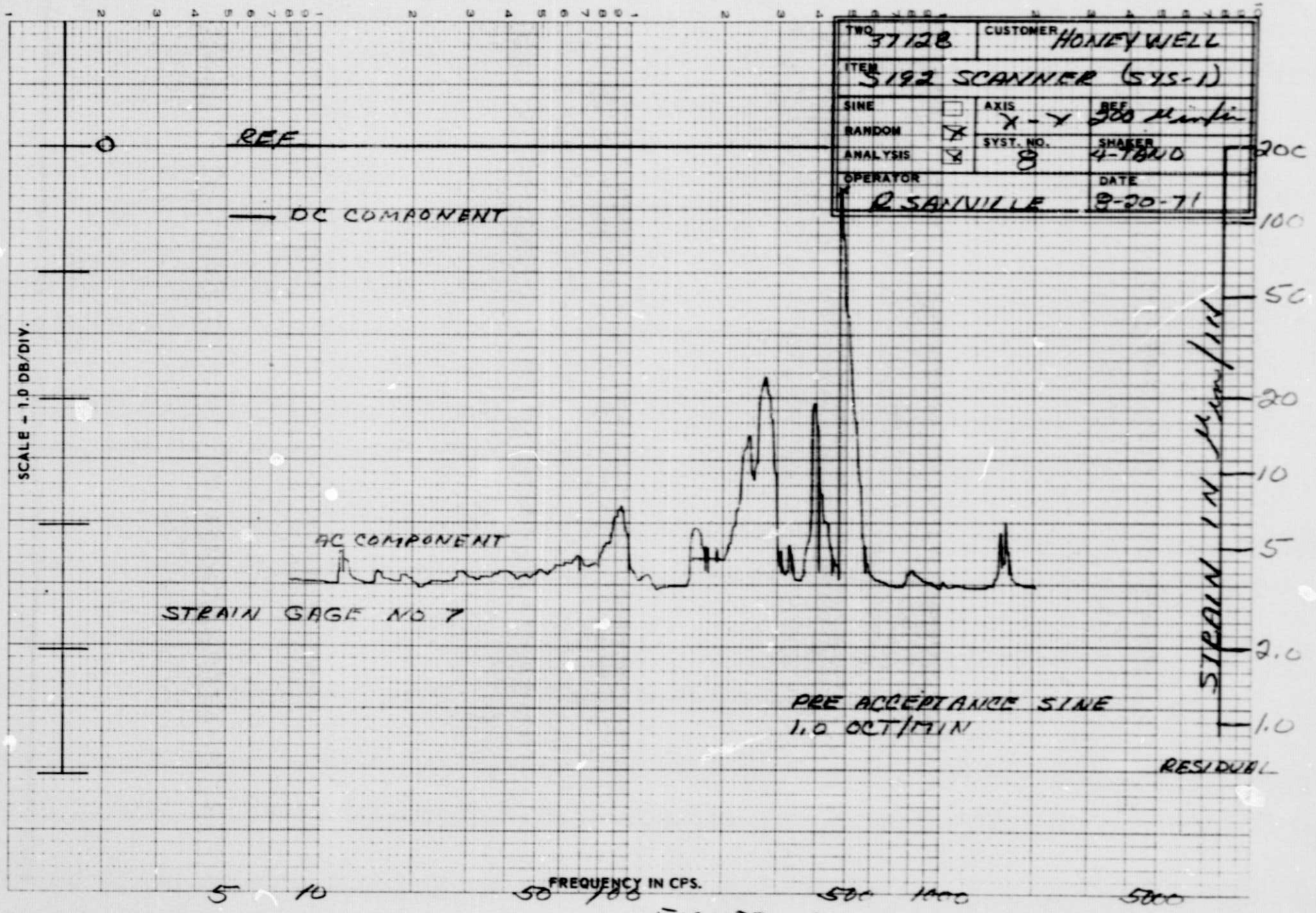

FIGURE

10

6-2478
7-68

TWO 37128	CUSTOMER HONEY WELL
ITEM 5192	SCANNER (2)S 1)
SINE ☒ RANDOM ☐ ANALYSIS ☐	AXIS X-X / SYST. NO. 8 / REF. 200 Hz Sine / SHAKER 4-TENDER
OPERATOR P SANVILLE	DATE 8-20-71

REF

DC COMPONENT

AC COMPONENT

STRAIN GAGE NO 9

PRE ACCEPTANCE SINE
1.0 OCT/MIN

RESIDUAL

SCALE - 1.0 DB/DIV.

0 -10

20G 100 50 20 10 5 2.0 1.0

5 10 50 100 500 1000 5000

FREQUENCY IN CPS.

FIGURE 3

6-2478
7-68

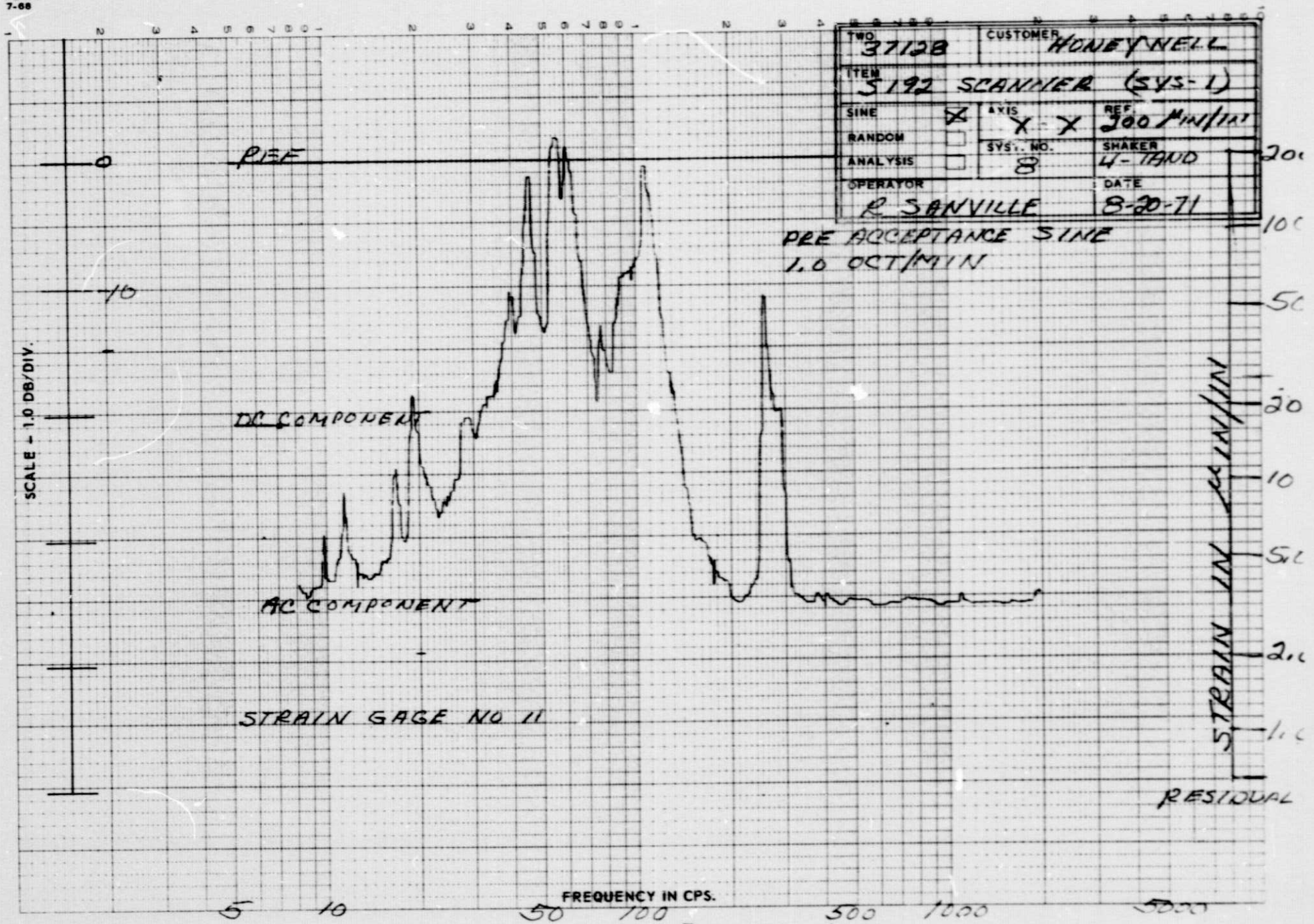

FIGURE 4

6-2478
7-68

TWO 37128	CUSTOMER HONEYWELL		
ITEM 5192 SCANNER (SYS-1)			
SINE X	AXIS X-Y	REF. 200 MINIM	
RANDOM	SYST. NO. 8	SHAKER H-STAND	
ANALYSIS			
OPERATOR RSANVILLE		DATE 8-30-71	

PRE ACCEPTANCE SINE
1.0 OCT/MIN

0 REF

-10

SCALE - 1.0 DB/DIV.

DC COMPONENT

STRAIN GAGE NO. 15

AC COMPONENT

RESIDUAL

STRAIN IN G²/CPS

20
10
5
2.0
1.0

5 10 50 100 500 1000 5000

FREQUENCY IN CPS.

FIGURE 5

SEMI-LOGARITHMIC
4 CYCLES X 10 DIVISIONS PER INCH

6-2478
7-68

TWO 3712B	CUSTOMER HONEYWELL
ITEM S 192 SCANNER (SYS 1)	
SINE ☒ RANDOM ☐ ANALYSIS ☐	AXIS X-X / SYST. NO. 8 / REF. 1.0 g (PK) / SHAKER 4 - TANDEM
OPERATOR R MIDDLETON	DATE 8-20-71

PRE ACCEPTANCE SINE
1.0 OCT/MIN

TR = 6.3

TR = 2.0

REF

ACCEL NO 6-4
X-DIRECTION

SCALE - 1.0 DB/DIV.

ACCEL IN G (PK)

8.0
4.0
2.0
1.0
.50
.250
.125

FREQUENCY IN CPS.

5 10 50 100 500 1000 5000

AIX

FIGURE 6

14

6-2478
7-68

TNO 37128	CUSTOMER AIRKEY WELL
ITEM S 192 SCANNER (SYS 1)	
SINE ☒ RANDOM ☐ ANALYSIS ☐	AXIS X-X
	SYST. NO. 3
	REF. 7.0 G (PK)
	SHAKER 4-TANDEM
OPERATOR R MIDDLETON	DATE 8-20-71

TR = 11.2

TR = 6.3

TR = 5.0

REF

SCALE - 1.0 DB/DIV.

+10

0

-10

ACCEL NO 6-C
X-DIRECTION

PRE ACCEPTANCE SINE
LO OCTAVIN

ACCEL IN G (PK)

8.0
4.0
2.0
1.0
.50
.25

FREQUENCY IN CPS.

5 10 50 100 500 1000 5000

FIGURE 7

A3X

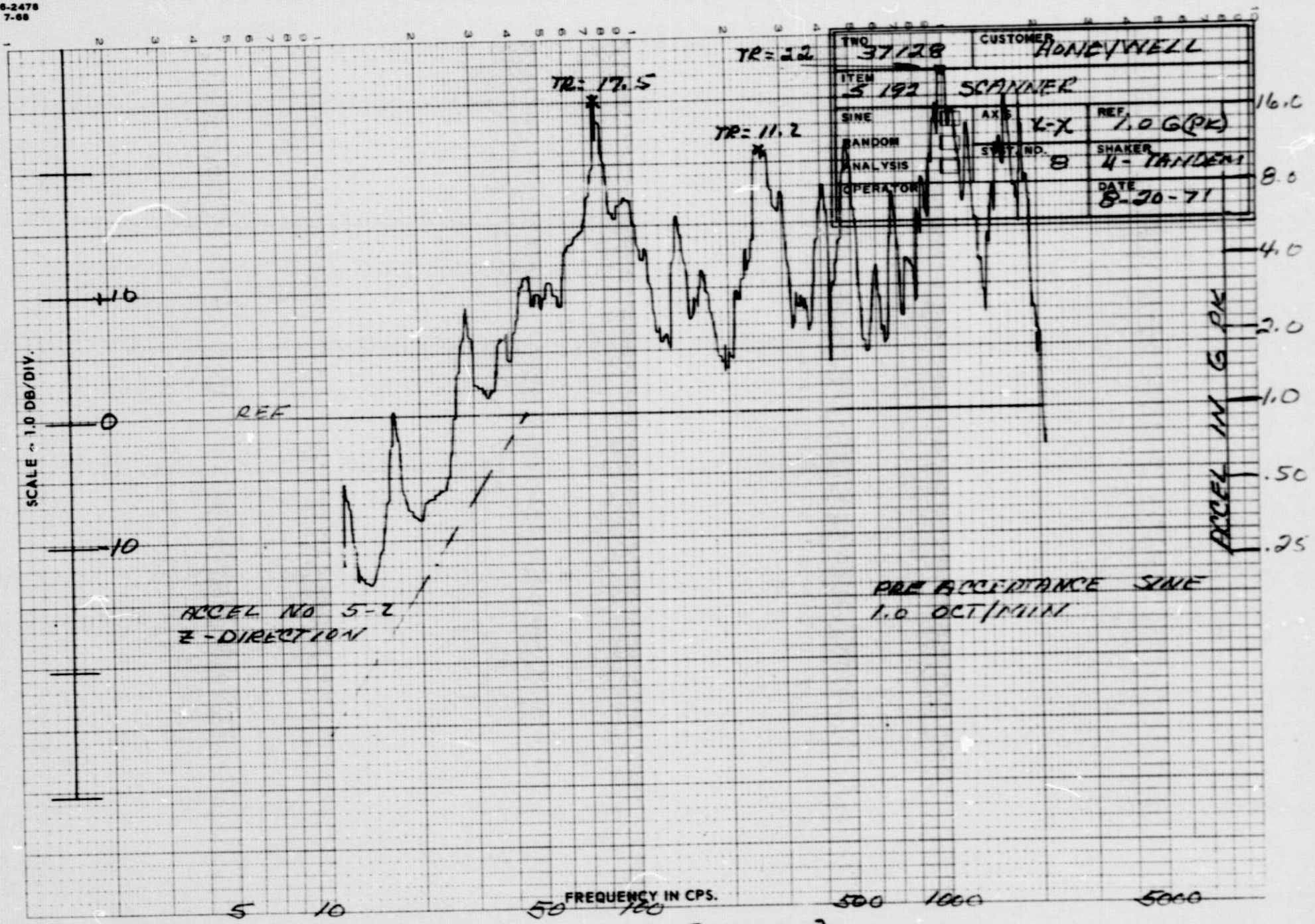
SEMI-LOGARITHMIC
4 CYCLES X 10 DIVISIONS PER INCH
6-2478
7-68
TR= 22
TR= 17.5
TR= 11.2
TNO 37128
CUSTOMER HONEYWELL
ITEM S 192
SCANNER
SINE
RANDOM
ANALYSIS
OPERATOR
AXIS Y-Y
SWEEP NO. 8
REF 1.0 G(PK)
SHAKER 4- TANDEM
DATE 8-20-71
SCALE = 1.0 DB/DIV.
+10
0
-10
REF
ACCEL NO 5-2
Z-DIRECTION
PRE ACCEPTANCE SINE
1.0 OCT/MIN
ACCEL IN G PK
16.0
8.0
4.0
2.0
1.0
.50
.25
5
10
50
100
500
1000
5000
FREQUENCY IN CPS.

A42

FIGURE 8

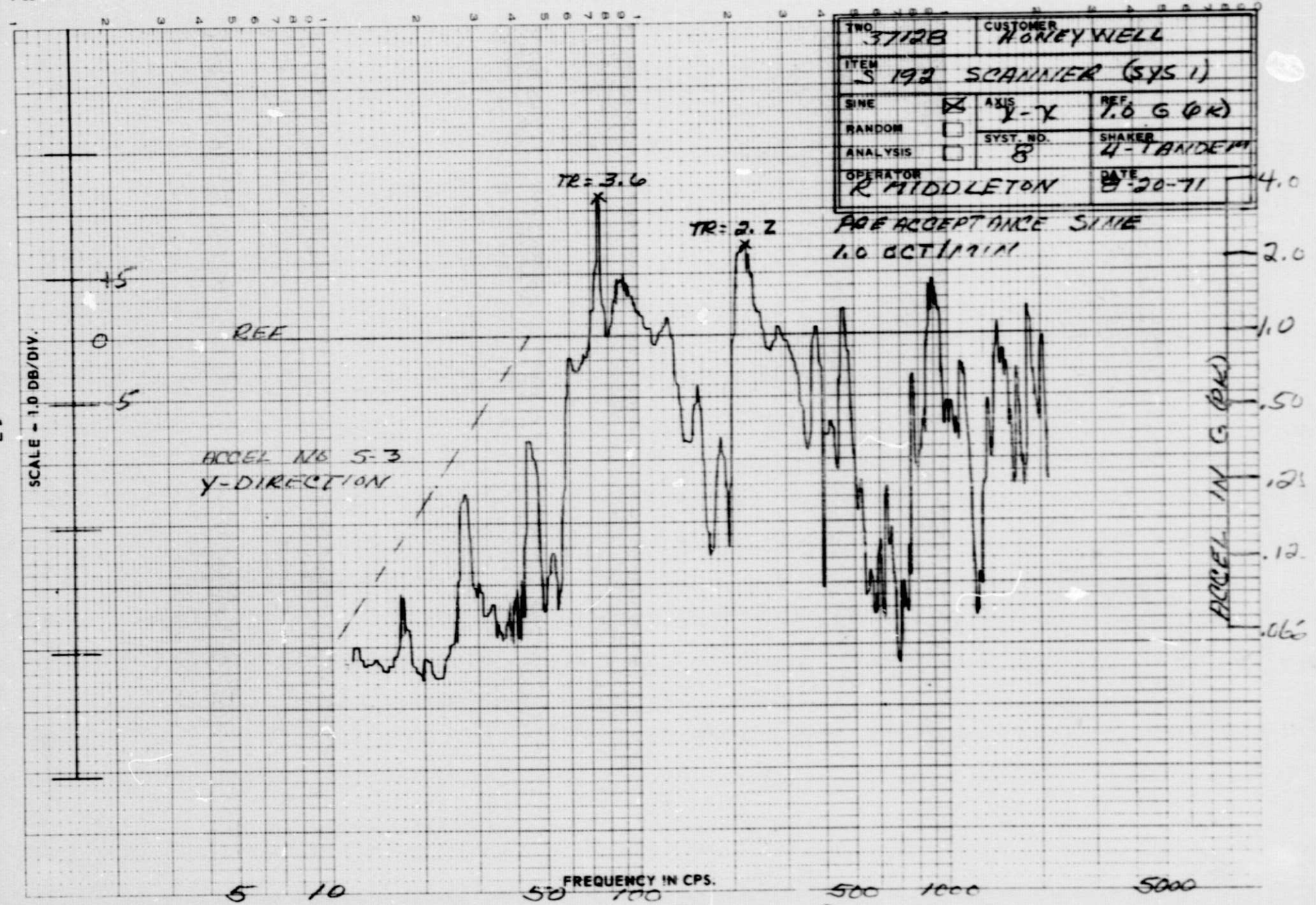
TWO 3712B
CUSTOMER HONEYWELL
ITEM S 192 SCANNER (SYS 1)
SINE ☒
RANDOM ☐
ANALYSIS ☐
AXIS Y-X
REF. 1.0 G (RMS)
SYST. NO. 8
SHAKER 4-TANDEM
OPERATOR R MIDDLETON
DATE 8-20-71
TR = 3.6
TR = 2.2
ACCEPTANCE SINE
1.0 OCTAVE
REF
+5
0
-5
SCALE - 1.0 DB/DIV.
ACCEL NO 5-3
Y-DIRECTION
4.0
2.0
1.0
.50
.25
.12
.06
ACCEL IN G (RMS)
5
10
50
100
500
1000
5000
FREQUENCY IN CPS.

A5Y

FIGURE 9

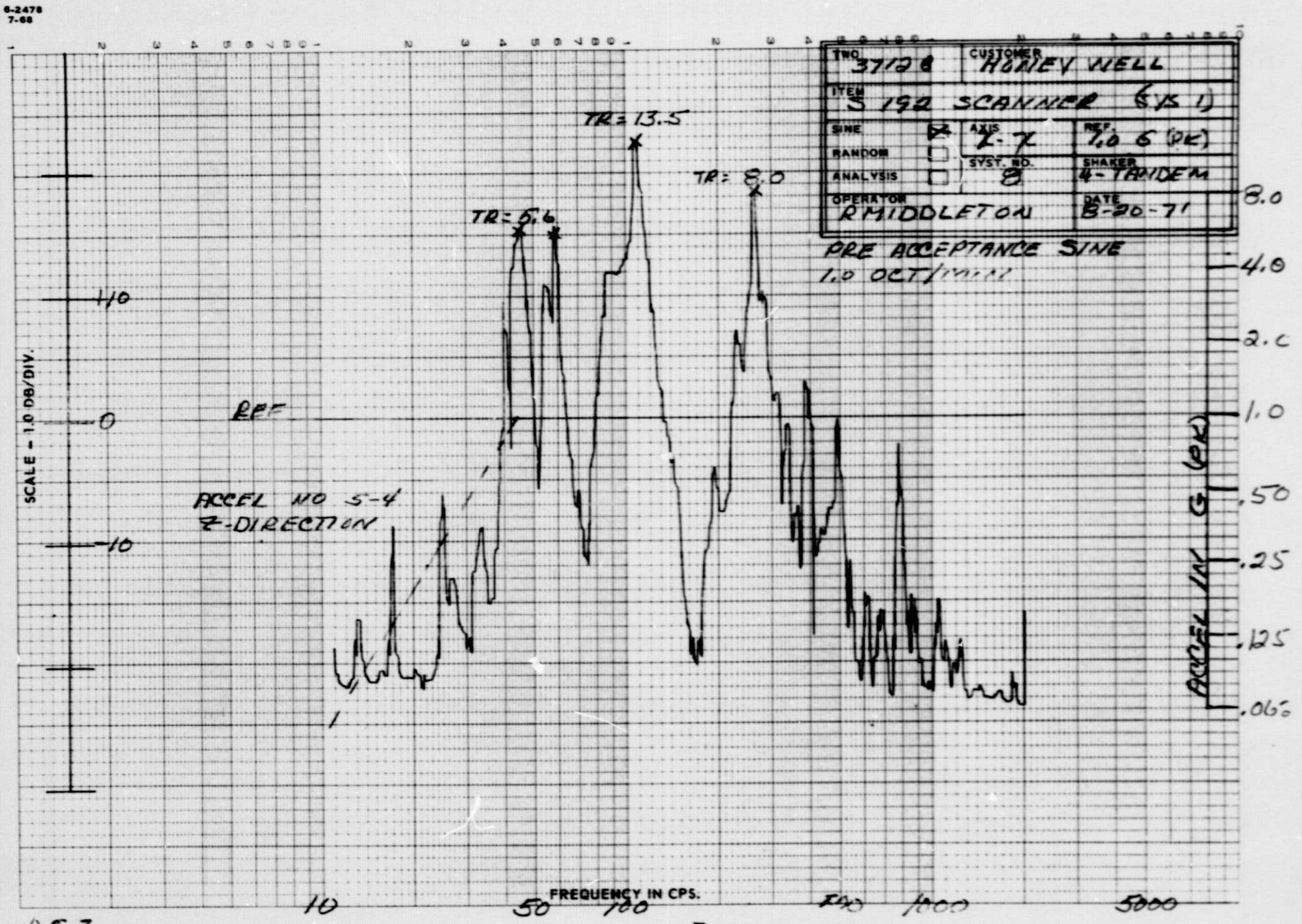

TNO. 37126	CUSTOMER HONEY WELL
ITEM S 192 SCANNER (SYS 1)	
SINE ☒ RANDOM ☐ ANALYSIS ☐	AXIS Z-7 SYST. NO. 8
REF. 7.0 G (PK) SHAKER 4-TANDEM	
OPERATOR RMIDDLETON	DATE 8-20-71

A6 Z

FIGURE 10

6-2478
7-68

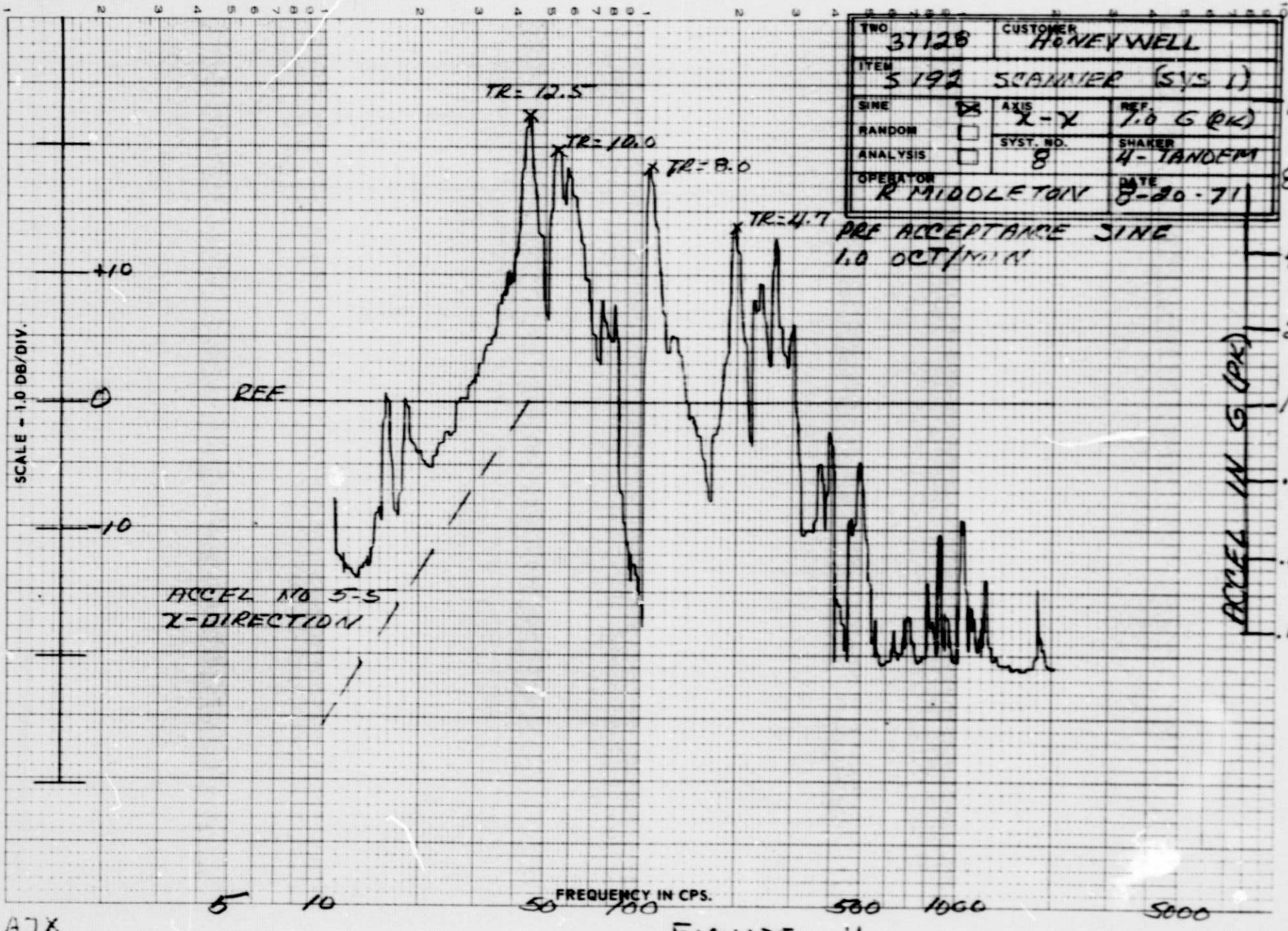

A7X

FIGURE 11

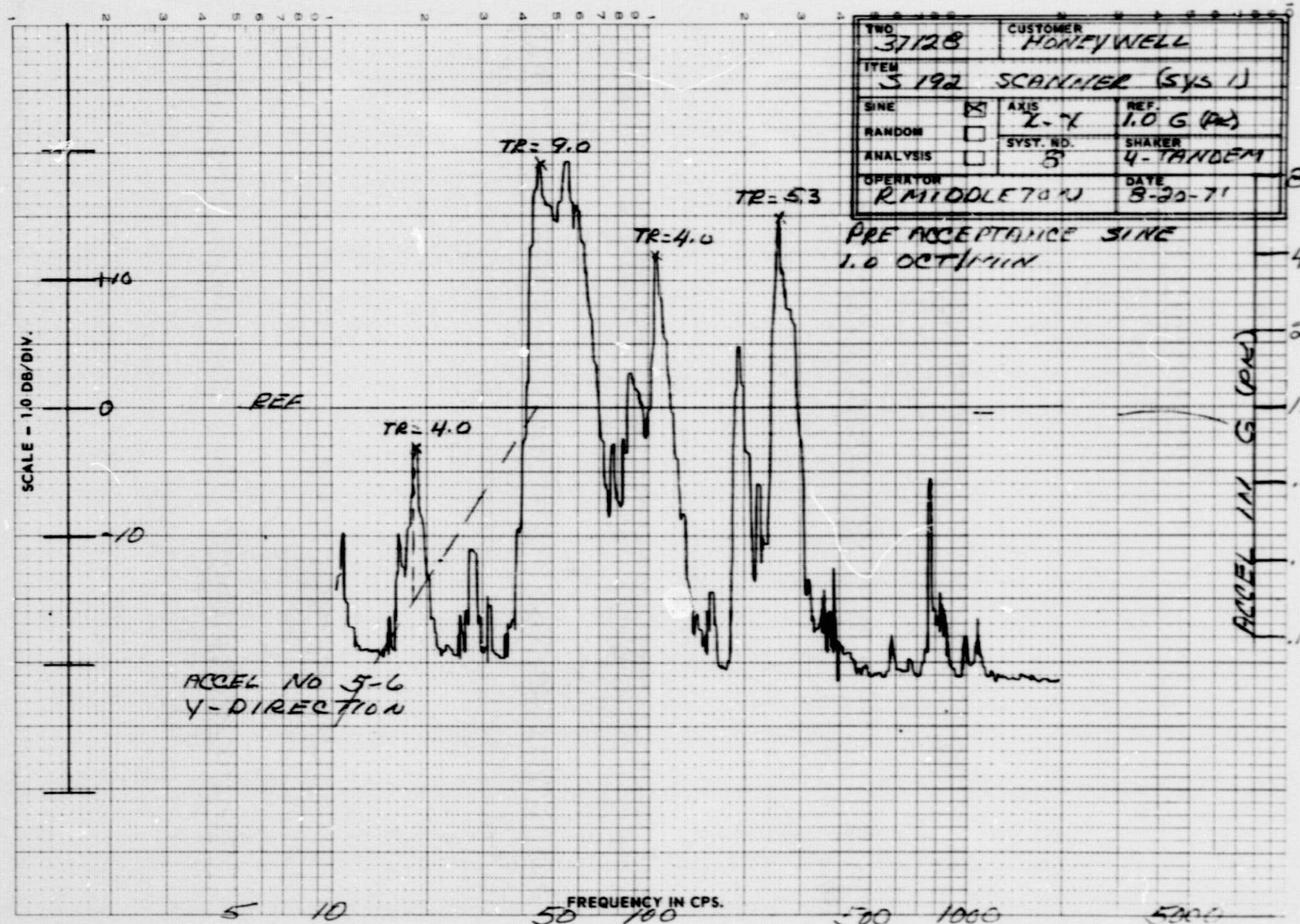
TWO 37128
CUSTOMER HONEYWELL
ITEM 3192 SCANNER (SYS 1)
SINE
RANDOM
ANALYSIS
AXIS Z-Y
SYST. NO. 5
REF. 1.0 G (PK)
SHAKER 4-TANDEM
OPERATOR RMIDDLETON
DATE 8-20-71
PRE ACCEPTANCE SINE
1.0 OCT/MIN
TR=9.0
TR=5.3
TR=4.0
TR=4.0
REF
+10
0
-10
SCALE - 1.0 DB/DIV.
ACCEL NO 5-6
Y-DIRECTION
FREQUENCY IN CPS.
5
10
50
100
500
1000
ACCEL IN G (PK)
8.0
4.0
2.0
1.0
.5
.25
.125

FIGURE 12

SEMI-LOGARITHMIC
4 CYCLES x 10 DIVISIONS PER INCH

6-2478
7-68

TWO 37128	CUSTOMER HONEYWELL
ITEM S 192 SCANNER (SYS 1)	
SINE ☒ RANDOM ☐ ANALYSIS ☐	AXIS X-Y
	REF. 1.0 G (PK)
	SYS. NO. B
	SHAKER 4-TANDEM
OPERATOR RMIDDLETON	DATE 8-20-71

TR=9.0
TR=4.5
TR=2.5
TR=4.5
REF
0
ACCEL. NO 4-5
Z-DIRECTION
PREVIOUS TOLERANCE SINE
1.0 OCT/MIN

SCALE – 1.0 DB/DIV.

ACCEL (1/4 G (PK))

8.0
4.0
2.0
1.0
.50
.25
.125

FREQUENCY IN CPS.

5 10 50 100 500 1000 5000

A97

FIGURE 15

6-2478
7-68

TWO 37128	CUSTOMER HONEYWELL
ITEM S 192	SCANNER (SYS 1)
SINE ☒ / RANDOM ☐ / ANALYSIS ☐	AXIS X-X; SYST. NO. 69
REF. 1.0 G(PK)	SHAKER 4-TANDEM
OPERATOR R SANVILLE	DATE 8-20-71

TR= 8.0

TR= 4.7

REF

SCALE = 1.0 DB/DIV.

+10

0

-10

ACCEL NO 13
Y-DIRECTION

PRE ACCEPTANCE SINE
1.0 OCTAVE/MIN

FREQUENCY IN CPS.

5 10 50 100 500 1000 500

ACCEL LEVEL G (PK)

8.0 4.0 2.0 1.0 .50 .25 .125

FIGURE 14

6-2478
7-68

TWO 37128	CUSTOMER HONEYWELL
ITEM S 192 SCANNER (SYS 1)	
SINE ☒ RANDOM ☐ ANALYSIS ☐	AXIS X-X / SYST. NO. 8
REF. 1.0 G PK / SHAKER 4- TANDEM	
OPERATOR R SANVILLE	DATE 8-20-71

SCALE - 1.0 DB/DIV.

+10

0 REF

-10

ACCEL NO 15
Y DIRECTION

PRE ACCEPTANCE SINE
1.0 OCT/MIN

ACCEL IN G (PK)

4.0
2.0
1.0
.50
.25
.12

FREQUENCY IN CPS.

5 10 50 100 500 1000 5000

FIGURE 15

SEMI-LOGARITHMIC
4 CYCLES X 10 DIVISIONS PER INCH

6-2478
7-68

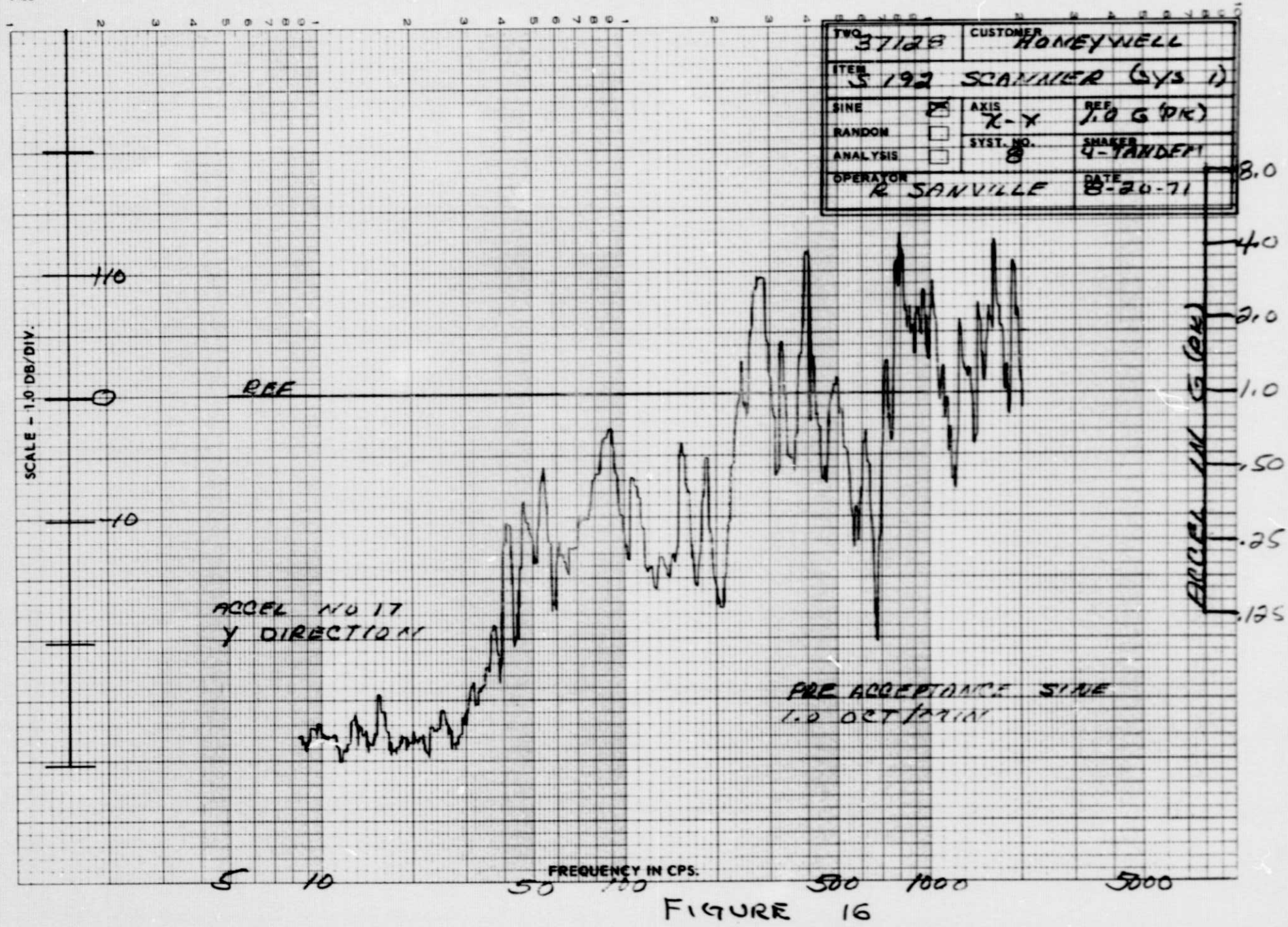

FIGURE 16

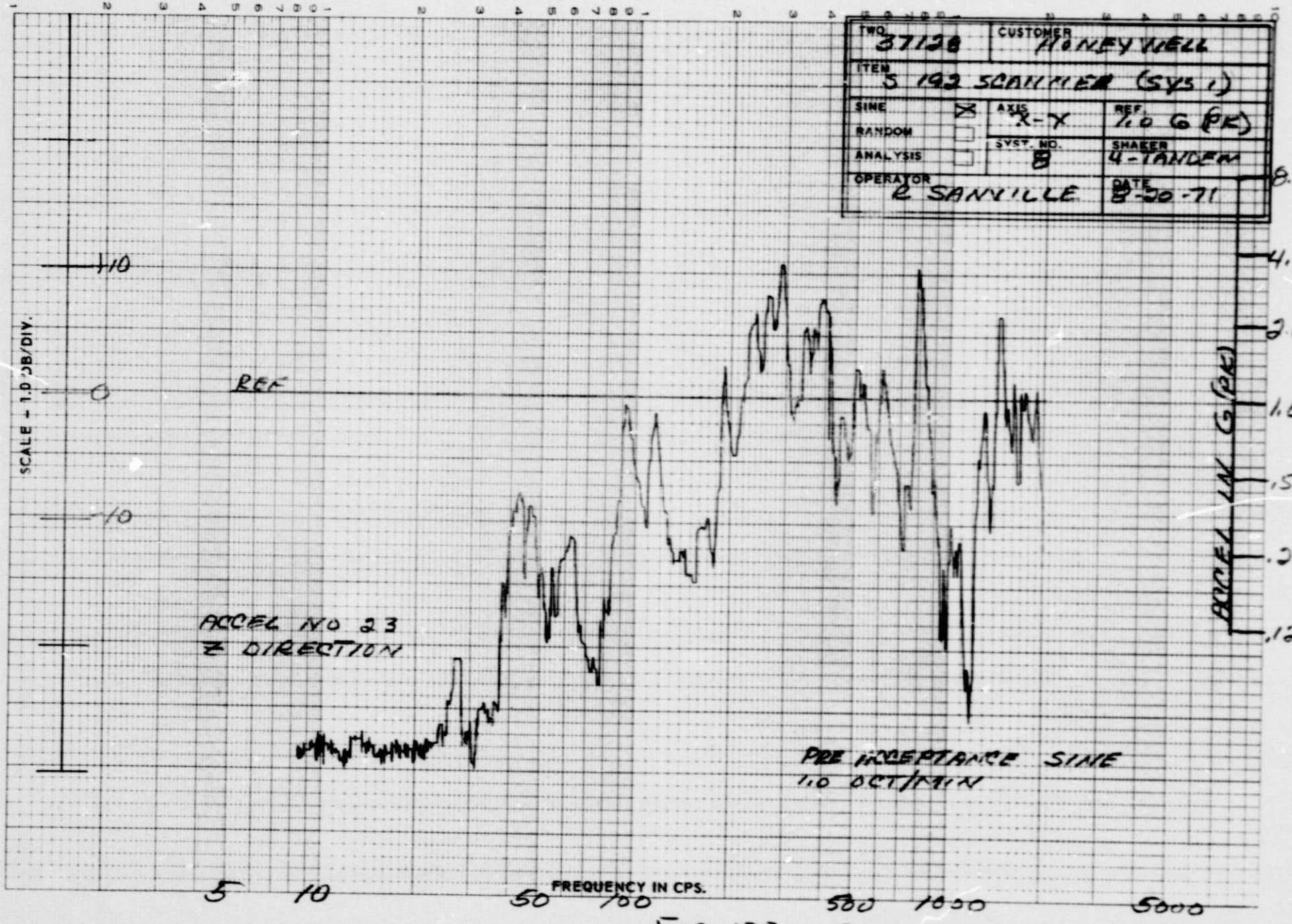

FIGURE 17

SEMI-LOGARITHMIC
4 CYCLES X 10 DIVISIONS PER INCH

6-2478
7-68

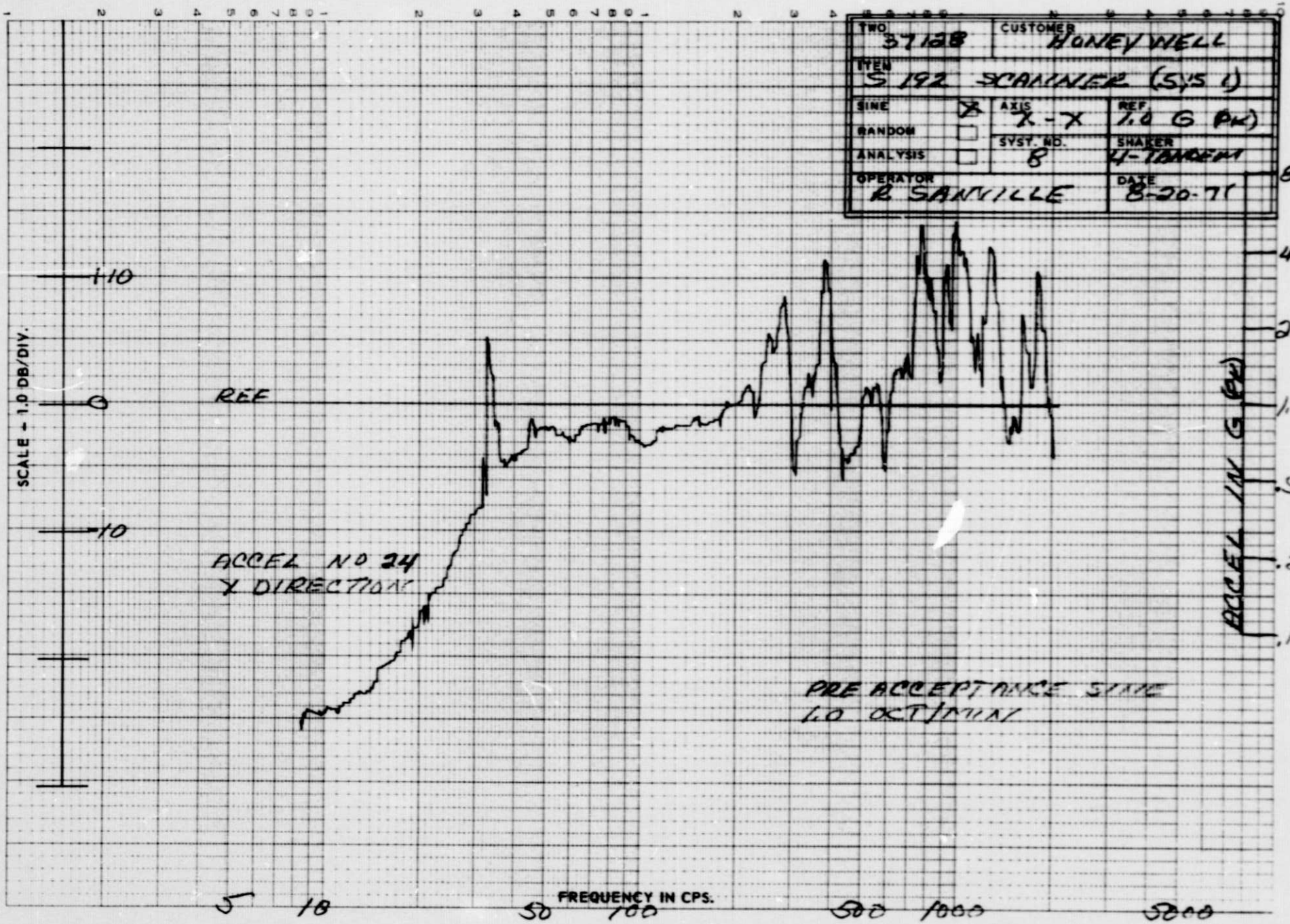

FIGURE 18

6-2478
7-68

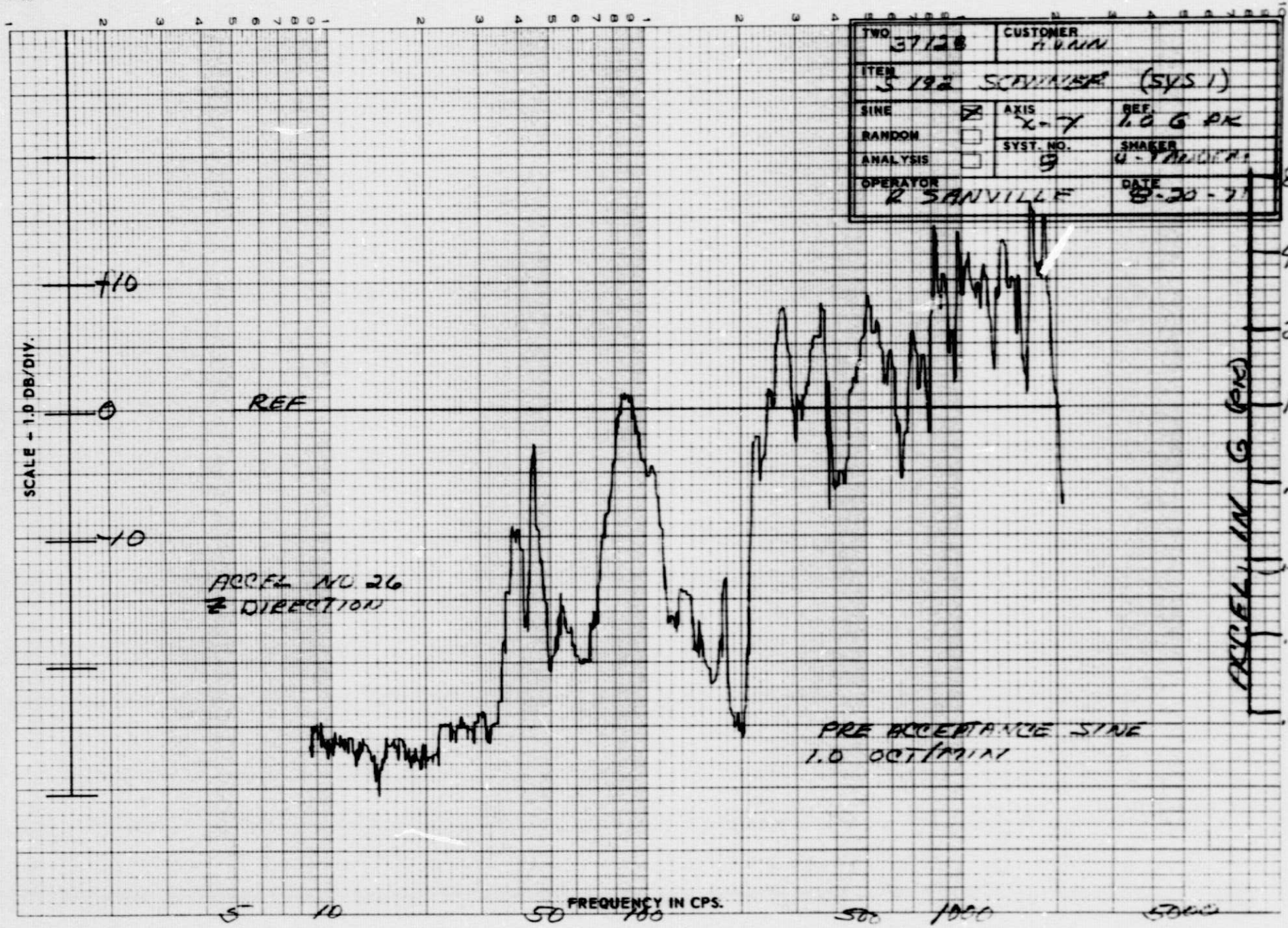

FIGURE 19

SEMI-LOGARITHMIC
4 CYCLES X 10 DIVISIONS PER INCH

6-2478
7-68

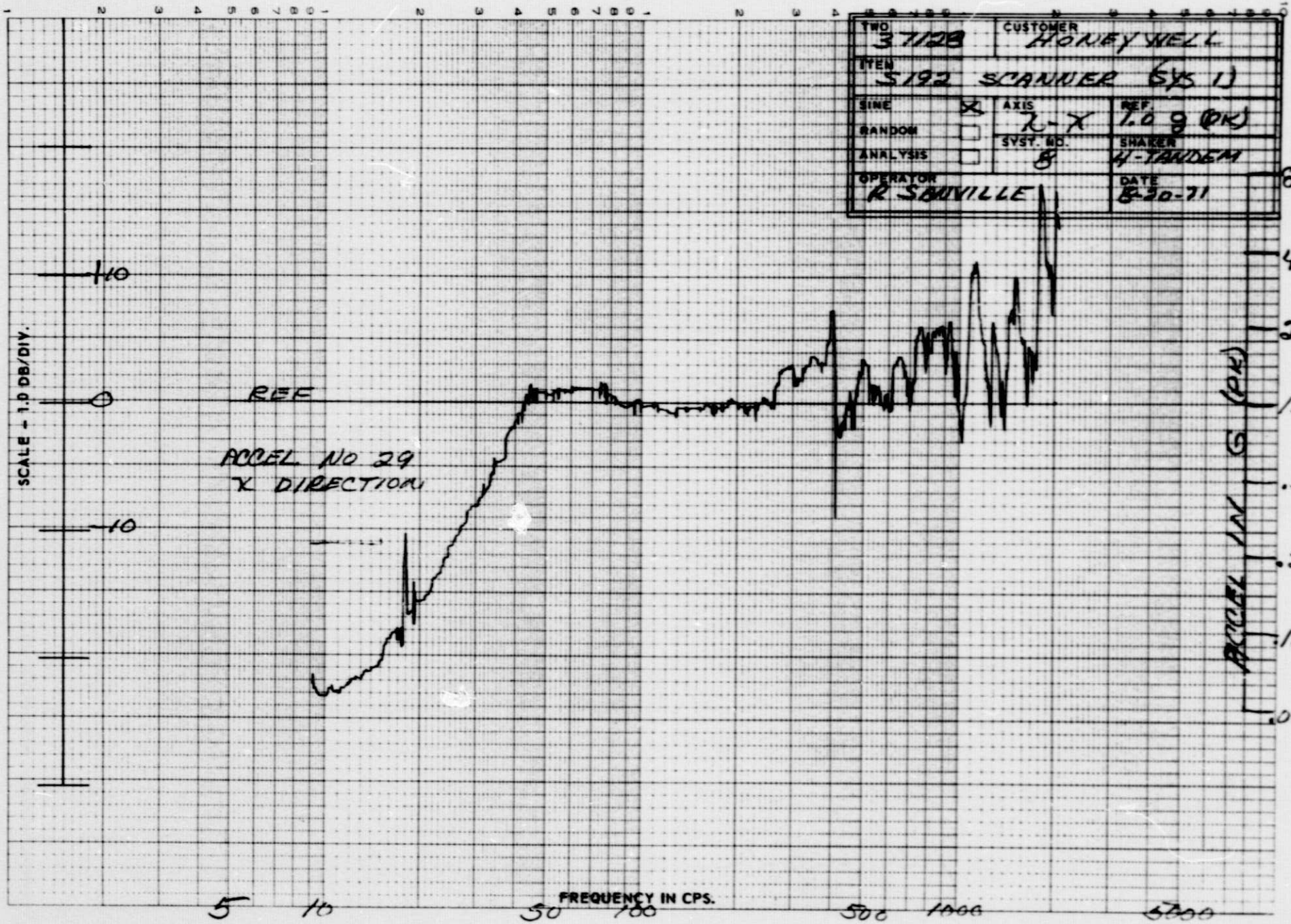

FIGURE 20

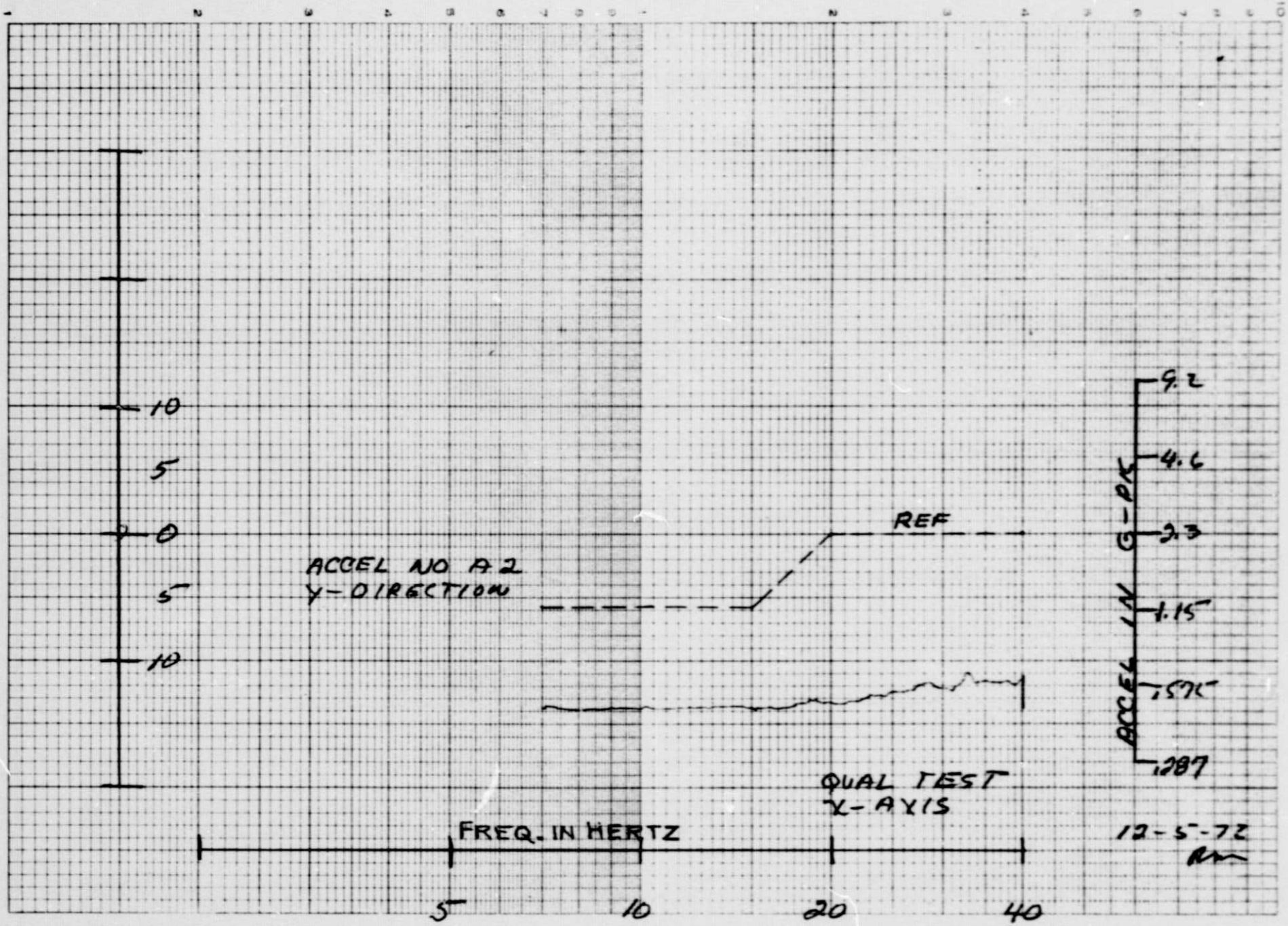
10
5
0
5
10
ACCEL NO A2
Y-DIRECTION
REF
9.2
4.6
2.3
1.15
.57
.287
G-PK
ACCEL
QUAL TEST
X-AXIS
FREQ. IN HERTZ
5
10
20
40
12-5-72

FIGURE -21

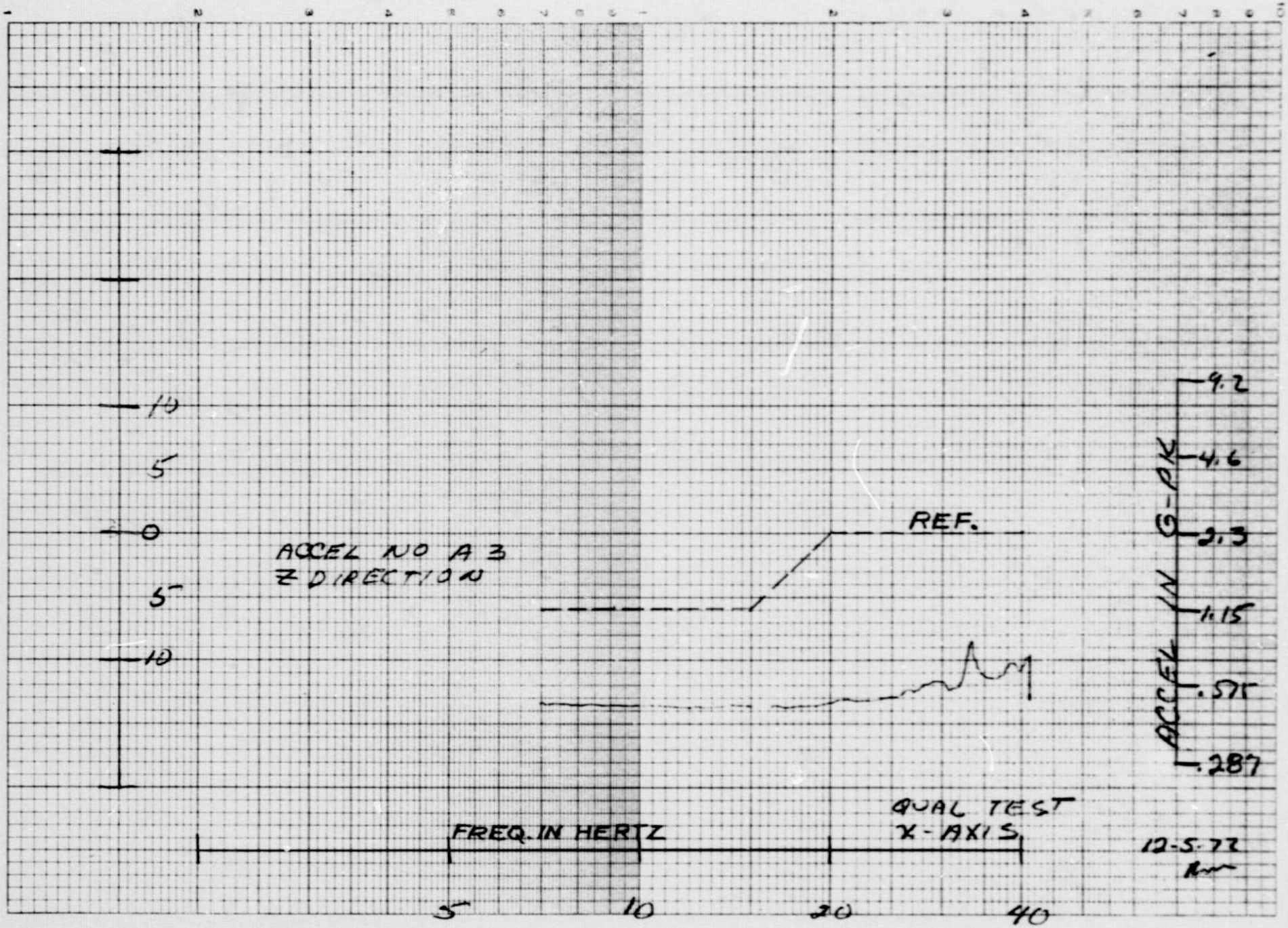
15
5
0
5
10
ACCEL NO A 3
Z DIRECTION
REF.
9.2
4.6
2.3
1.15
.575
.287
G-PK
G-RMS
ACCEL
FREQ. IN HERTZ
5
10
20
40
QUAL TEST
X-AXIS
12-5-77

FIGURE 22

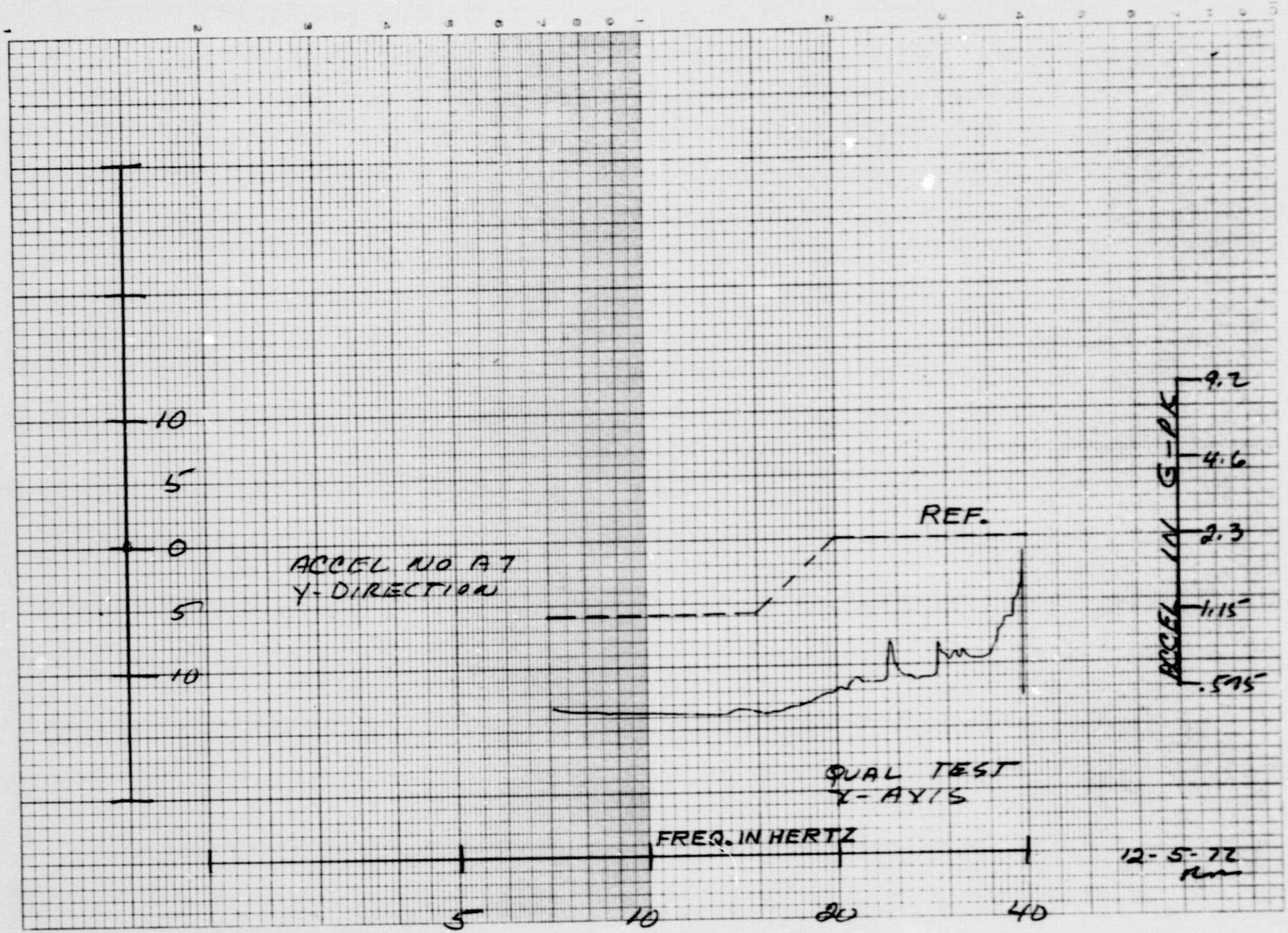
10
5
0
5
10
ACCEL NO A7
Y-DIRECTION
REF.
9.2
4.6
2.3
1.15
.575
G-PK
ACCEL
QUAL TEST
Y-AXIS
FREQ. IN HERTZ
5
10
20
40
12-5-72

FIGURE 23

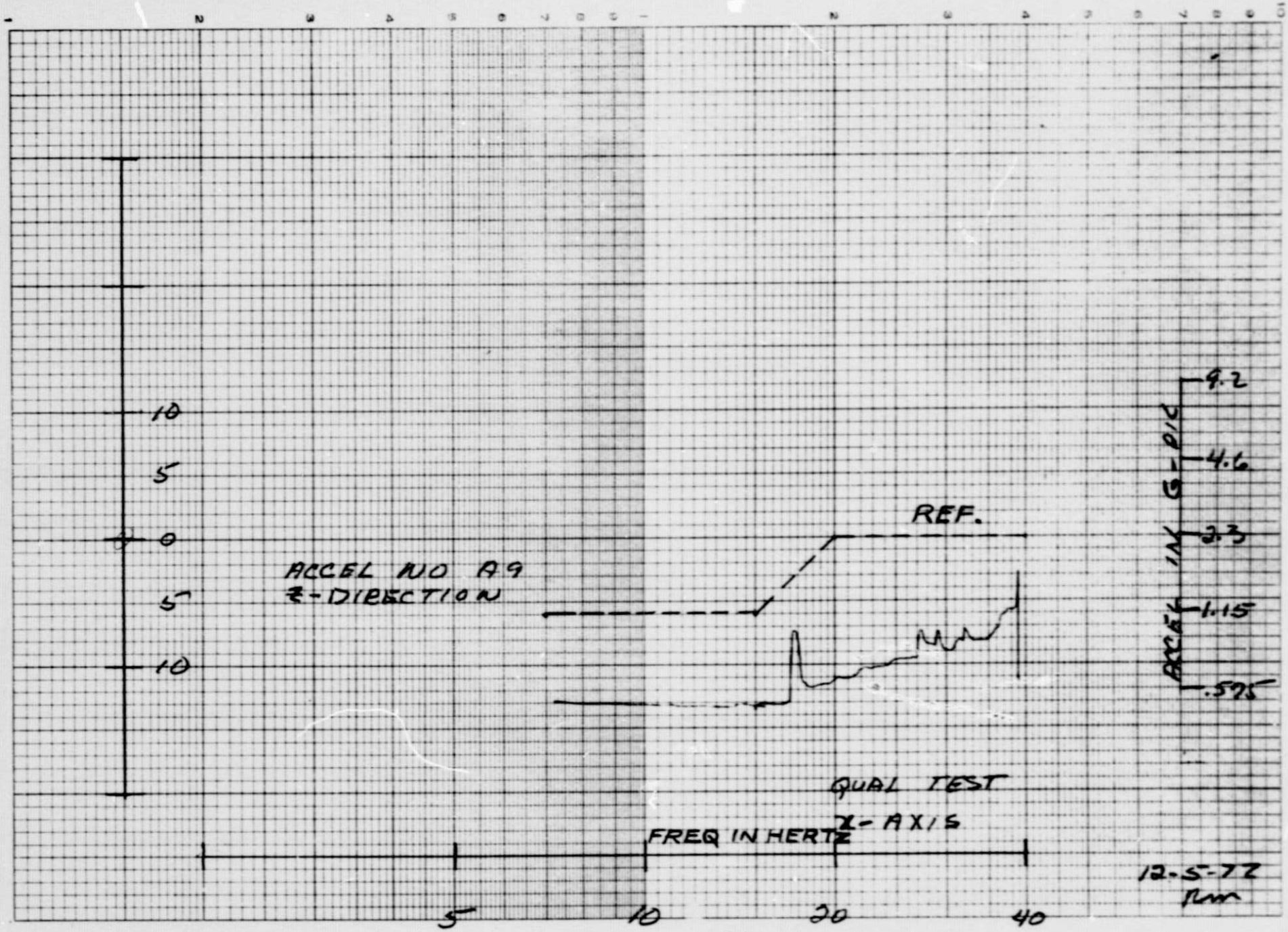
10
5
0
5
10
REF.
ACCEL NO A9
Z-DIRECTION
9.2
4.6
2.3
1.15
.575
G-PK
IN
ACCEL
QUAL TEST
X-AXIS
FREQ IN HERTZ
5
10
20
40
12-5-72

FIGURE 24

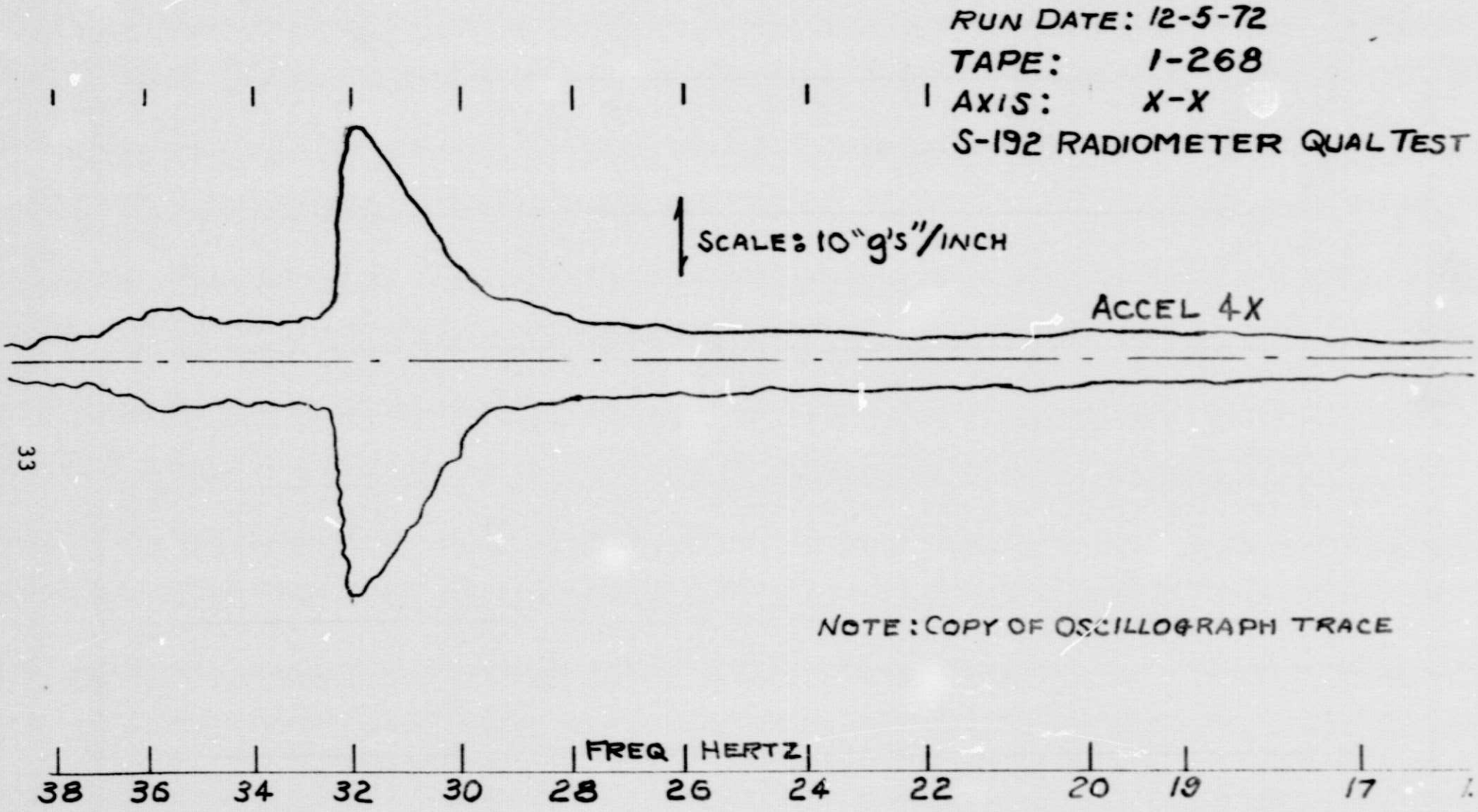
RUN DATE: 12-5-72
TAPE: 1-268
AXIS: X-X
S-192 RADIOMETER QUAL TEST
SCALE: 10 "g's"/INCH
ACCEL 4X
33
NOTE: COPY OF OSCILLOGRAPH TRACE
FREQ HERTZ
38 36 34 32 30 28 26 24 22 20 19 17

FIGURE 25

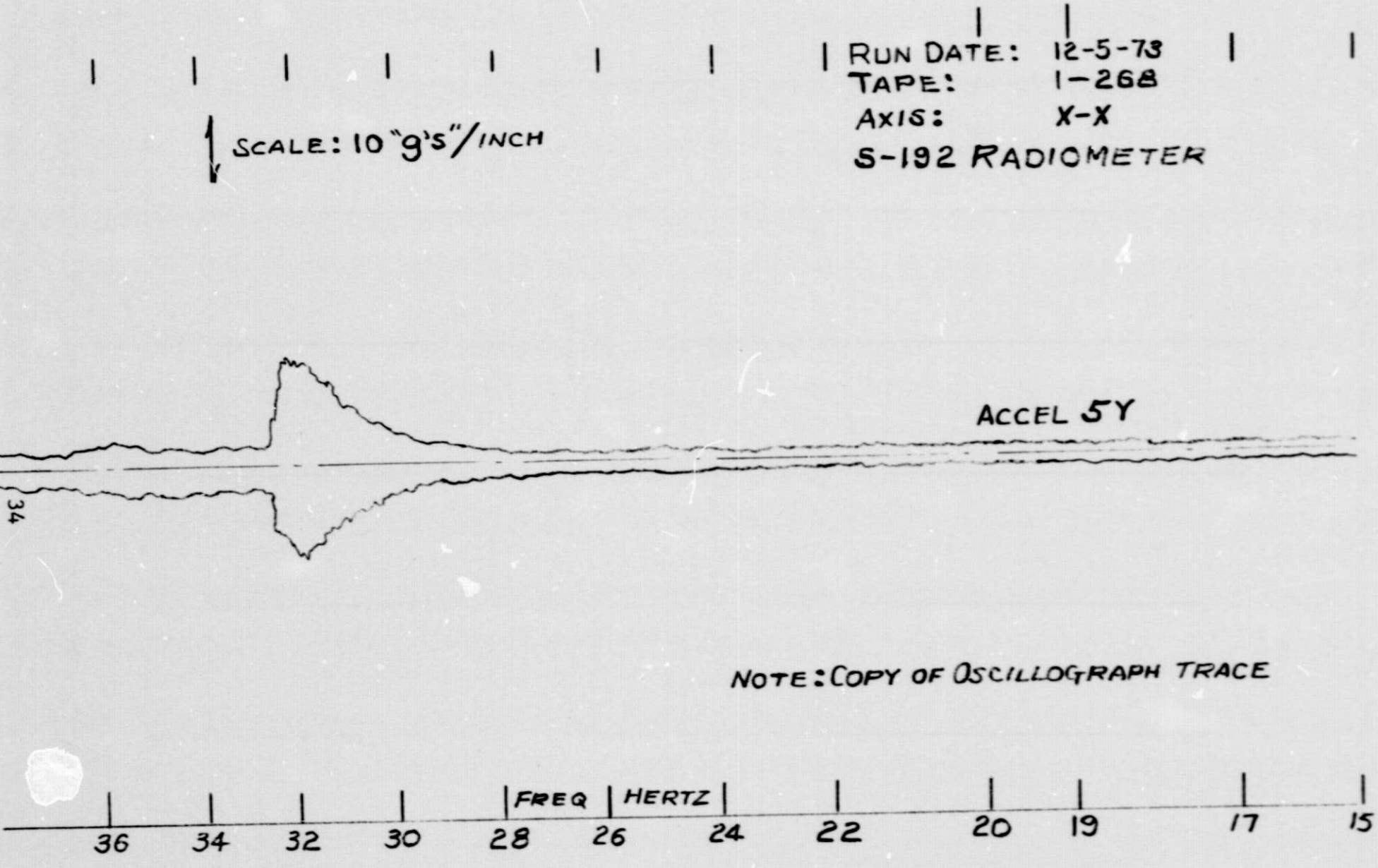
RUN DATE: 12-5-73
TAPE: 1-268
AXIS: X-X
S-192 RADIOMETER
SCALE: 10 "g's"/INCH
ACCEL 5Y
34
NOTE: COPY OF OSCILLOGRAPH TRACE
FREQ
HERTZ
36
34
32
30
28
26
24
22
20
19
17
15

FIGURE 26

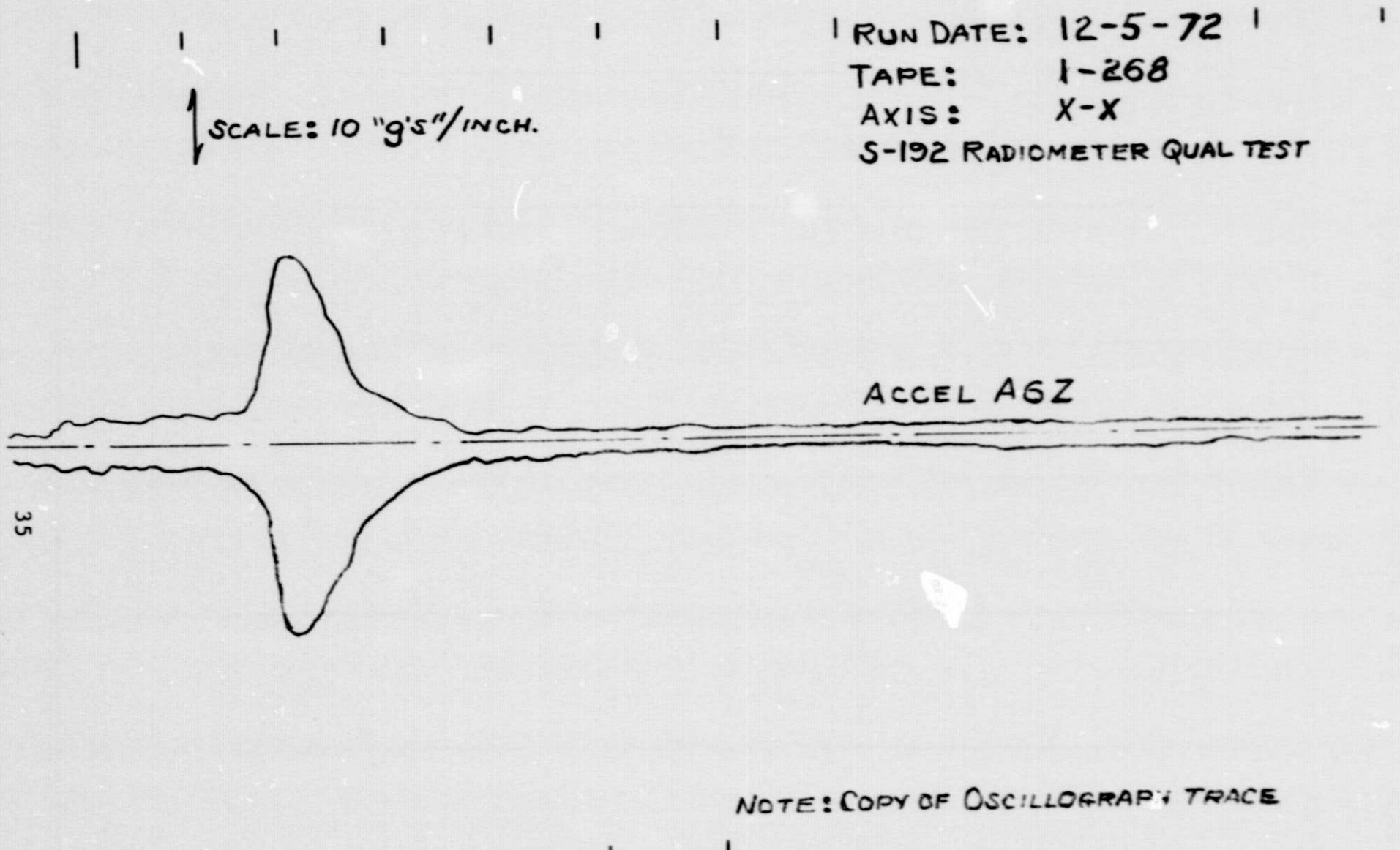
RUN DATE: 12-5-72
TAPE: 1-268
AXIS: X-X
S-192 RADIOMETER QUAL TEST
SCALE: 10 "g's"/INCH.
ACCEL A6Z
NOTE: COPY OF OSCILLOGRAPH TRACE
FREQ IN HERTZ
36
34
32
30
28
26
24
22
20
19
17
15

FIGURE -7

S-192

VIBRATION ANALYSIS · S/N 329 COOLER

RUN # 1

8-16-73

(1) MOTOR VOLTAGE = 27.49V ON LOW SPEED WINDING

(2) ACCELEROMETER LOCATED ON COOLER BODY, NEAR FLANGE.

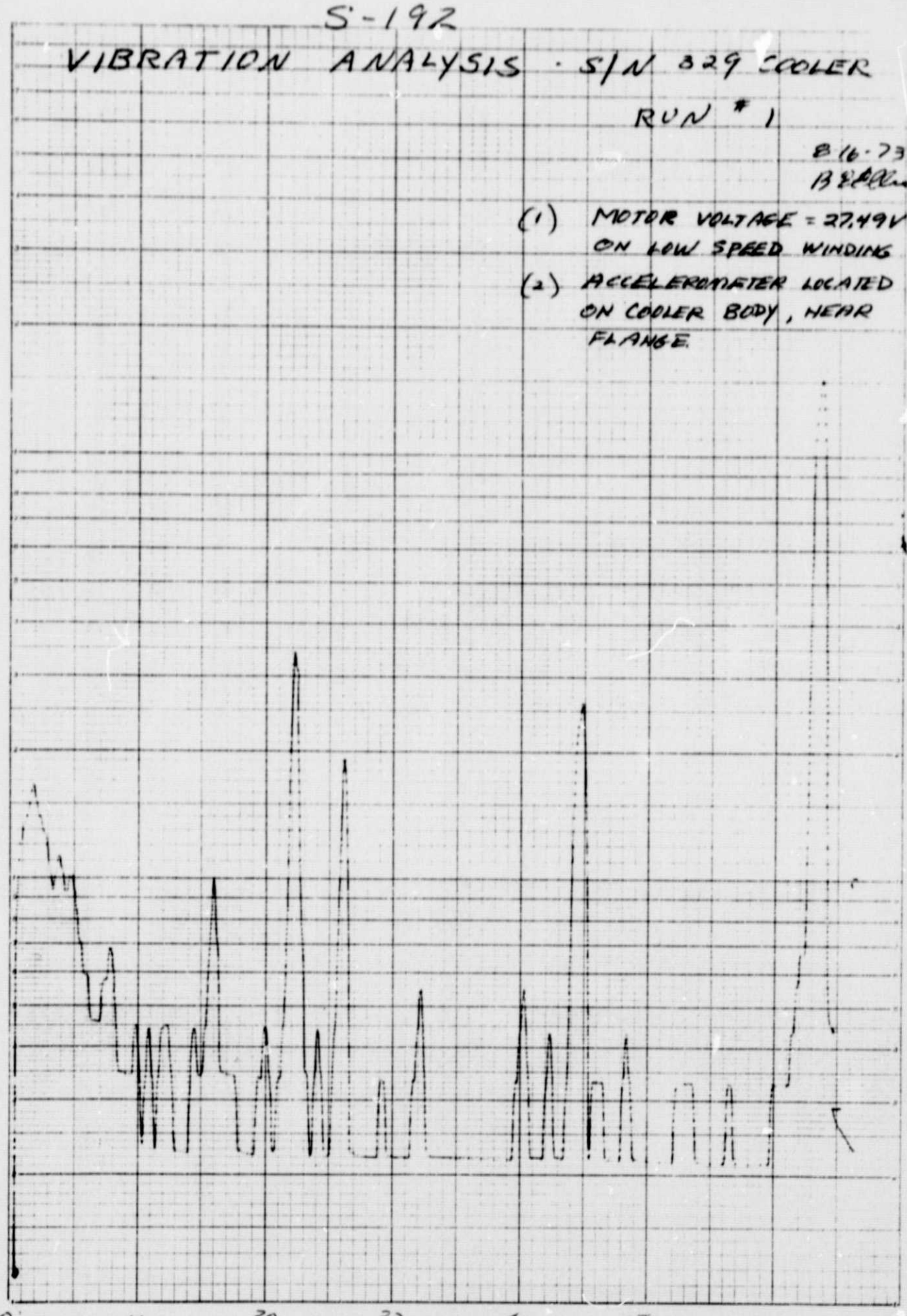

FIGURE 2

S-192

VIBRATION ANALYSIS
S/N 329 COOLER

RUN #2
8-16-73

(1) MOTOR VOLTAGE = 25.99V ON LOW SPEED WINDING.

(2) ACCELEROMETER LOCATED ON COOLER BODY NEAR FLANGE.

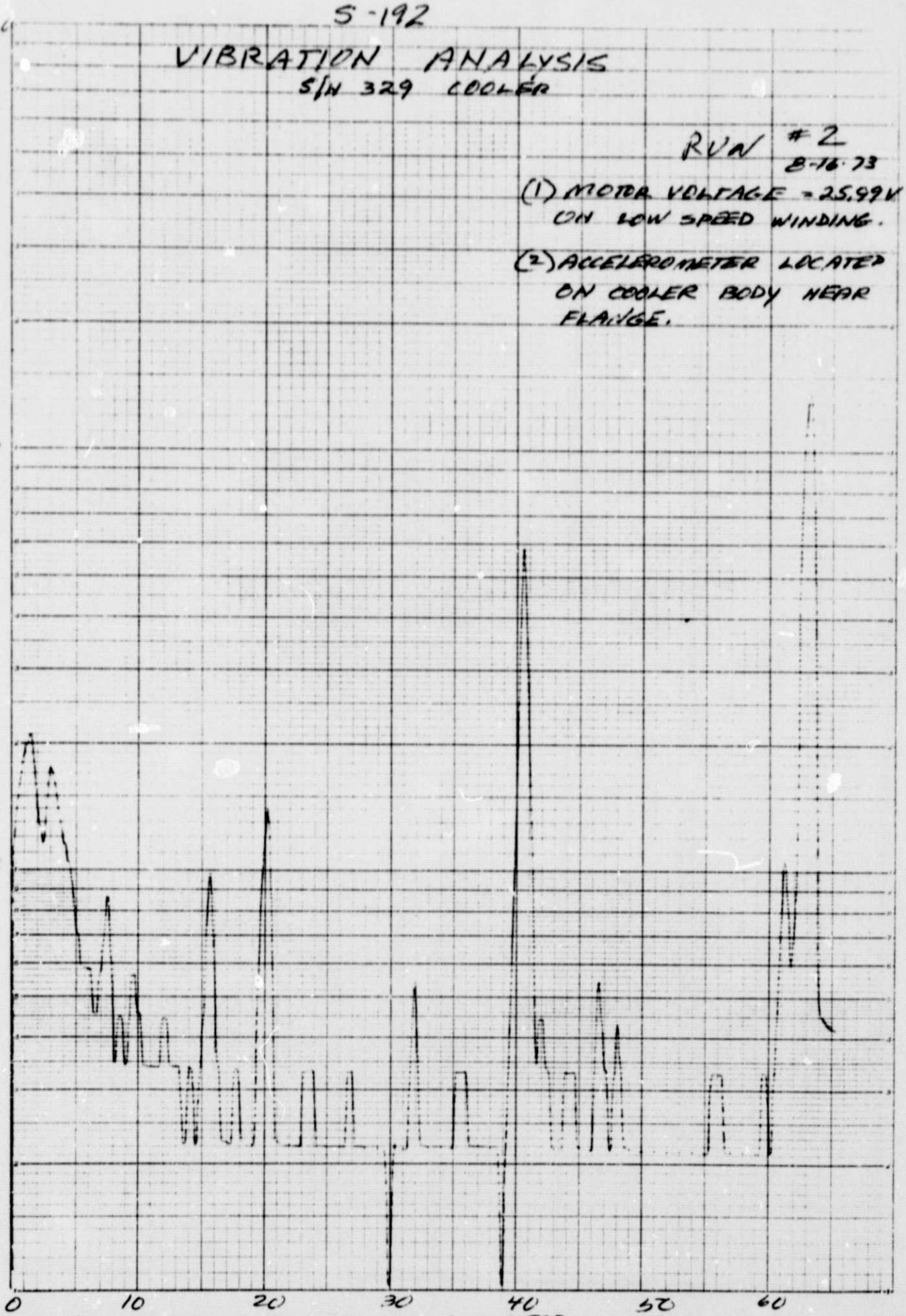

FIGURE 29

S-192

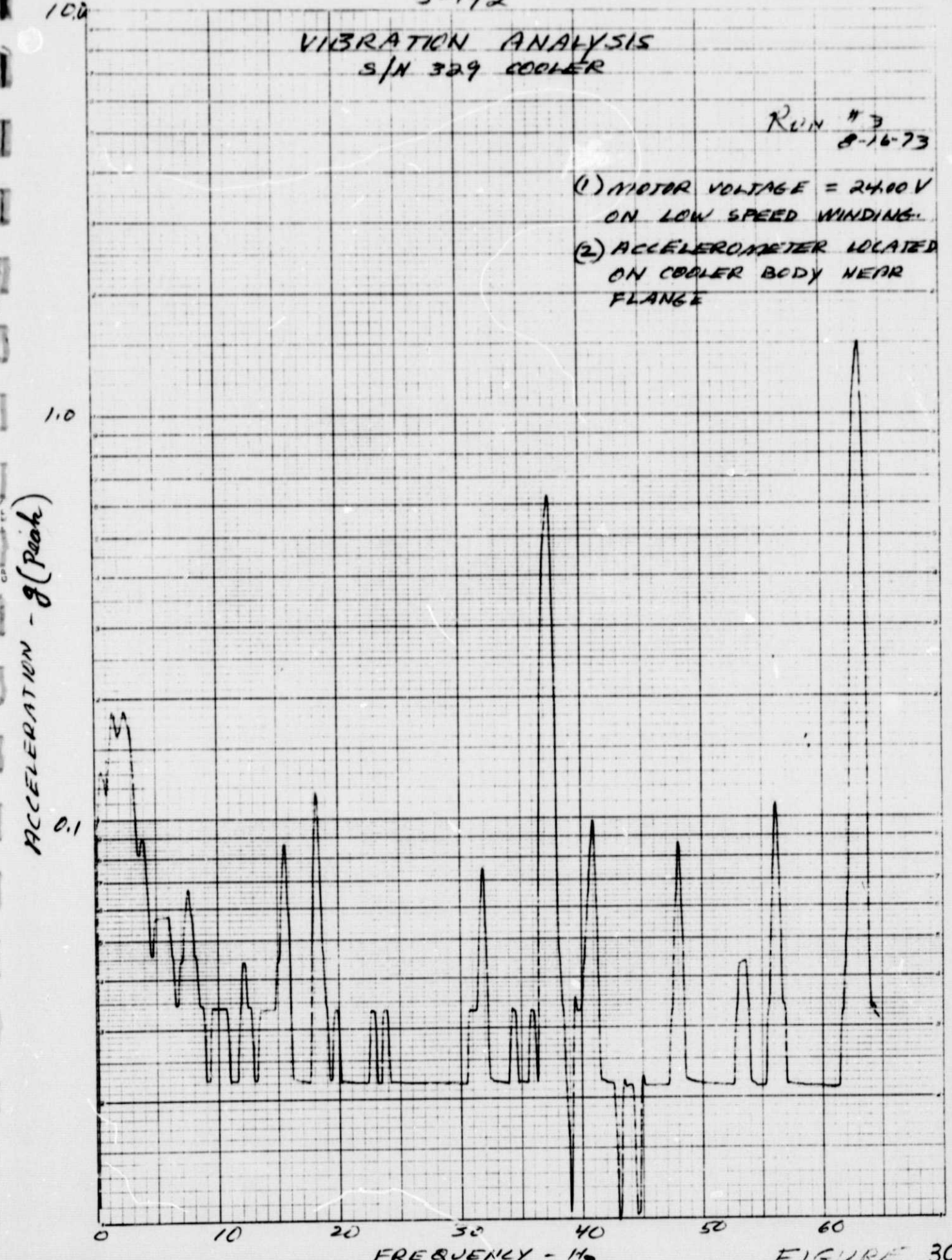

FIGURE 30

S-192

VIBRATION ANALYSIS
S/N 329 COOLER

Item 4
8-16-73
(1) MOTOR VOLTAGE = 22.00 V ON LOW SPEED WINDING
(2) ACCELEROMETER LOCATED ON COOLER BODY NEAR FLANGE.

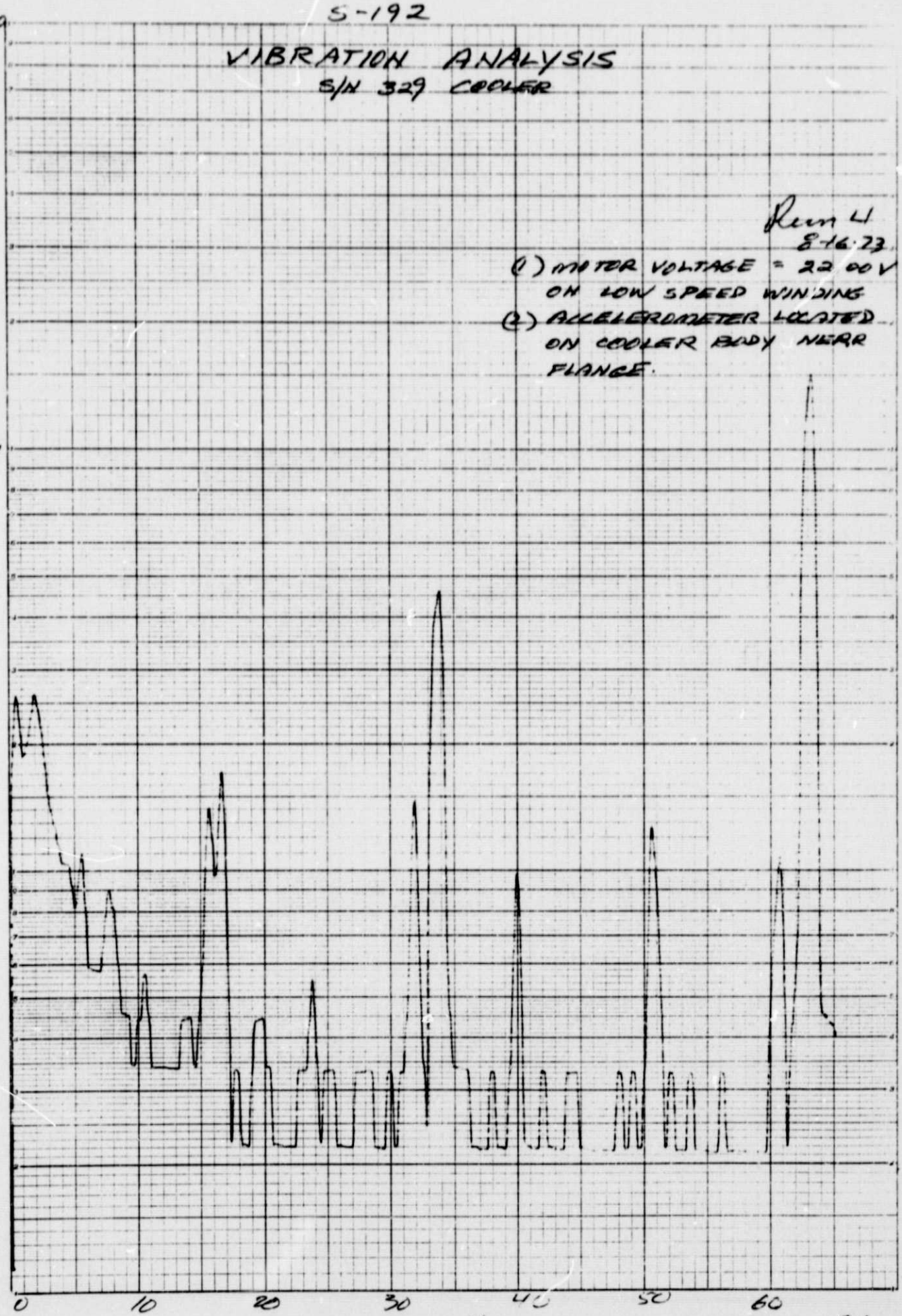

FIGURE 31

S-192

VIBRATION ANALYSIS
S/N 329 COOLER

Run #5
8-16-73
(1) MOTOR VOLTAGE = 20.00 V ON LOW SPEED WINDING.
(2) ACCELEROMETER LOCATED ON COOLER BODY NEAR FLANGE

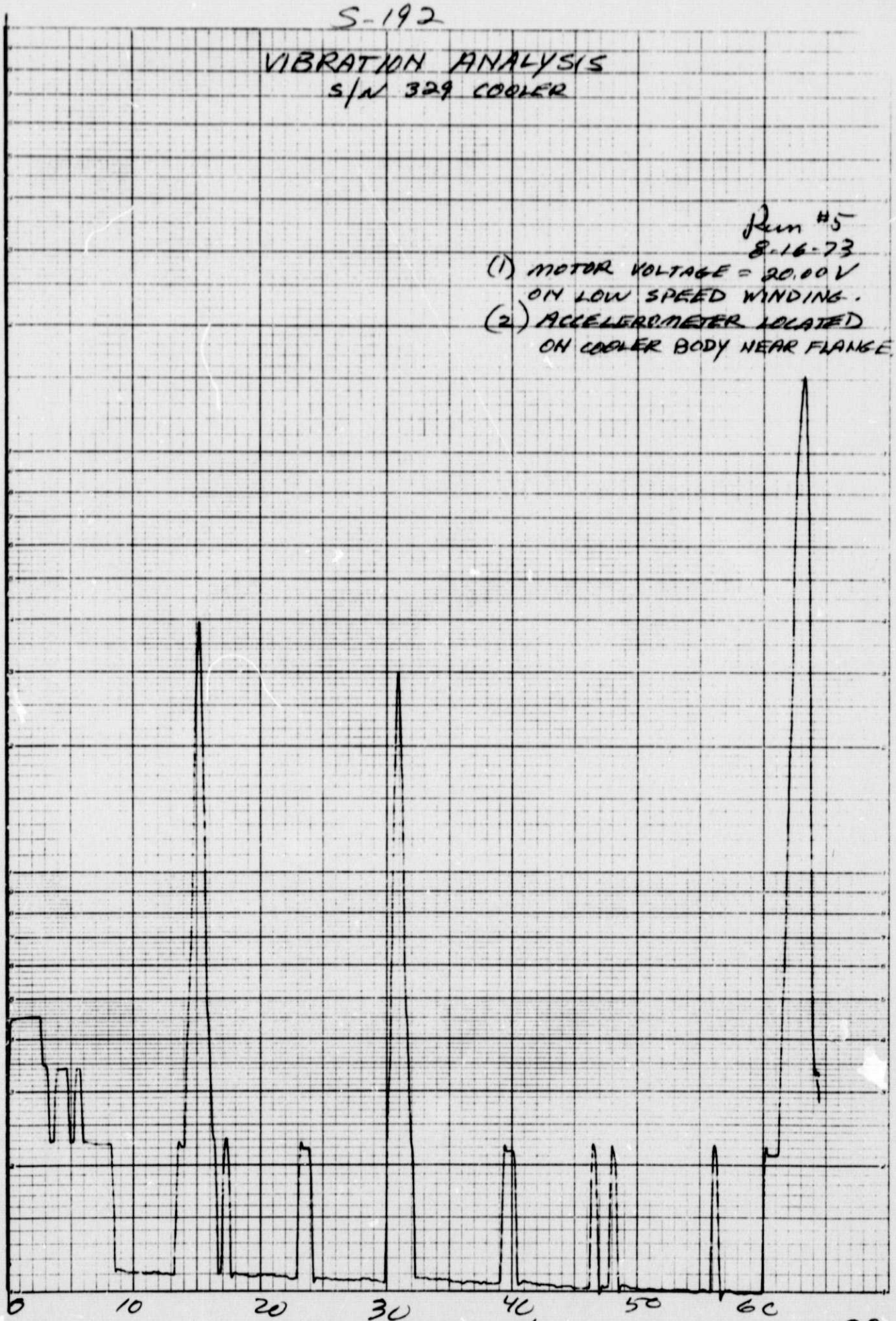

FIGURE 32

S-192

VIBRATION ANALYSIS

S/N 369 COOLER

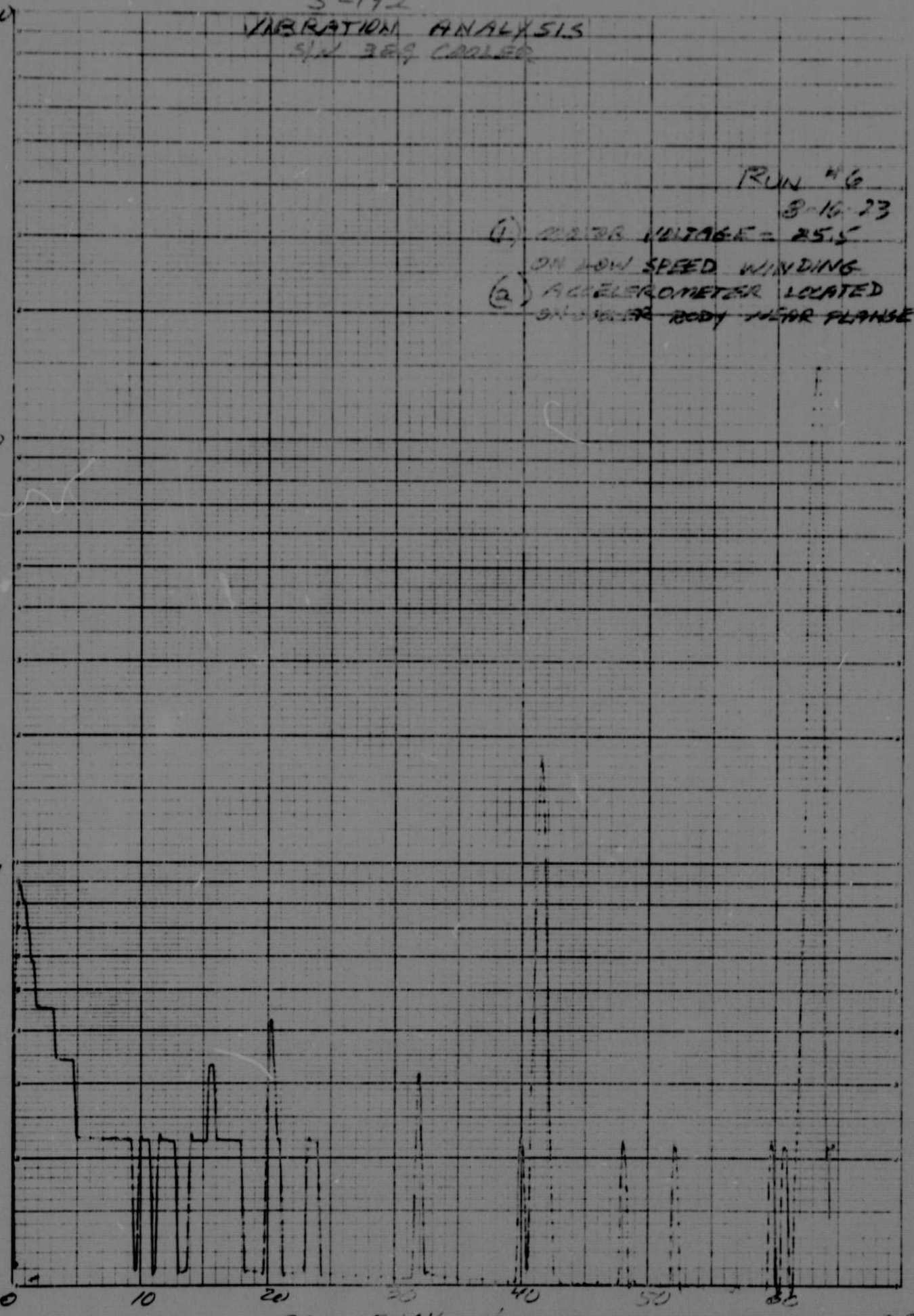

FIGURE 33

S-192

VIBRATION ANALYSIS
S/N 329 COOLER

RUN # 7
8-16-73

① MOTOR VOLTAGE = 25.37 V ON LOW SPEED WINDING,
② ACCELEROMETER LOCATED ON COLD FINGER

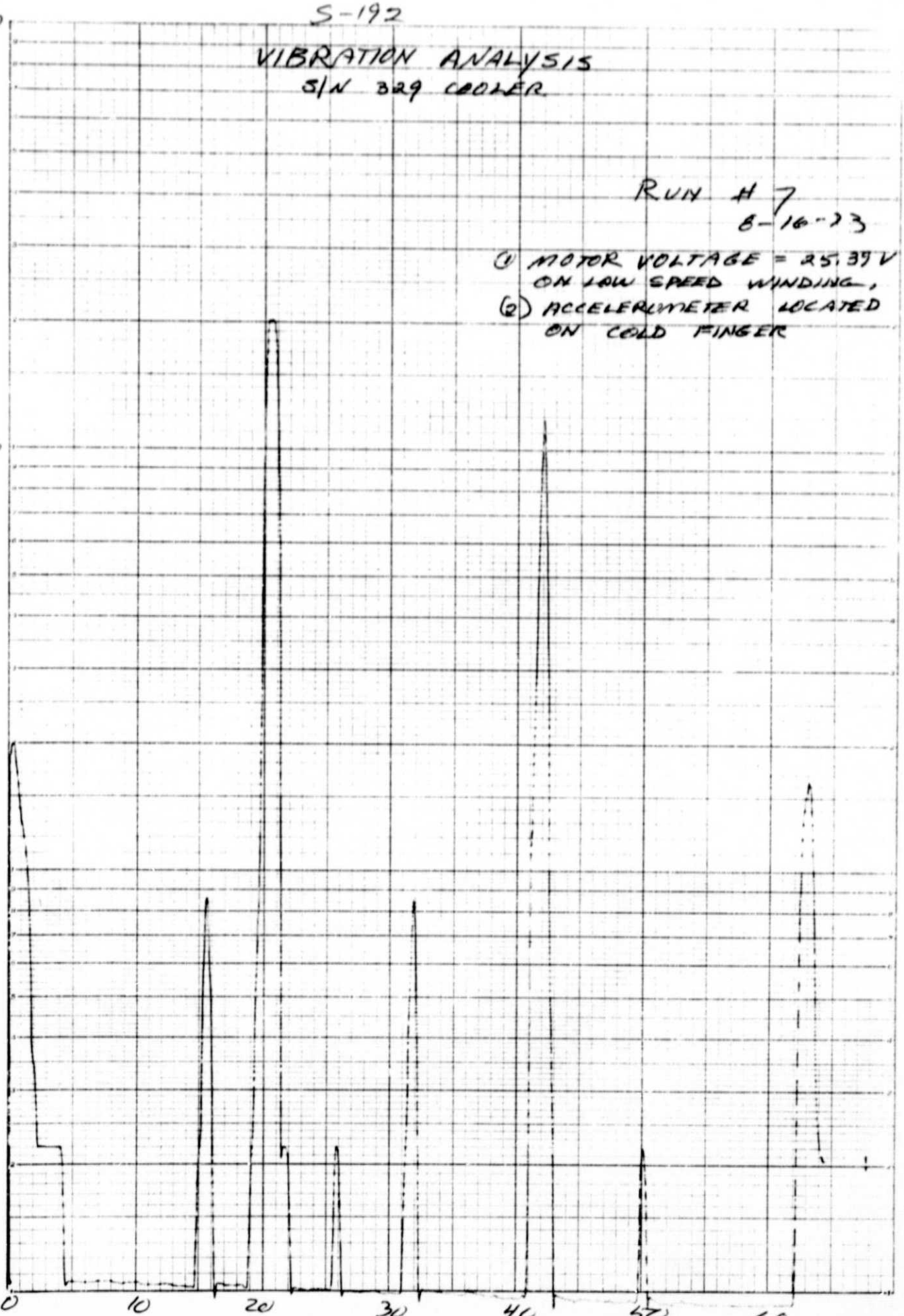

FIGURE 34

S-192

VIBRATION ANALYSIS
S/N 329 COOLER

R. Ohl + S. 8-16-73

(1) MOTOR VOLTAGE = 25.49 V ON LOW SPEED WINDING

(2) ACCELEROMETER LOCATED ON COLD FINGER

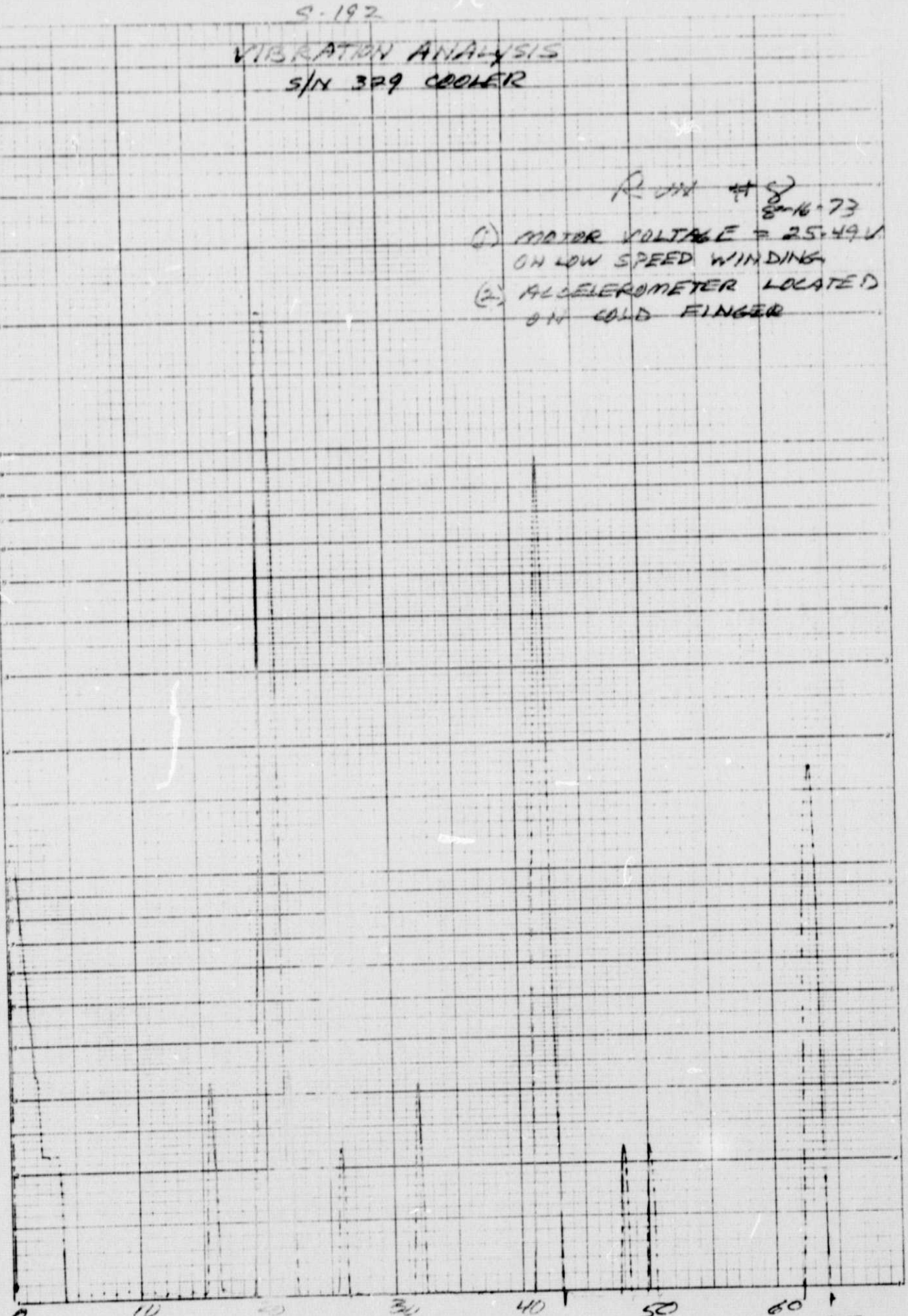

35

S-192

VIBRATION ANALYSIS
S/N 329 COOLER

RUN # 9 8.16.73

(1) MOTOR VOLTAGE = 24.00V ON LOW SPEED WINDING.

(2) ACCELEROMETER LOCATED ON COLD FINGER.

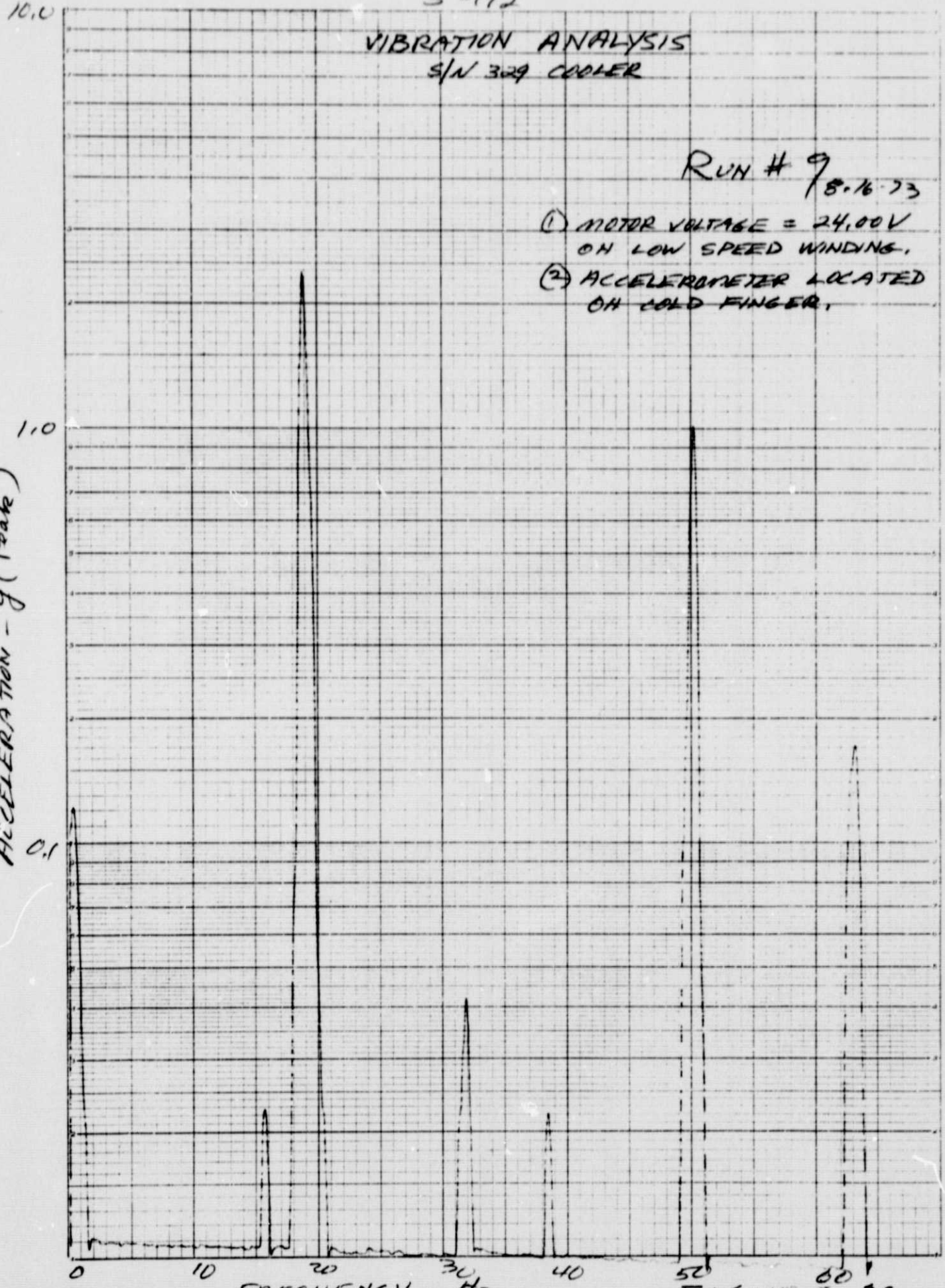

FIGURE 36

S-192

VIBRATION ANALYSIS
S/N 329 COOLER

RUN #10

(1) MOTOR VOLTAGE = 22.00 V ON LOW SPEED WINDING.

(2) ACCELEROMETER LOCATED ON COLD FINGER.

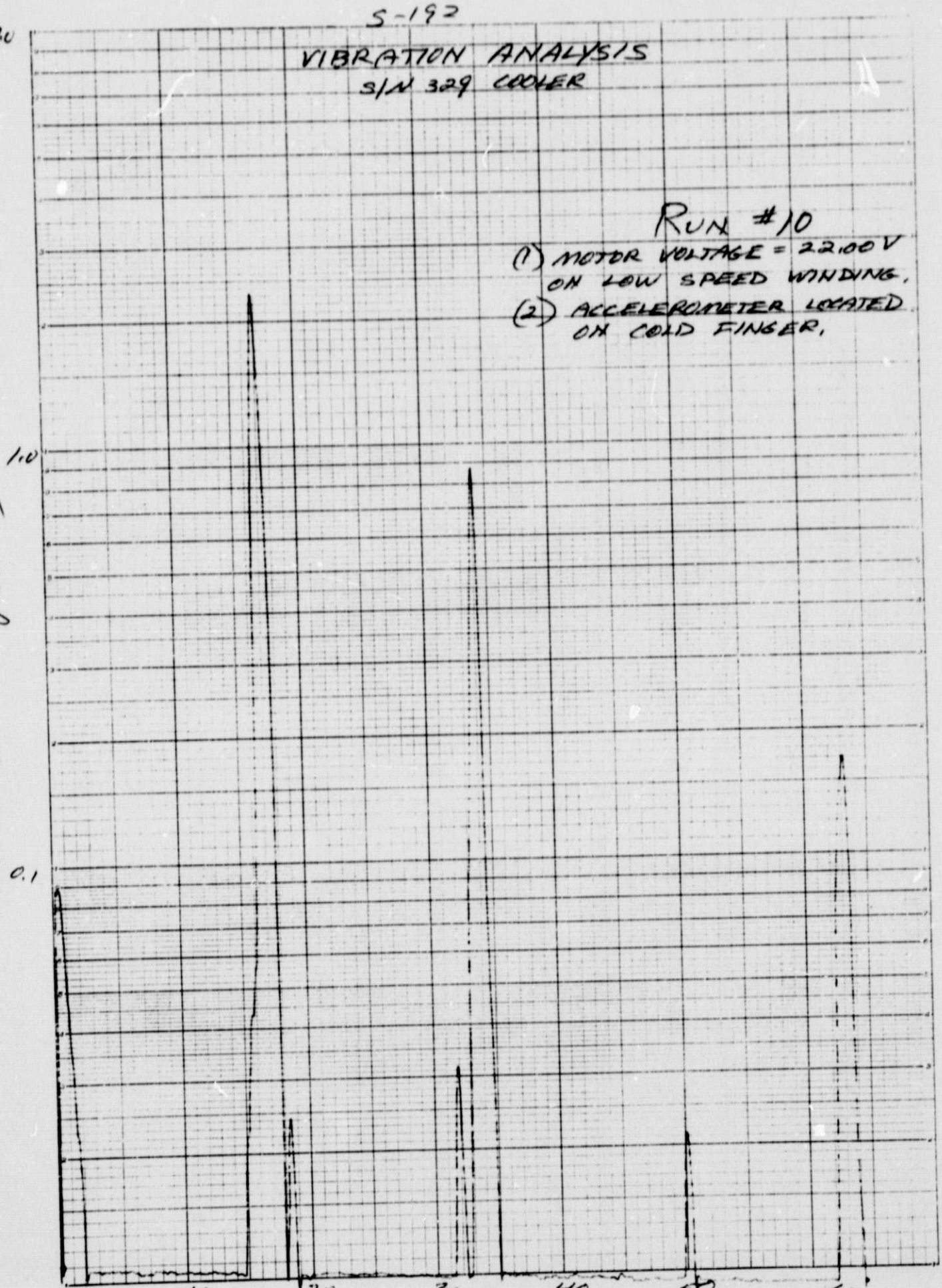

FIGURE

S-192

VIBRATION ANALYSIS
S/N 329 COOLER

Room #11 8-16-73

(1) MOTOR VOLTAGE = 20.00 V ON LOW SPEED WINDING.

(2) ACCELEROMETER LOCATED ON COLD FINGER

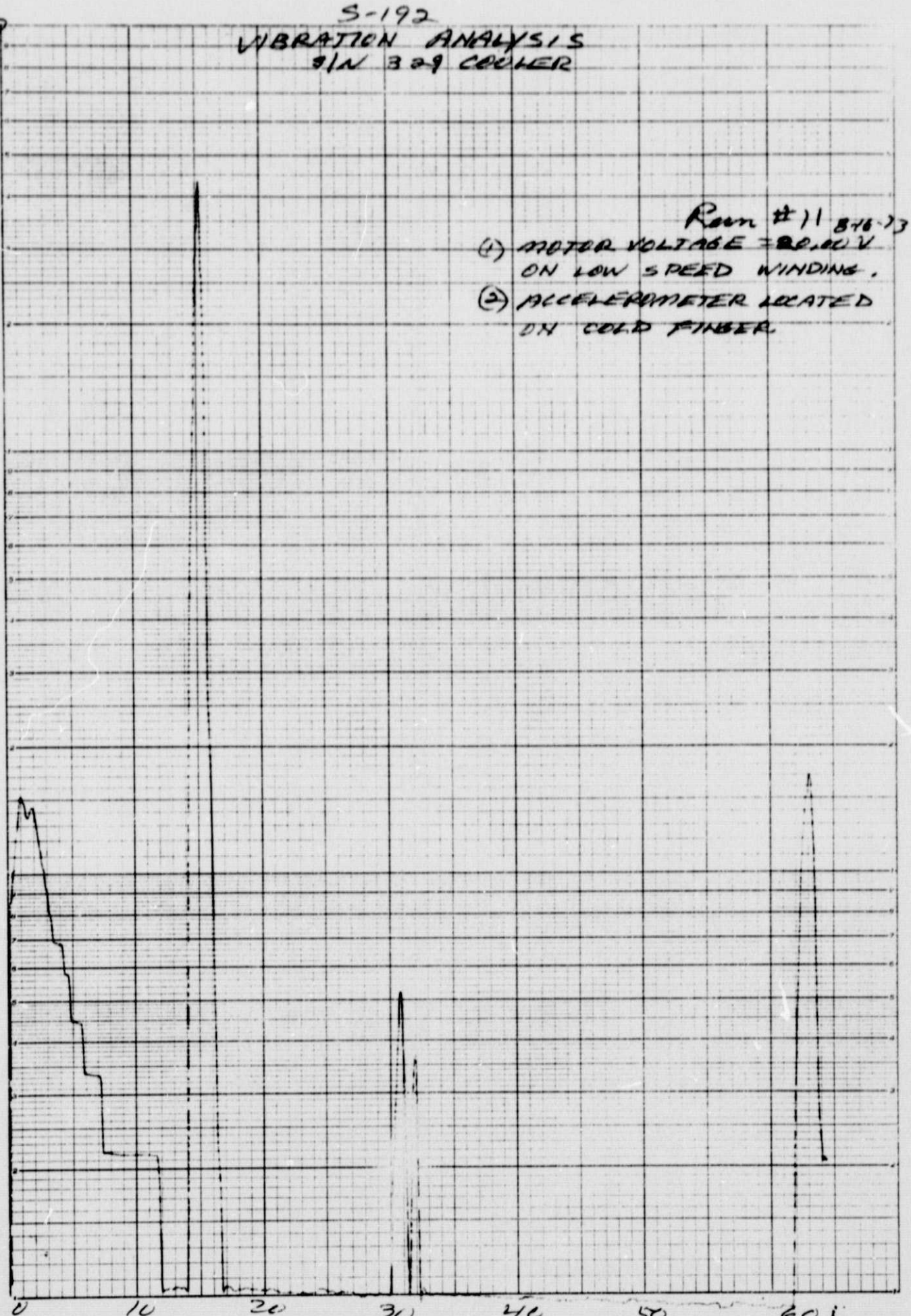

S-192

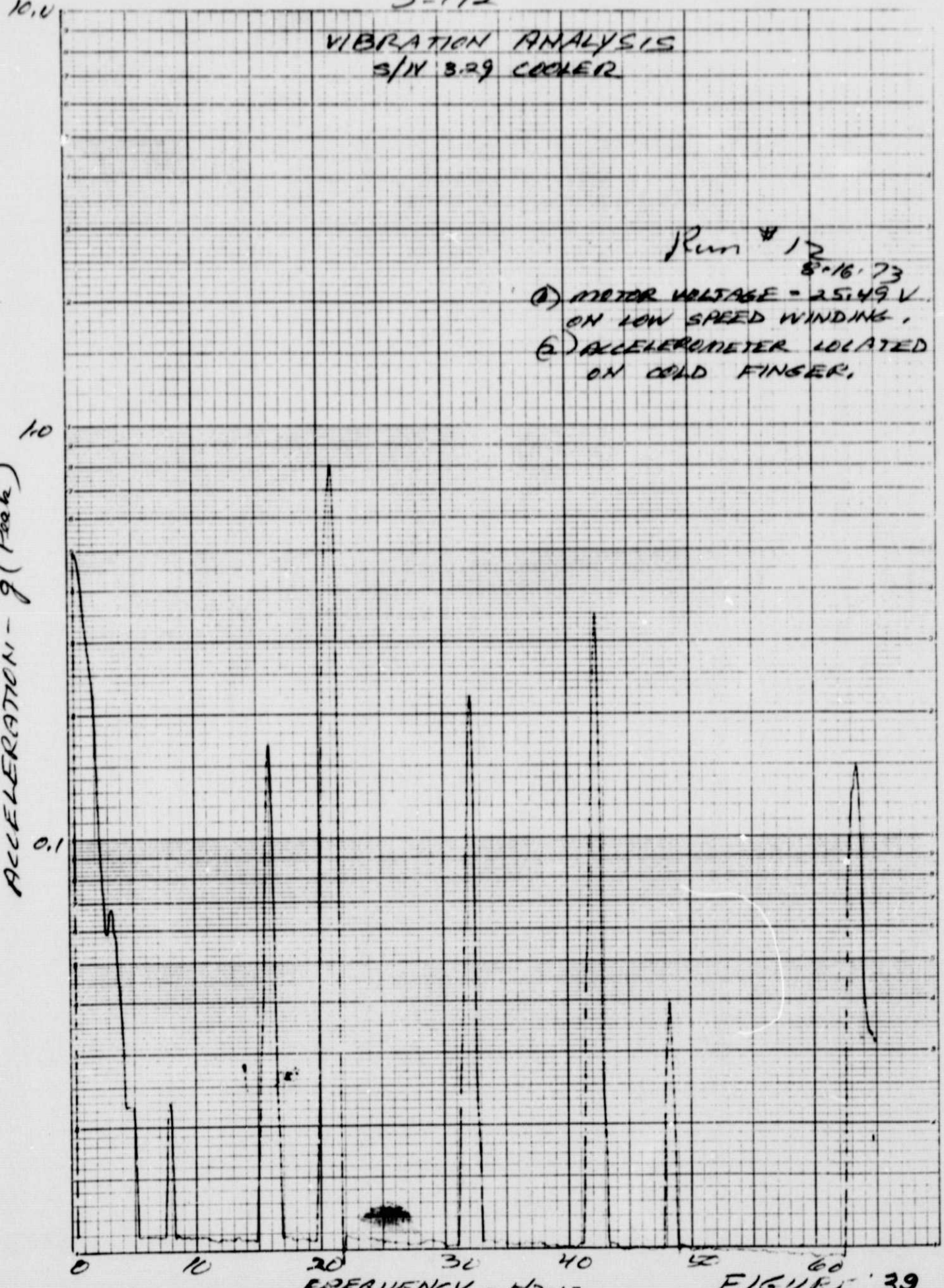

FIGURE 39

S-192

VIBRATION ANALYSIS
S/N 329 COOLER

BACKGROUND NOISE

RUN #13
BACKGROUND NOISE
8-16-73

(1) MOTOR VOLTAGE = 0.00V
(2) ACCELEROMETER LOCATED ON COLD FINGER.

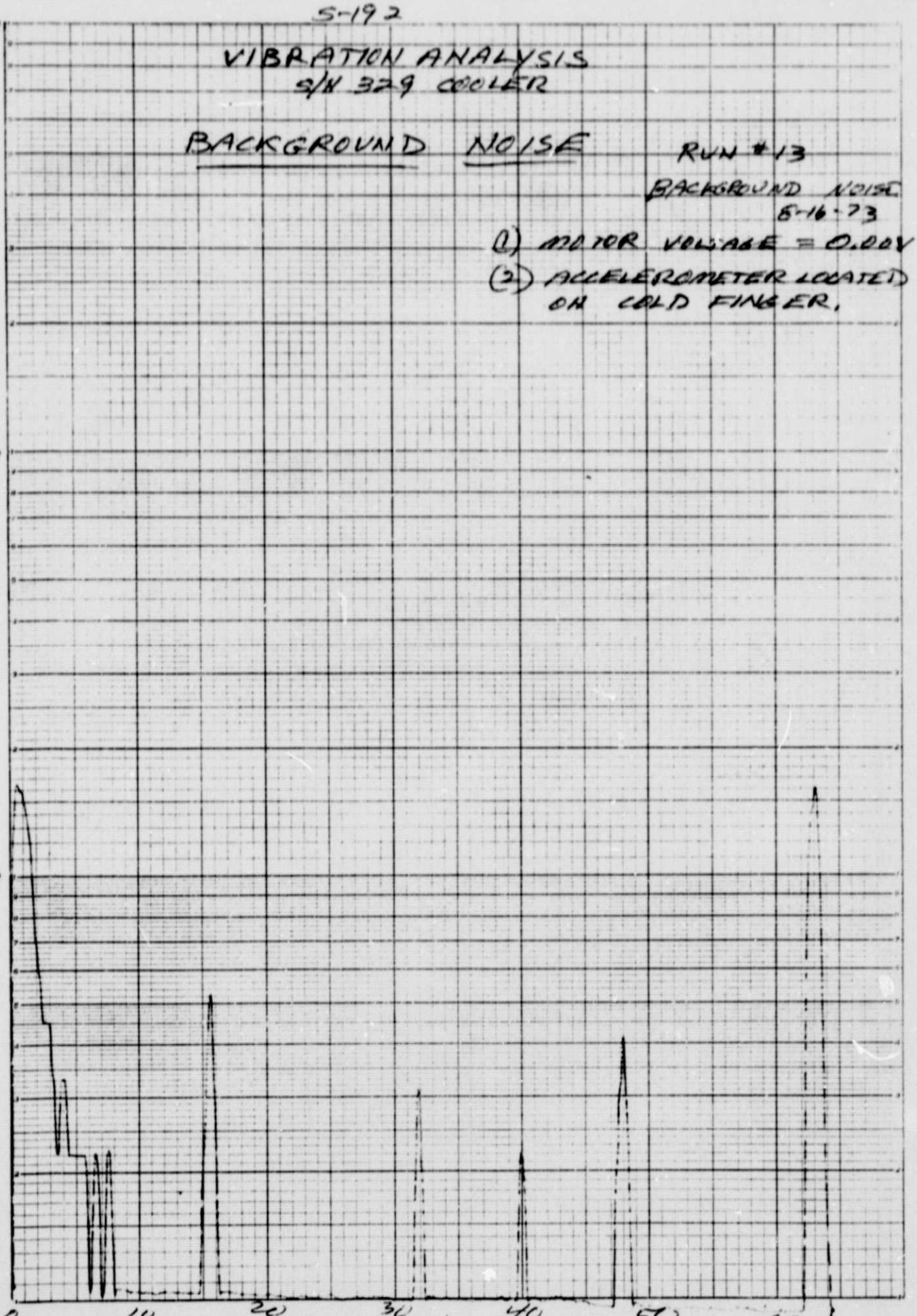

FIGURE 40

SECTION 2

ANALYSIS OF THE NATURAL FREQUENCIES OF DEWAR LEADS

Dewar wire assemblies were analyzed for natural frequencies to check if any individual wires could have low frequencies approximately within the 20-Hz range. As shown in Table II , the lowest natural frequency, 131 Hz, was the stainless steel wire. Frequencies of other wires for fixed-hinged and fixed-fixed end conditions are higher than those documented for simple support.

Assuming the glass adhesive did not hold for both the gold and copper leads and that the detached adhesive became a mass on the wire at the two attachment locations, an analysis showed the lowest possible natural frequency would be 267 Hz.

Table II

WIRE LEADS NATURAL FREQUENCIES

CALCULATED

S-192 DEWAR ASSEMBLY

SIMPLE SUPPORT

MATERIAL EACH WIRE SPAN	WIRE RADIUS INCH	WIRE SPAN INCH	FREQUENCY, HERTZ				
			f_1	f_2	f_3	f_4	f_5
GOLD	.0005	.18	985	3943	8874	15771	24655
COPPER	.0025	.34	2340	9365	21076	37459	58560
STAINLESS STEEL	.0025	1.70	131	524	1179	2095	3275
KOVAR	.005	.42	3669	14683	33046	58732	91815

SECTION 3

S-192 COOLER AND SUPPORT STRUCTURE ANALYSIS

A study of the S-192 Cooler and its supporting structure was performed to determine analytically if any detrimental exciting frequencies exist.

The Cooler itself was analyzed as a cantilever beam, fixed at its mounting flange (flange assumed to be rigid). This gives a fundamental frequency of 272 Hz.

The next area of investigation was the cooler flange. The initial analysis was made assuming the cooler to be a rigid insert acting on a simply supported flexible circular plate (diameter is that of the mounting bolt circle). This analysis shows the system to have a frequency of 192 Hz. A more refined analysis of the flange was conducted using the Stardyne Finite Element computer program. This was done to obtain a more accurate simulation of the four point support. The results of this analysis indicated a system frequency of the cooler and flange at 112 Hz.

Additional various parts of the cold tip were analyzed to determine their frequencies. The analysis indicates the cold tip to have a fundamental frequency well above 200 Hz.

As it became apparent that the cooler, its mounting flange and the cold tip assembly had relatively high frequencies, attention was focused on the aluminum adapter structure. This structure connects the cooler assembly to the optical bench. The

initial area of concern was the flange to which the cooler assembly is bolted. With all the weights of the cooler, cold tip, dewar, and electronics supported by this flange, the structure had a low frequency of 34 Hz. The results are summarized in Table III.

A tabulation of weights and mass inertias of all components connected to the adapter plate was made and were subsequently used with a computer model of the adapter plate as inputs for a frequency analysis of the adapter plate.

The plate frequency with weights and inertias applied, including the spare cooler and dewar assembly, was 25 Hz.

When the inertia of the spare assembly was removed, the frequency was slightly higher at 25.4 Hz.

The above plate frequencies were taken at approximately the center of the plate.

Table III

COOLER AND SUPPORT RESONANT FREQUENCIES

ITEM	RESONANT FREQUENCY (HERTZ)	REMARKS
1.0 Cold Finger	228	Roark's formulas for stress & strain
2.0 Head of Cold Tip-Support for Detectors	13595	Roark's
3.0 Cooler & support Flange	192	Roark's
4.0 Cooler & Support Flange	113 221 485	Finite Element Computer Program
5.0 Cooler/Dewar/Preamp Subassy & Support Flange	34	Finite Element Computer Program

STABILITY IN THE FORWARD SIGNAL PATH OF THE THERMAL CHANNEL

4.1 INTRODUCTION

Low frequency noise in the form of discrete oscillations has been observed in the S192 thermal channel output. The low frequency noise has components of 20 Hz and below. The same noise has been observed in the "span" and "zero" calibration signals of the thermal channel as well.

The thermal channel signal path was examined to determine obvious sources or causes of such oscillation. Figure 41 is a video processor math model of the signal path of the thermal channel.

The input radiance from the source or the calibration signals is transmitted through the front end optics and field stop to the detector. The electrical signal processing then falls into three separate sections consisting of (1) a preamplifier, (2) a video processor consisting of an automatic gain control circuit and a summing amplifier for the insertion of an automatic offset control signal, and (3) the output stage consisting of the digital processing electronics whose primary function is to provide A/D conversion.

Since the oscillations were noted in the span and zero calibration data, this part of the circuitry was looked at and analyzed in some detail.

We note that the agc and the offset control input signals are generated in respective feedback loops which gave rise to some suspicion that either of these loops might oscillate at low frequency. On the other hand, an oscillation might be generated due to interaction or cross-coupling between the two loops.

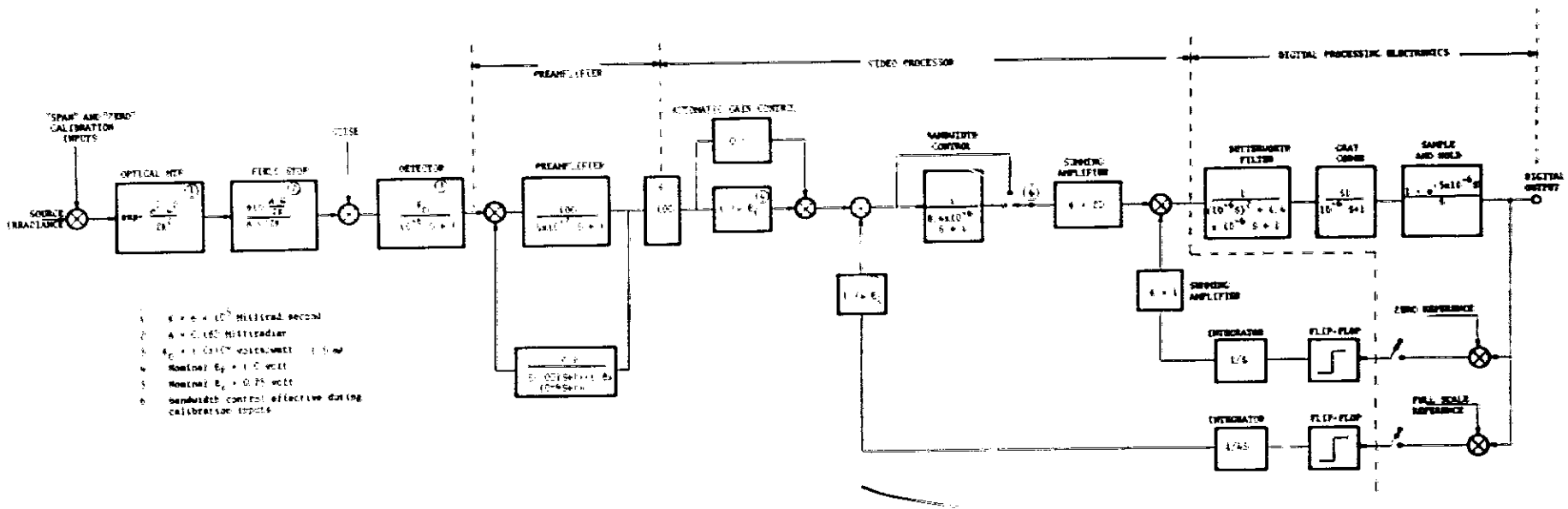

Figure 41 S192-SIGNAL PROCESSING MODEL - CHANNEL 13

We also note another feedback path in the signal path, namely, an integrator feedback around the preamplifier. Therefore, this circuit was also analyzed to determine its stability characteristics.

Other possible electrical causes of oscillation that were considered at this time in addition to those mentioned were the bias supply for the detector not shown in the block diagram and, also, the primary power supplies used in the system.

4.2 AGC AND AOC LOOPS

The agc loop was modeled in the following way. Any agc which involves variable gain introduces a system nonlinearity. The variable gain is obtained with an FET used as a variable resistor in an attenuator circuit:

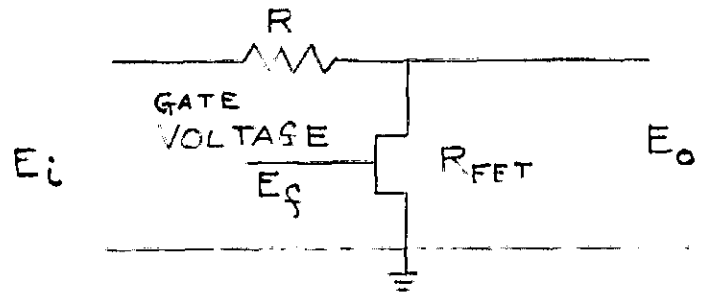

The FET resistance is controlled by the FET gate voltage. The gain as a function of R_{FET} is given by:

$$G = \frac{R_{FET}}{R_{FET} + R}$$

As can be seen, the gain is a nonlinear function of R_{FET}. Using a piece-wise linear approach, we can assume linearity about the operating point for small gain changes. A total dynamic range of at least ±6 dB can easily be achieved in the circuit.

About the operating point the gain can be represented as:

$$G = A\ E_f + b$$

and for a typical situation the constants are determined to give the following:

$$G = 1.74\ E_f - 0.5$$

Therefore, the output from the agc circuit is given by the following:

$$E_o = (1.74\ E_f - 0.5)\ E_c$$

Dynamically, the gain through the agc is given by:

$$G_1 = \left.\frac{\Delta E_o}{\Delta E_f}\right|_{E_c \text{ constant}} = 1.74\ E_c$$

$$G_2 = \left.\frac{\Delta E_o}{\Delta E_c}\right|_{E_f \text{ constant}} = 1.74\ E_f - 0.5$$

This is modeled in the following way:

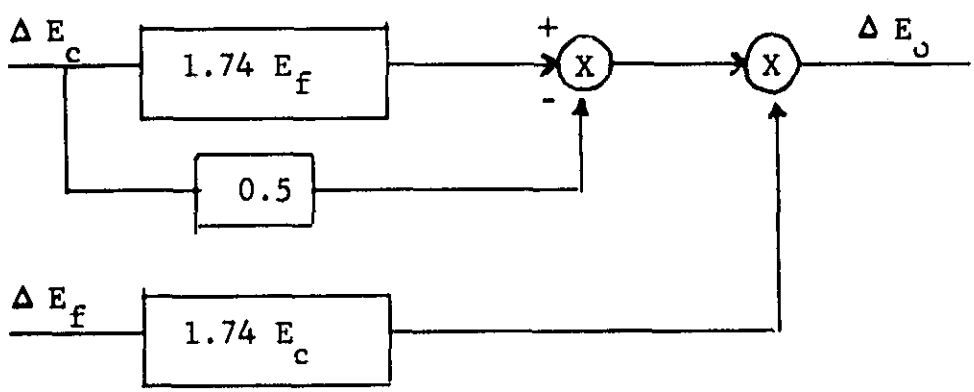

The agc and offset control (AOC) loops are now represented in Figure 42 with appropriate gain and frequency characteristics. The loops perform in the following way and under the following conditions:

The calibration sources are sampled once each scan cycle for a period of 14 IFOV's or 72 microseconds out of 0.01 second. The sampling is indicated by the switches in the input lines to the loops to indicate the sequential nature of the sampling, plus the switches shown schematically prior to the flip-flops to indicate that the loops are only closed for a very short time. Essentially then, the cal sources are sampled and compared to a reference input to determine the span and zero errors and the loops are then open. The polarity of the error signal then enables the flip-flop to introduce a fixed voltage input to the integrators. The integrators continue to integrate the error signal to bring about respective changes at the summing points to reduce the error. This cycle then repeats itself every 0.01 second.

To summarize, the calibration signals are sampled and compared to the reference inputs in a matter of 72 microseconds, the polarity of the error is sensed, the loop is opened, and the integrator continues to integrate the fixed input signal in an open loop mode until the next cycle.

The open loop gain of the agc loop is 33 dB. Due to the non-linearity of the flip-flop, the gain decreases with increasing input signal, to reduce the loop gain. With effectively a single log due to the integrator and the sample and hold within the bandpass of the loop(the butterworth filter and the bandwidth control circuit not shown have breakpoints at 167 kHz and

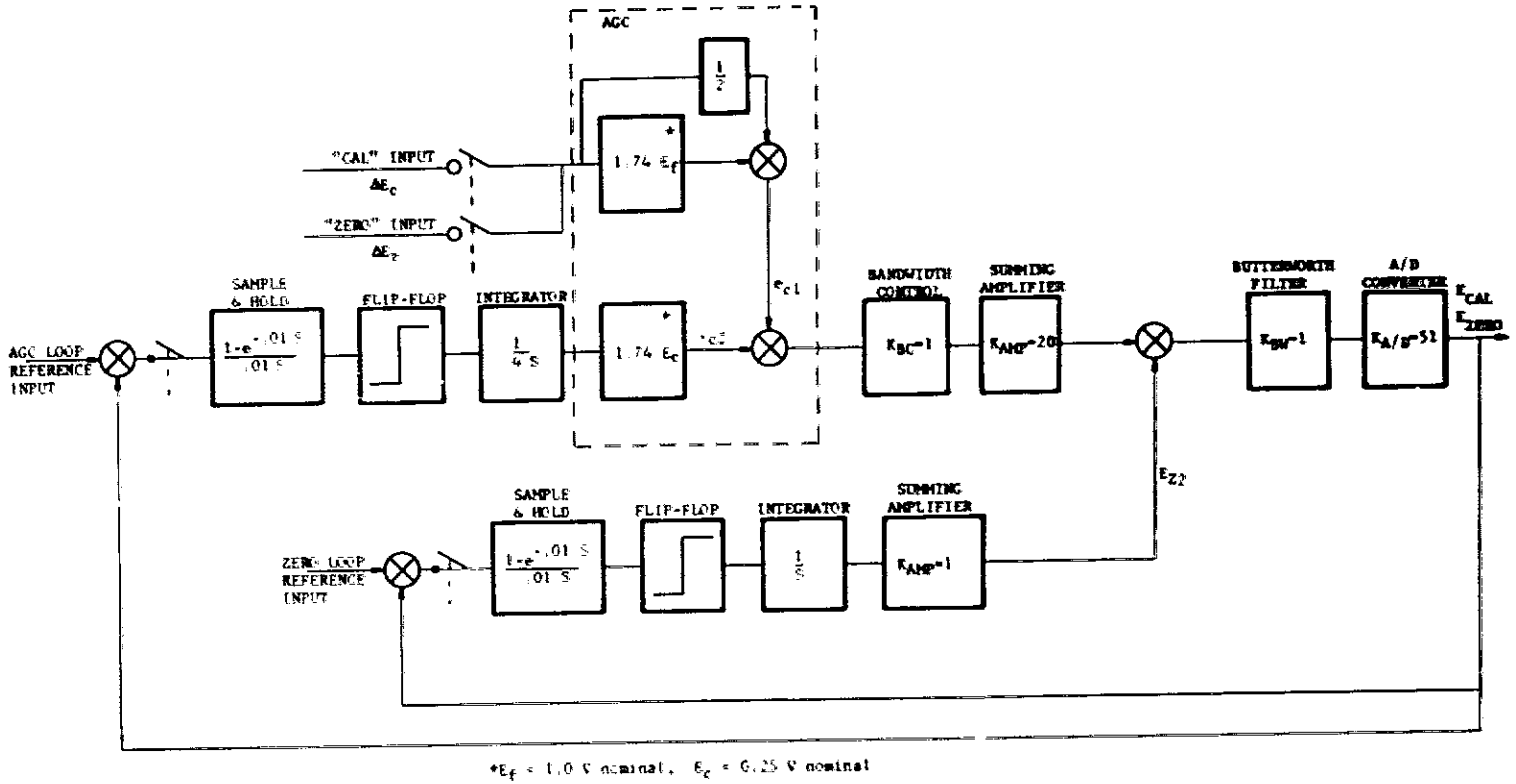

Figure 42 AGC AND AOC CONTROL LOOPS

and 20 kHz respectively), the zero crossover occurs at approximately 7 Hz with a phase of 90 degrees. With changes in the operating point of the agc which would result in lower gain and also with decreased gain through the flip-flop, the bandpass would be reduced to less than 7 Hz.

Also, the offset control loop has an open loop gain of 26 dB with a zero crossover of approximately 3 Hz and a phase angle of 104° giving a 76° phase margin.

With this kind of loop dynamics, there is more than adequate margin to prevent any low frequency oscillation.

4.3 AGC AND AOC CROSS COUPLING

There is another aspect to the agc and AOC loops that has to be considered with regard to stability. That is the possibility of cross-coupling in a manner to give rise to a low frequency oscillation.

The transient response of the output of the A/D converter was determined for effectively simultaneous step changes to the span and zero input signals. Any periodic interaction between the two loops whose period would be determined by the time constants within the loops would show up as an instability at the output.

From the block diagram of Figure 42, the output of the A/D converter is related to the calibration input by:

$$E_{CAL} = K_{A/D} K_{AMP} (e_{c1} - e_{c2}) - K_{A/D} E_{z2}$$

where $e_{c1} = (1.74 E_f - 0.5) \Delta E_c = A(\Delta E_c)$

$e_{c2} = 1/4 (1.74 E_c) 0.2t = Bt$

E_{CAL} = deviation from the full scale reference input

and is related to the "zero" input by:

$$E_{ZERO} = K_{A/D} [K_{AMP} e_{c1} - E_{z2}]$$

where $e_{c1} = (1.74 E_f - 0.5) \Delta E_z = A(\Delta E_z)$

$E_{z2} = 0.2t$

E_{ZERO} = deviation from the zero reference input

We note that E_{CAL} is a function E_{z2}, the output of the zero loop integrator. This gives rise to a cross coupling into the agc loop. On the other hand, we note that there is no cross coupling term from the agc loop into the zero control loop. The output response of the agc loop to a step change ΔE_c is given by:

$$E_{CAL} = K_{A/D} \left\{K_{AMP} [A(\Delta E_c) - B_m \Delta t] - 0.2n\Delta t\right\}$$

where m = number of scan cycles of the agc loop

n = number of scan cycles of the zero loop

Δt = .01 second period of one cycle.

The number of scan cycles of one loop does not need to equal the other, i.e., $m \neq n$ since one loop can achieve steady state in a shorter time than the other.

Since the zero loop couples into the agc loop, as a worse case, let's assume that $m\,\Delta t < n\,\Delta t$, i.e., the agc loop achieves gain balance before the zero loop achieves zero balance. Therefore, E_{CAL} equals zero under the condition that:

$$K_{AMP}[A(\Delta E_z) - B_m\,\Delta t] - 0.2\,m\Delta t = 0$$

Since the zero loop is not balanced, then $E_z 2$ will continue to change until:

$$K_{AMP}\,A(\Delta E_z) - 0.2\,n\Delta t = 0$$

This represents a change in $E_z{}^2$ amounting to $0.2\,(n-m)\Delta t$ which has to be compensated by the agc loop such that

$$K_{AMP}\,B(n-m)\,\Delta t = 0.2\,(n-m)\,\Delta t$$

Therefore, the effect of this cross-coupling is to extend the response time of the agc loop until the zero loop is balanced to zero.

Since the agc slew rate is faster than the zero loop slew rate, the agc loop has no problem keeping up with the zero loop.

There is no inherent instability in this performance and in the limit both outputs converge to zero deviation from the reference inputs.

Also, since there is no comparable effect in reverse, the agc can take a longer time to come to steady state than the zero loop without correspondingly affecting response time of the zero loop.

4.4 PREAMPLIFIER

The preamplifier is a dc coupled amplifier with an integrator in the feedback path. The integrator provides a low frequency cut-off or break point at 1.5 Hz in the gain frequency characteristic so that no dc is passed.

The transfer characteristics are shown below:

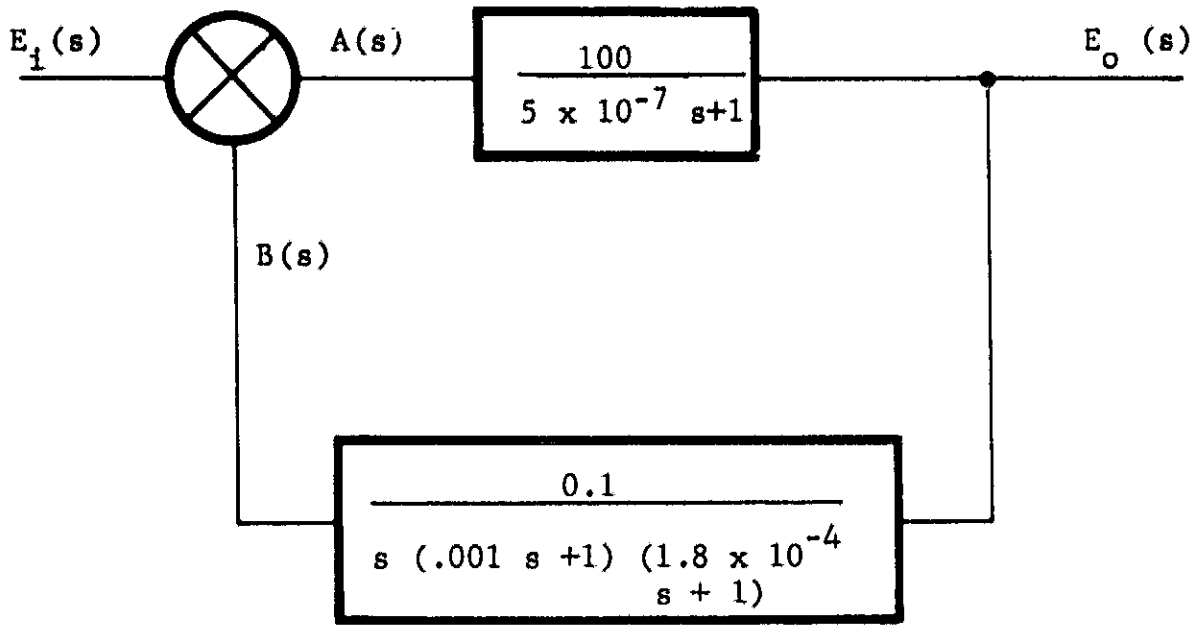

PREAMPLIFIER BLOCK DIAGRAM

The open loop transfer characteristic is given by

$$\frac{B(s)}{A(s)} = \frac{10}{S(.001\ S+1)(1.8 \times 10^{-4}\ S+1)(5 \times 10^{-7}\ S+1)}$$

The preamp has a zero dB crossover point at 1.5 hertz. With the next break at 160 Hz ($\tau = .001$ second) which is two decades removed, the phase lag at the crossover point of unity gain is 90°. This gives a phase margin of 90° and a gain margin in excess of 40 dB

for a very stable loop.

The closed loop transfer function is given by the following.

$$\frac{E_o(s)}{E_i(s)} = \frac{100\ S(1001\ S+1)\ (1.8 \times 10^{4}\ S+1)}{[S(.001\ S+1)(1.8 \times 10^{-4}\ S+1)\ (5 \times 10^{-7}\ S+1) +10]}$$

At low frequencies the terms $(1.8 \times 10^{-4}\ S+1)$ and $(5 \times 10^{-7}\ S+1)$ are effectively equal to unity. Therefore, the low frequency characteristics are given by

$$\left.\frac{E_c(s)}{E_i(s)}\right|_{Low} = \frac{100\ S(.001\ S+1)}{S(.001\ S+1) +10}$$

$$= \frac{100\ S(.001\ S+1)}{(.001\ S^2 +S +10)}$$

Factoring this reduces to

$$\left.\frac{E_o(s)}{E_i(s)}\right|_{Low} = \frac{10S}{0.1\ S+1}$$

This is plotted in Figure 43. The integrator in the feedback path makes the amplifier behave as a differentiator at low frequencies with a low frequency break point at 10 rad/s (1.6 hertz).

At high frequencies the gain of the feedback path through the integrator effectively goes to zero. Therefore, the transfer characteristic approaches that of the feed forward path with a high frequency break at $\tau = 5 \times 10^{-7}$ seconds.

The input circuit to the preamplifier is a balanced Wheatstone bridge with the thermal detector as one of the arms of the bridge. Detector bias is supplied with a precision regulator which is only used in this circuit to eliminate any crosscoupling with other circuits.

Any residual dc unbalance in the bridge is not passed by the

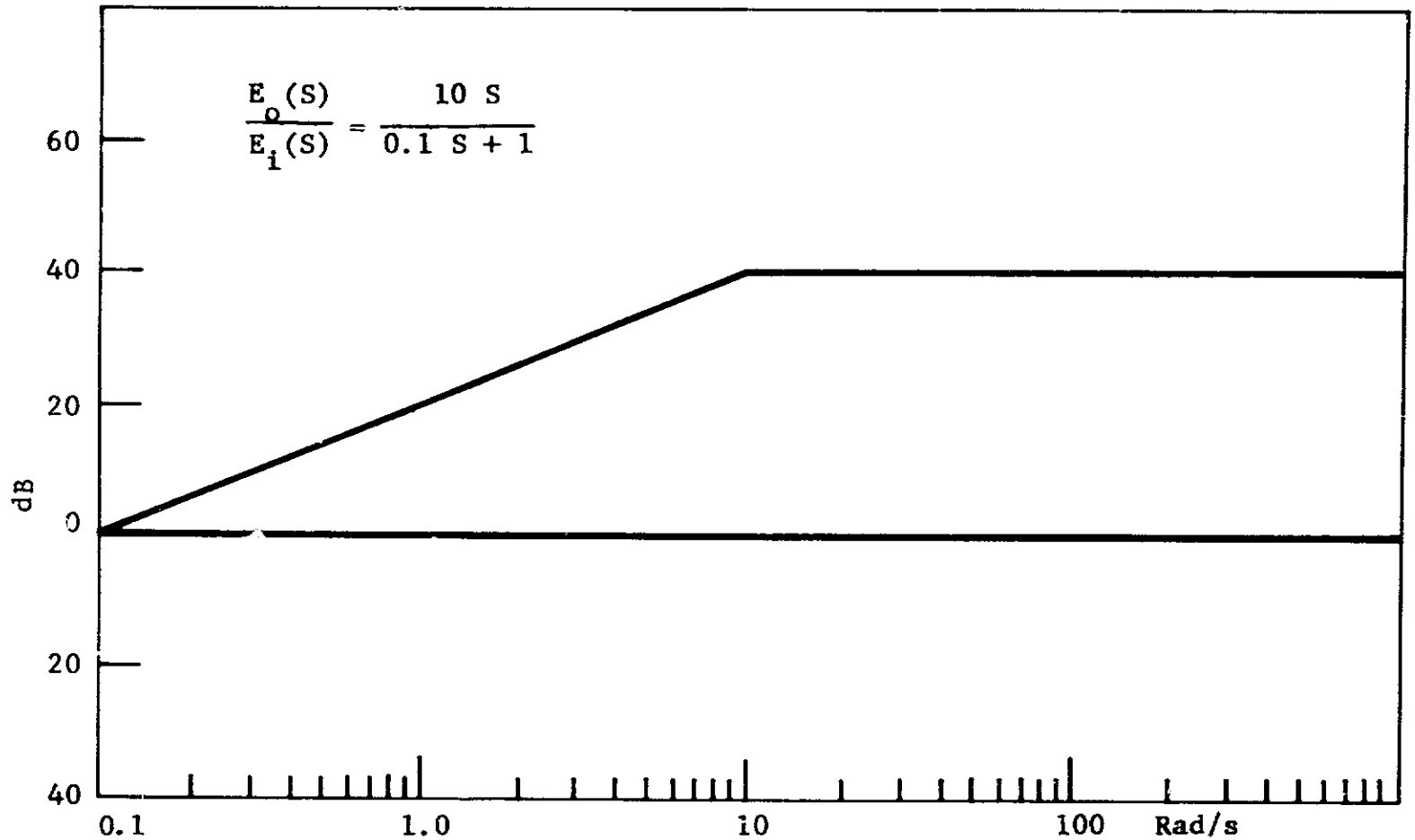

Figure 43 PREAMP-CLOSED LOOP (LOW FREQUENCY RESPONSE)

preamplifier due to the low frequency cut-off at 1.5 hertz. The integrator in the feedback path provides an equal and opposite voltage to any unbalance to reduce the input to zero.

Any drift voltages in the input circuit from whatever source will be attenuated for frequencies below 1.5 hertz. However, at frequencies above 1.5 hertz, drift voltages or other induced voltages particularly in the region of 20 hertz will be passed.

4.5 SUMMARY

There seems to be no internal source in the forward signal path of the thermal channel for low frequency oscillations of the order of 20 hertz. The possible sources were the preamplifier and the agc and the AOC circuitry because of the feedback used in the design.

The preamplifier has a low frequency cut-off at 1.5 hertz below which all signals will be attenuated and even dc offsets will be compensated to zero. Low frequency noise above 1.5 hertz, however, will be passed.

In the discussion on the agc and AOC loops, it was pointed out that both of these loops have narrow bandwidths of less than 7 hertz. Therefore, the agc and AOC cannot respond to 20 hertz noise and such noise will appear at the output of the signal path.

SECTION 5

HISTORY OF MICROPHONICS AND LOW FREQUENCY MODULATION INVESTIGATIONS

5.1 MICROPHONICS FROM COOLER OPERATION, SEPT.-OCT. 1971

The first identification of microphonically induced noise was made during cooler-dewar-preamplifier assembly testing in September, 1971. The major microphinic output appeared on the thermal channel, Band 13, when the Malaker cooler was operating at low speed. Wide band noise output of approximately 150 millivolts peak-to-peak dropped to approximately 20 millivolts pk-pk when the cooler was turned off. To further determine whether this output contribution was microphonic in origin, the assembly was shocked mechanically with detector cooled but with cooler power off, while observing output waveforms on an oscilloscope. Waveforms from mechanical shock were nearly identical to those obtained with cooler operating. The source of disturbance was, therefore, judged to be microphonic, from cooler vibration.

Outputs from Bands 1 through 12 were also measured. These all showed microphonic contributions approximately equal to the system noise with the cooler not operating (i.e., cooler detector noise). The unit tested was a complete cooler-dewar-preamplifier assembly with the 79 V detector array.

Similar results were obtained with a second cooler-dewar-preamplifier assembly (51 V array) in all above respects.

As a further check, both assemblies were subjected to a resonance search frequency analysis of thermal channel noise, Band 13, with coolers running at low speed. Microphonic peak

outputs were measured with a wave analyzer (Δf = 6 Hz). One assembly showed peak output of 5 mV at 1.33 kHz, and the other of 5 mV at 1.9 kHz. These peaks could be "tuned" in frequency by adjusting cooler motor speed, further indicating the microphonic origin. The comparable wave analyzer outputs were less than 1 mV, with cooler power off. Other noise components greater than 1 mV were noted at frequencies from 0.8 to 3 kHz. Interestingly, no low frequency components were noted (20 Hz and below).

Investigation within the dewar assemblies revealed two problems:

1) Movement of thermal channel detector leads.
2) Possible movement of Bands 1 through 12 detectors on their common mounting, due to a bonding failure.

These problems were attacked separately. The two thermal channel detector lead wires were further immobilized by adding cemented supports of insulating material near the midpoints of their spans. The mounting boards of the visible and near IR band detectors were recemented with different techniques. A subsequent retest of the 79 V Cooler-Dewar Assembly with breadboard preamplifier showed no microphonic outputs for any of the 13 bands under even more severe conditions than previously used (Cooler motor at high speed vs previous tests at low speed). No microphonic outputs were observed from mechanical shock to the cooler assembly after it had cooled the detectors, but was then turned off. The microphonics problem was considered to have been reduced below detection at this time, and system integration was resumed.

5.2 LOW FREQUENCY MODULATIONS WITHOUT COOLER OPERATION, MAY 1972

The first identifications of 0.3 to 3.5 Hz modulations of digital scientific data outputs (SDO's) were found during analyses of the magnetic tapes made during Flight Unit No. 2's first EREP system operation, the Bench Tests at MDAC-E, St. Louis, May 1972. These modulations are not necessarily microphonic in origin. Modulations were first seen on strip chart recordings (QCWS S6806, 6-1072), then investigated further with NASA/JSC power spectral density plots (PSD's). From the latter investigation came FIAR S192-8176A written 7-19-72 during the Data Review at Houston. Identified were low frequency modulations of both noise and signal at 2.5 to 3.5 Hz. Modulations were seen on 17 SDO's, none of which were thermal channel outputs. The PSD's themselves were incapable of identifying such low frequencies because of their short sample times (0.18 and 0.36 seconds in the first runs of June and early July 1972). The strip chart recordings, however, permitted frequency measurement of noise and signal over continuous periods of one to four minutes. The short time losses of synchronization in the data displays of this era did not disturb the measurements of 0.3 to 3.5 Hz modulations on dark noise and on signal.*

---

*The "loss of sync" and "illegal sync" problems attributed solely to S192 flight hardware did concern the investigators unduly, resulting in less attention given to other S192 problems. The losses of sync were primarily caused by ground station data handling difficulties. The "illegal sync" problems (injections of extra mainframe sync words in the middle of a frame) were caused by GSE auxiliary scan drive motor grounding and an encoder grounding problem in the S192 External Scanner. These corrections were not clearly demonstrated until November 1972 testing at KSC, however.

Low frequency noise components near 25 and 50 Hz were identified by PSD's for some visible and near IR bands during the Bench Test runs. These were referenced in the 19 July 1972 memo by Dr. C.L. Korb to W.E. Hensley and R. Blades, "Noise Reduction in the S192 Scanner." Figure 44 illustrates an early PSD of 0.18 seconds duration showing broad noise peaks at 30 and 50 Hz. Also prominent are noise spikes at the 94.8 Hz scan frequency and its harmonics.

The first PSD's did not show any Band 13 noise sources of the frequencies mentioned above. A later processing (31 July 1972) with a different fill technique between frame times out to 2.16 seconds did show Band 13 noise spikes at 15, 23, and 29 Hz on all three SDO's (Figure 45 for SDO 16, channel 13-2). Although these frequencies had first been suspected to be microphonically induced in Bench Tests; The Flight Primary Cooler-Dewar-Preamplifier Assembly (C-D-P Assembly) serial number 92-1069 with detector array Y3 was at this time outfitted with a Joule-Thomson gas expansion cooler. Other bands showed less prominent noise spikes at somewhat different frequencies: Band 2 at 17 Hz; Band 12 at 26 and 29 Hz (Figures 46, 47, and 48). The relative accuracy of PSD frequencies was not well established, however. Comparison with later figures from the Qualification Unit Bench Tests, September, 1973, show that PSD frequencies can be accurate to ± one Hz for the large Malaker cooler-induced noise spikes of those runs. Repetitions of runs with similar conditions show some PSD noise spikes of the same frequencies, and comparisons of double-sampled bands show very good frequency reproducibility between those PSD's from the adjacent SDO's. The relative amplitudes were very much greater in the September 1973 runs (Figures 49, 50 typical). The Malaker cooler evidently provides a large forcing function at discrete frequencies, as

Sensor - S192 SDO 3
Low Pass Filter Used .0
Norm. Std Error... .70716
Filter Bandwidths... 5.5550
Filter Start Points .0000

Time Slice (Seconds) .00001 to .18000
Standard Deviation.. 9.5124 Date Processed 05Jul77
Input Tape No.

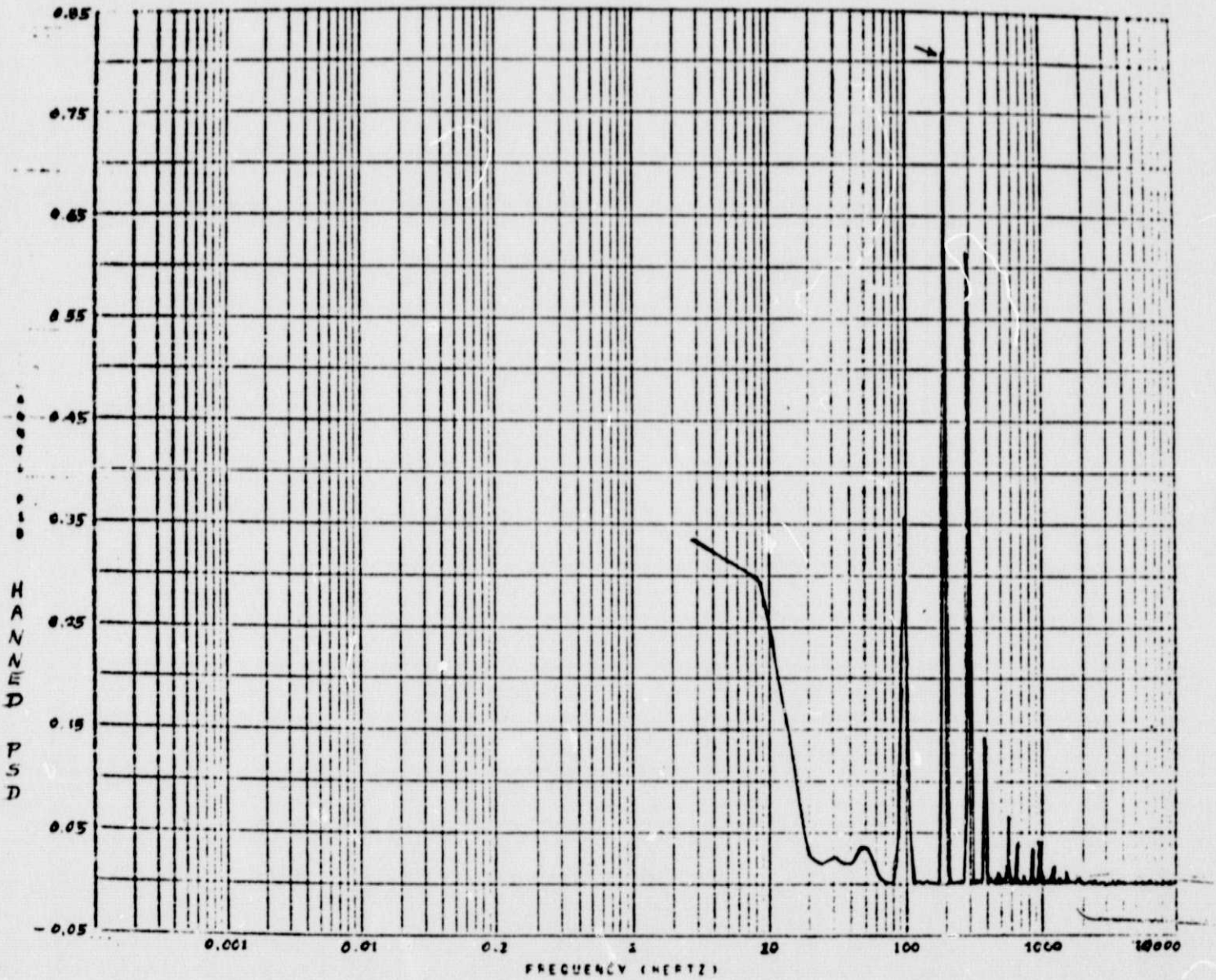

Figure 44 BAND 4 PSD FROM BENCH TESTS, MAY 1972

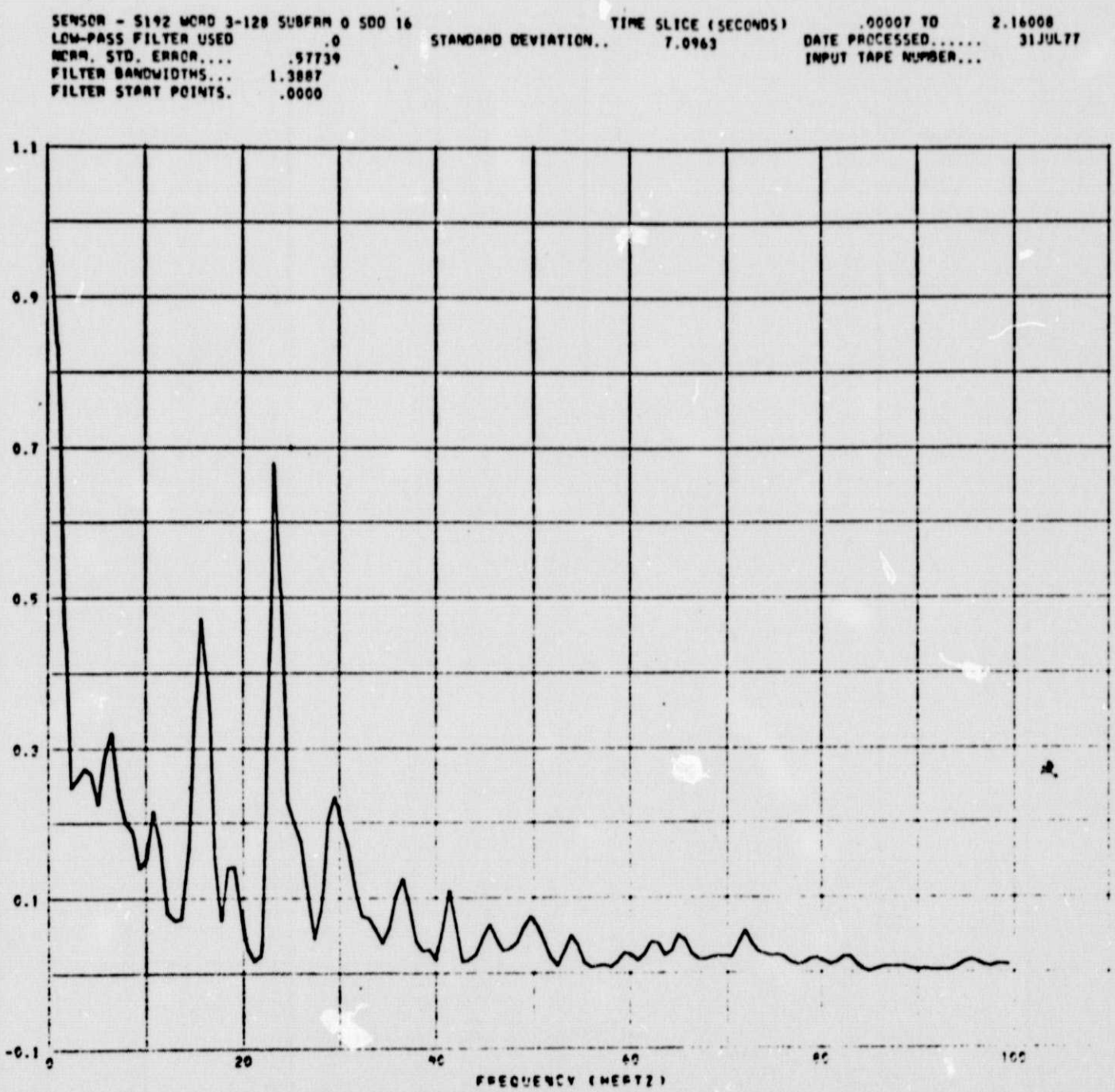

Figure 45 BAND 13 PSD FROM BENCH TESTS, MAY 1972

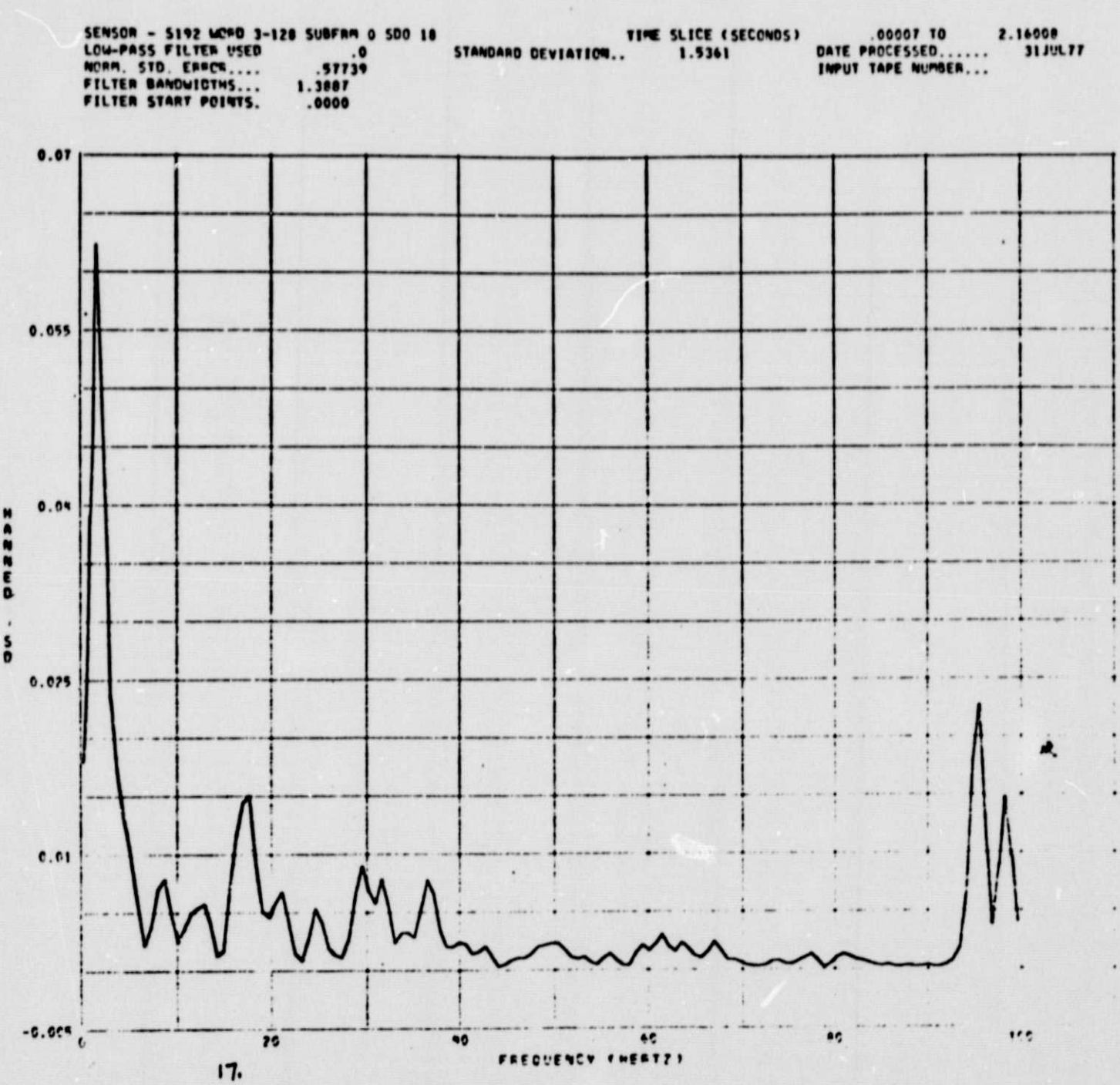

Figure 46 BAND 2 PSD FROM BENCH TESTS, MAY 1972

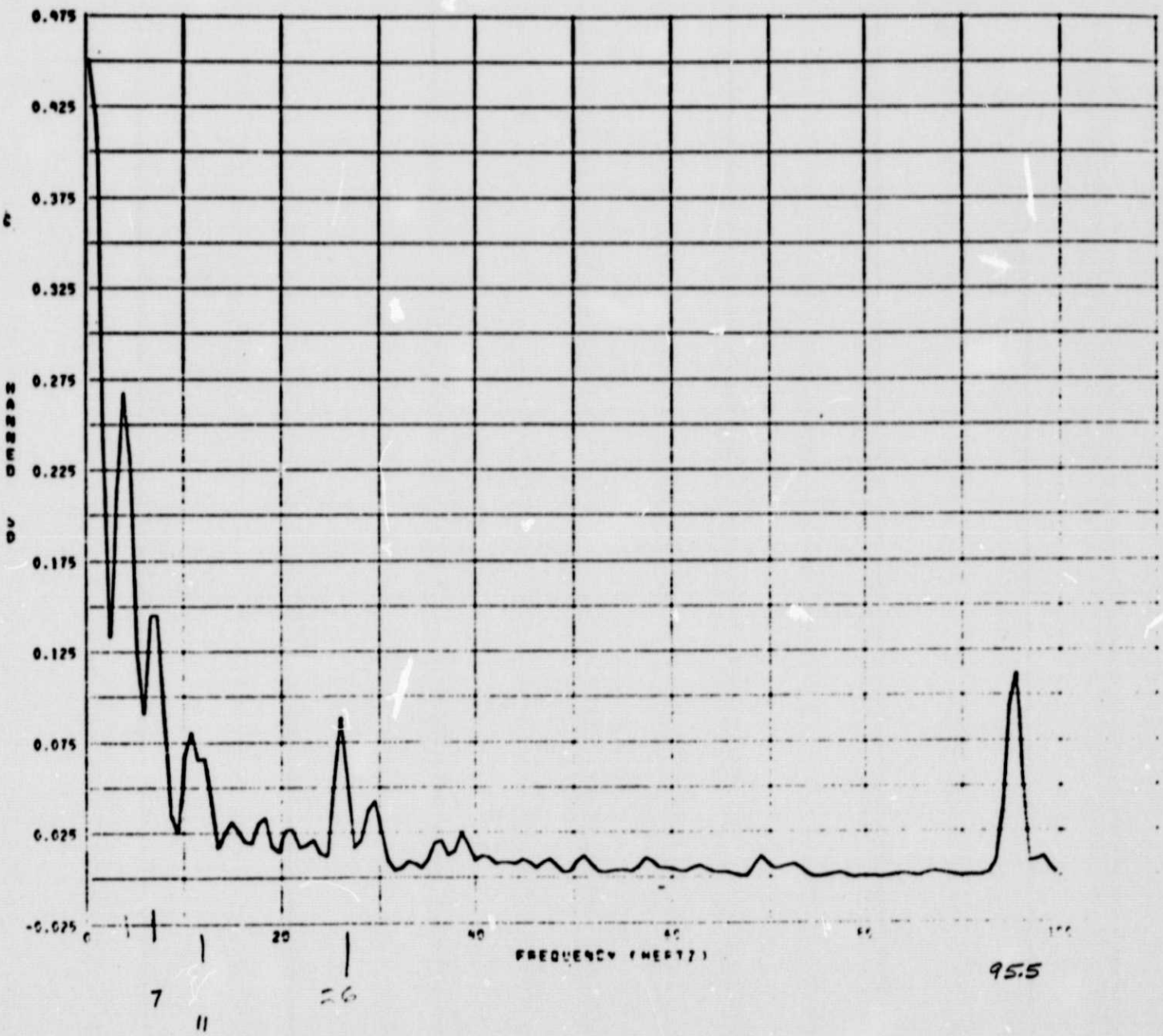

Figure 47 BAND 12 PSD FROM BENCH TESTS, MAY 1972

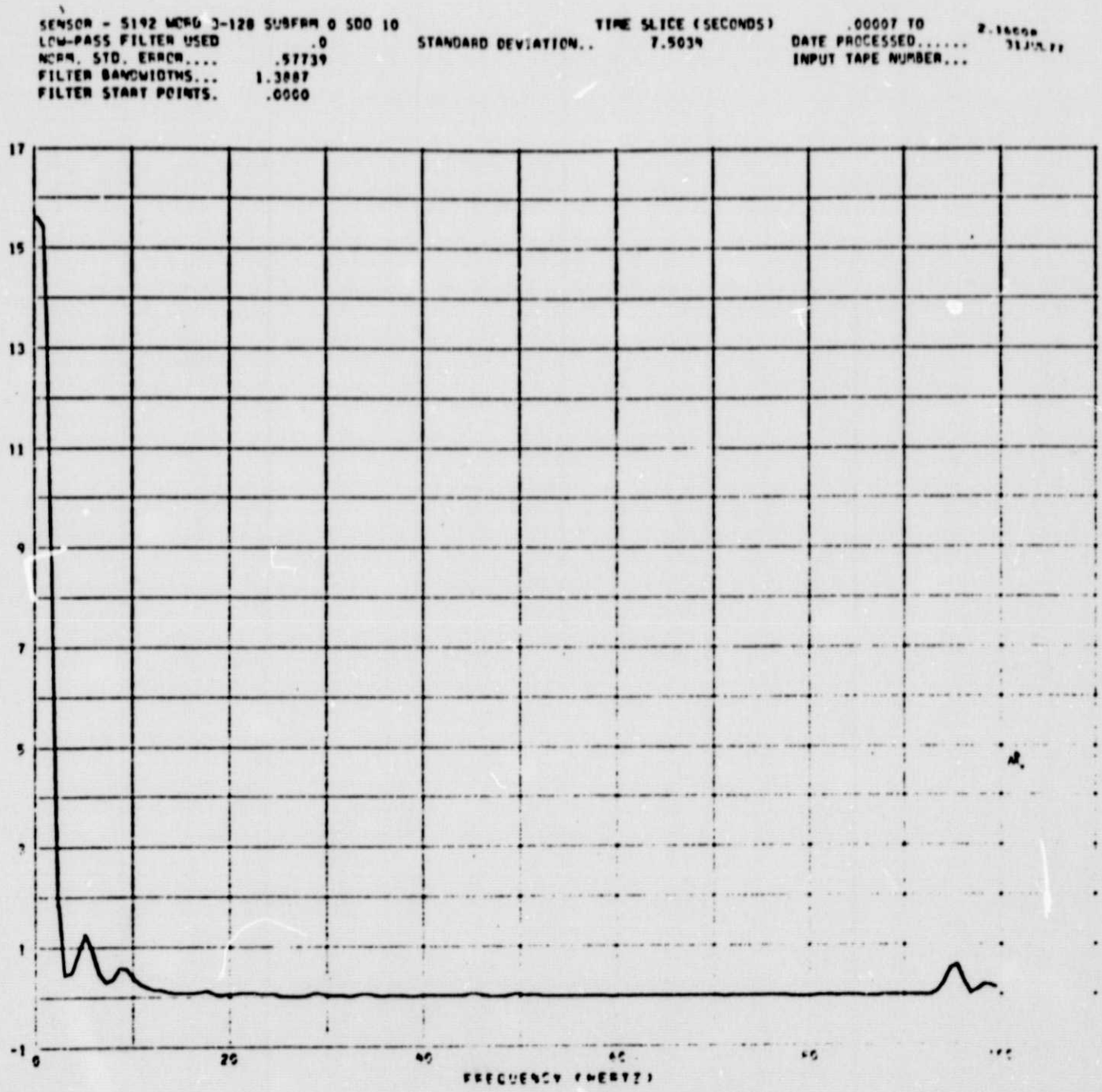

Figure 48 BAND 7 PSD FROM BENCH TESTS, MAY 1972

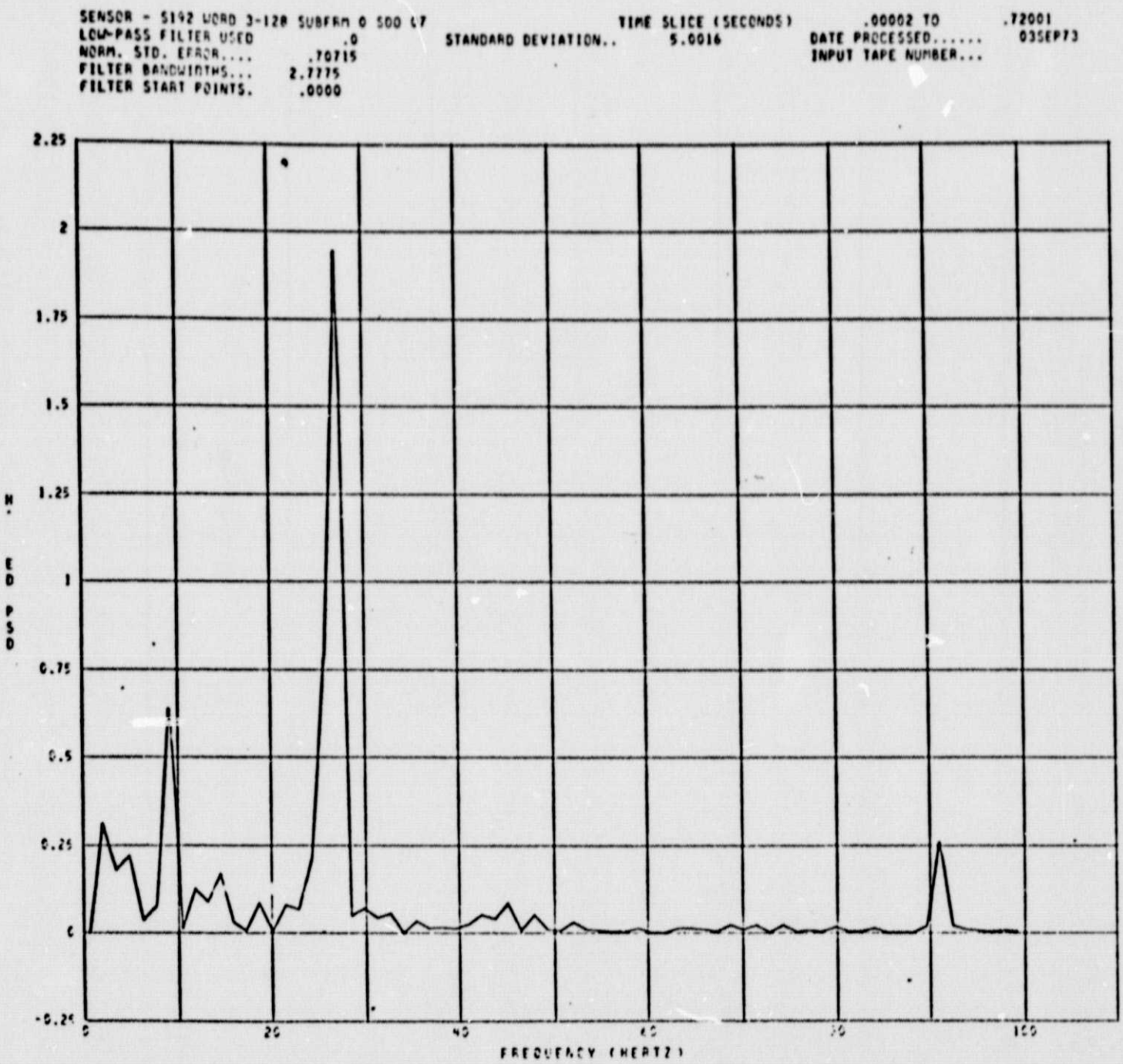

Figure 49 QUALIFICATION UNIT BAND 6 PSD, COOLER MOTOR ON, SEPTEMBER 1973

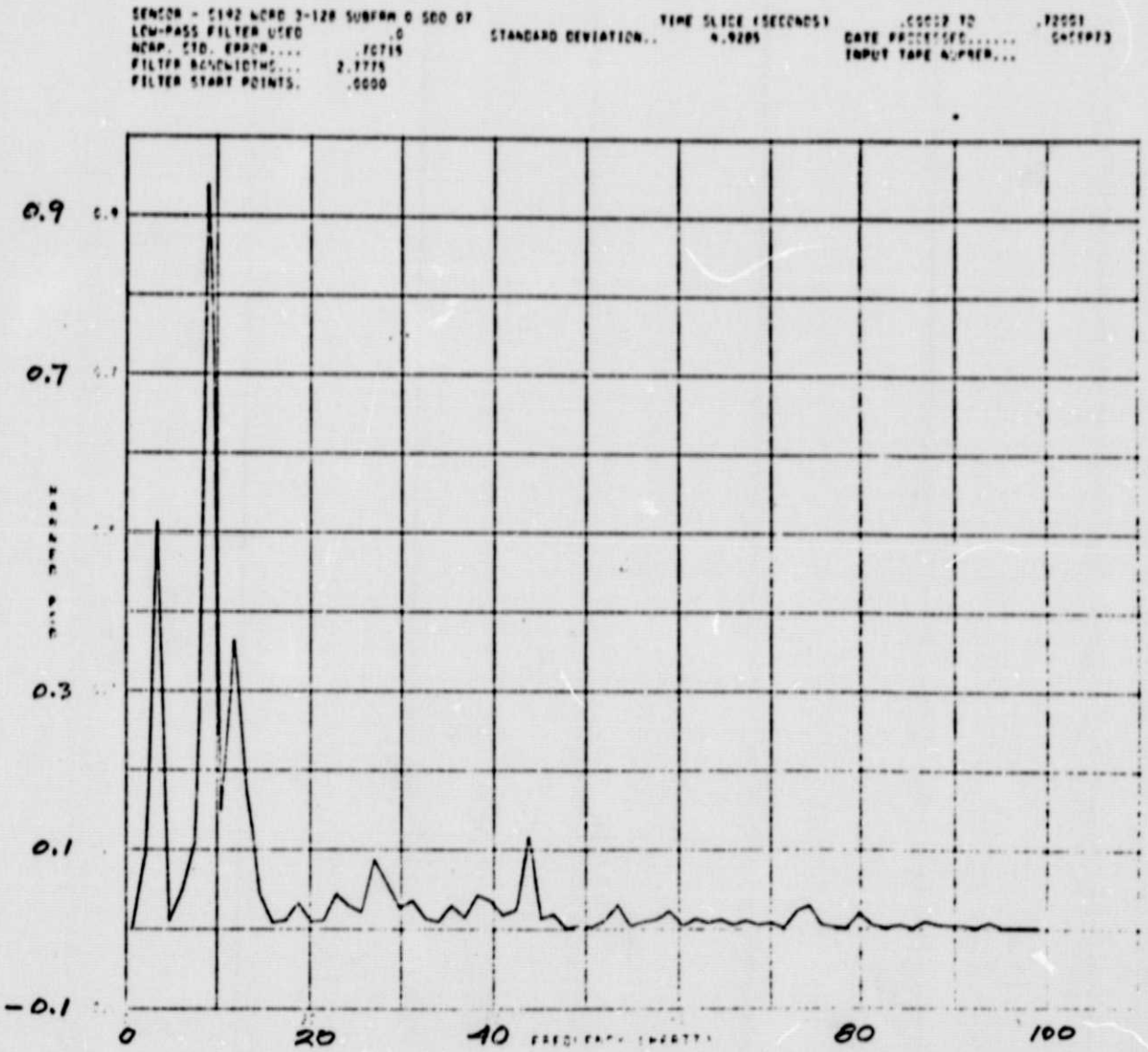

Figure 50 QUALIFICATION UNIT, BAND 6 PSD, COOLER MOTOR OFF, SEPTEMBER 1973

we shall see in later experiments. Some detector bands resonate more strongly than others, and indeed, seem to respond somewhat differently from test to test. A key indication of susceptibility to mechanically induced responses, however, was the differing low frequency noise seen from band to band in the first Bench Tests with no Malaker Cooler used. The GSE scan mirror auxiliary drive motor was a source of vibration, however.

The 95-Hz scan mirror frequency and its harmonics seen in the PSD's such as Figure 44 were not trusted since an artificial data fill system was required for Fourier analysis of wave trains longer than a frame time of 10 milliseconds (actually longer than a data time of 3 ms, but repeating at intervals of 10 ms). Relative amplitudes were still not meaningful, but the next series of tests to be cited at HRC from July to September 1972 did show the presence of scan-related frequencies and harmonics, as well as the presence of microphonic frequencies induced by the Malaker cooler motor.

5.3 MICROPHONICS FROM MALAKER COOLER OPERATION, JULY 1972

Malaker cooler serial number 327 had previously been installed onto the Flight Primary C-D-P Assembly; after return of the latter item from Bench Tests, the Joule-Thomson cooler was removed and Malaker Cooler No. 327 was again installed. A noise search was performed monitoring visible Band 7 preamplifier output with a wave analyzer (Δf = 6 Hz). Sixteen notable frequencies were listed with noise voltages well above those at surrounding frequencies (Table IV). The cooler motor was turned off as part of the test. When this was done, the following frequencies showed noise voltage drops:

22, 529, 550, 730, 835 Hz

At 22 Hz, voltage dropped to 1/5 its original value. All others showed drops nearly to zero (Table IV).

Voltages at none of these frequencies were affected when the scan motor was turned off, but the Malaker cooler kept running. Voltages at 10 other frequencies were affected when the cooler motor was turned off.

The 22-Hz noise voltage dropped to 1/5 for either of two other situations also:

(1) When no signal was allowed through the optical path (blocked at dewar window).

(2) When optical bias was turned off.

The 529-Hz noise voltage could be followed to higher or lower frequencies by increasing or decreasing cooler motor speed (using slightly higher or lower voltage to the motor). The noise component actually disappeared into background noise:

(1) When the cooler was operated at significantly higher speed.

(2) When optical bias was turned off.

Conclusion: The Malaker cooler motor was producing a mechanical movement of the visible detector array such that optical signal, or optical bias, produced a varying output.

The cooler normally runs at 4000 to 4600 rpm, and can go faster on demand. The compressor piston is driven through a 4:1 bevel gear reduction system. Piston frequency is, therefore, 16.7 to 19.2 cycles per second.

Table IV

RESONANCE SEARCH BAND 7

22 July 1972

Cooler-Dewar-Preamplifier Assembly No.92-1068

Cooler No. 327

Preamplifier output to H-P Model 302A Wave Analyzer,

Δf = 6 Hz

OPTICAL BIAS OPERATION

FREQUENCY (Hz)	WAVE ANALYZER OUTPUTS (millivolts)		
	Cooler On Scan Motor On	Cooler Off Scan Motor On	Cooler On Scan Motor Off
22	1.3	0.25	1.3
60	1.5	1.5	1.5
95	4.6	4.6	≈0
192	4.0	4.0	≈0
285	4.7	4.7	≈0
382	4.6	4.6	≈0
478	4.3	4.3	≈0
529	1.2	≈0	1.2
550	0.75	≈0	0.75
575	4.3	4.3	≈0
670	4.3	4.3	≈0
730	1.3	≈0	1.3
768	4.7	4.7	≈0
835	0.3	≈0	0.3
861	4.2	4.2	≈0
961	4.0	4.0	≈0
4000	0.04		

Reference = HRC Unit No. 2 Engineering Data Book No. 4, Page 50

Although the five frequencies noted above were linked to cooler motor operation, and 22 Hz itself to cooler piston motion, the individual noise voltage contributions at these five frequencies were relatively small compared to the total noise bandwidth of preamplifier output (out to 1.5 MHz). No further investigations were, therefore, pursued at this time. A more significant problem seemed to be scan - related harmonics and cooler-induced noise contributions about 1 kHz, to be discussed next.

5.4 MODULATIONS FROM SCAN MOTOR ROTATION FREQUENCY, JULY 1972

During Acceptance Thermal-Vacuum Environmental Testing, noise resonance searches were again performed on Bands 9 and 13 at low pressure, at 80,000 feet pressure, and at sea level pressure. Results are shown in Figures 51 through 56. Because the internal scanner video processor output was the only source of signal available outside the vacuum chamber, that output was fed to the wave analyzer. Its narrow band response to a discontinuous function (calibration sources, scan swath of target, retrace time, calibration sources next frame, etc.) gave the 94.8-Hz scanning mirror rotation frequency, plus harmonics, as the PSD's also had done. The only significant noise peaks are other frequencies: those shown at 45 and 80 Hz and 740-1135 Hz for Band 9 at high vacuum, for example. Those frequencies must be scaled down, however, to account for a wave analyzer calibration error for this run; 118 Hz indicated had to have been 94.8 Hz. This gives 22 and 57 Hz, which are possible cooler-induced frequencies for Band 9 at high vacuum. Band 9 at 20 torr also showed a strong 21 Hz spike; in this run the scan

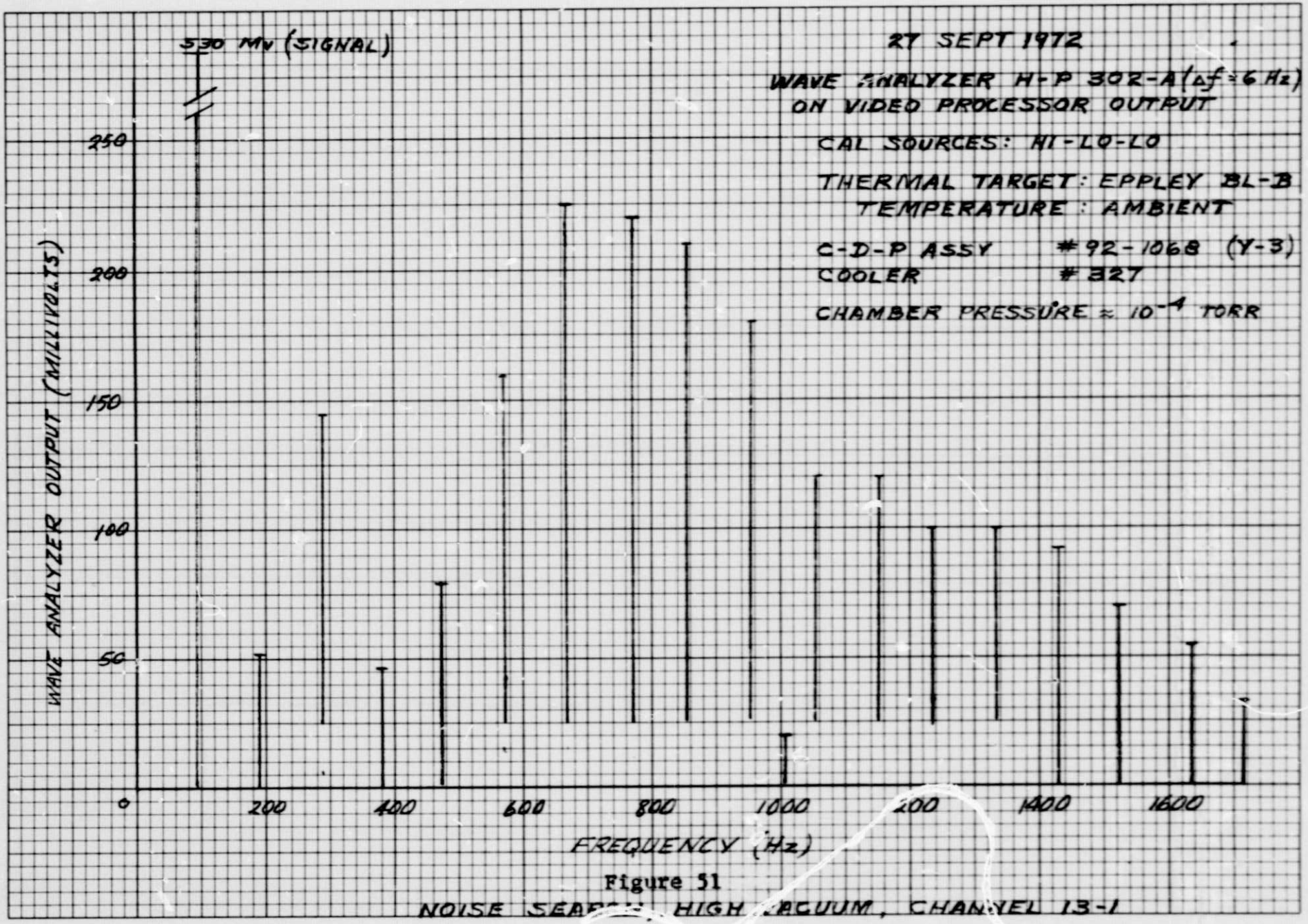

Figure 51

NOISE SEARCH, HIGH VACUUM, CHANNEL 13-1

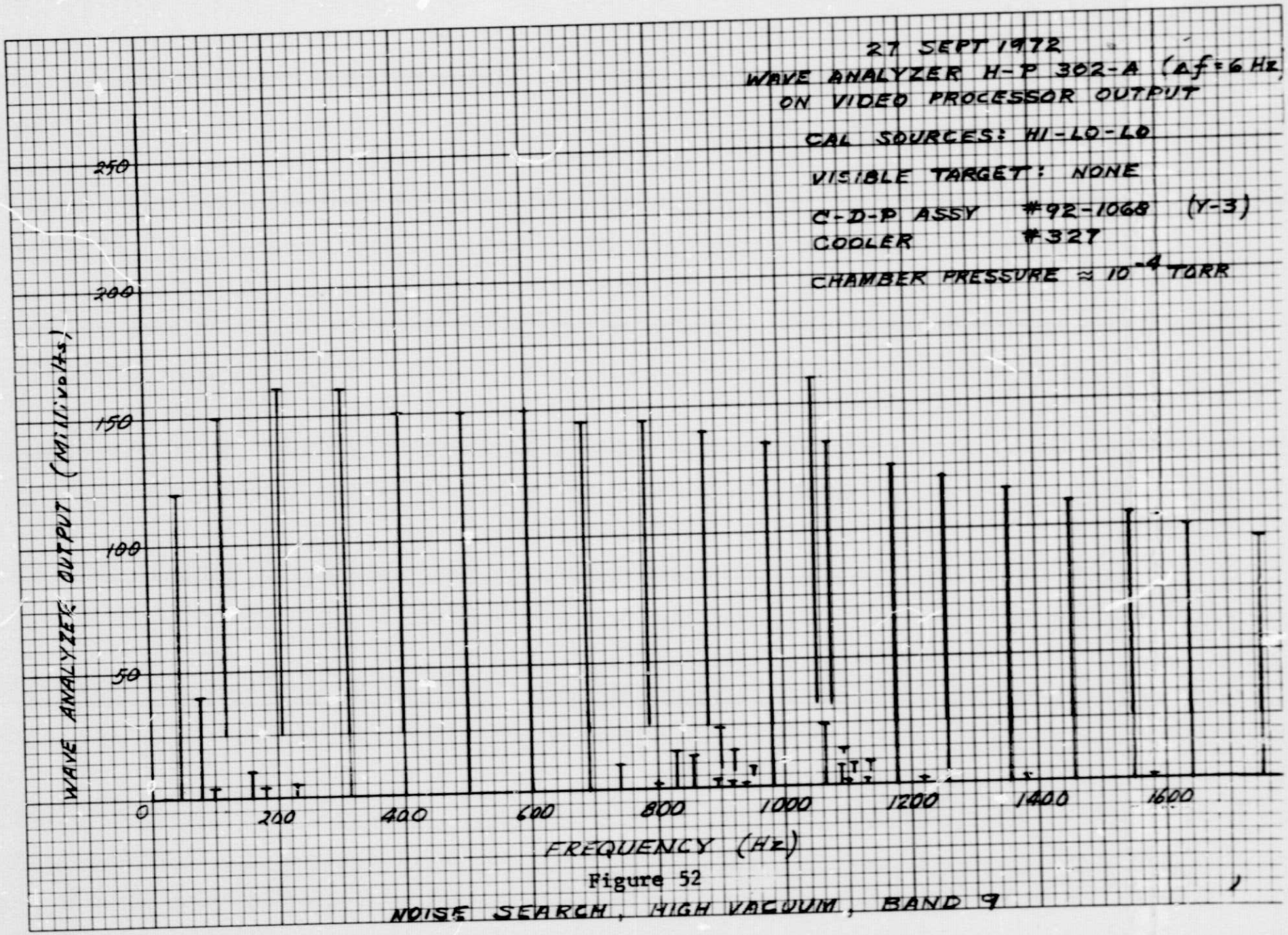

Figure 52

NOISE SEARCH, HIGH VACUUM, BAND 9

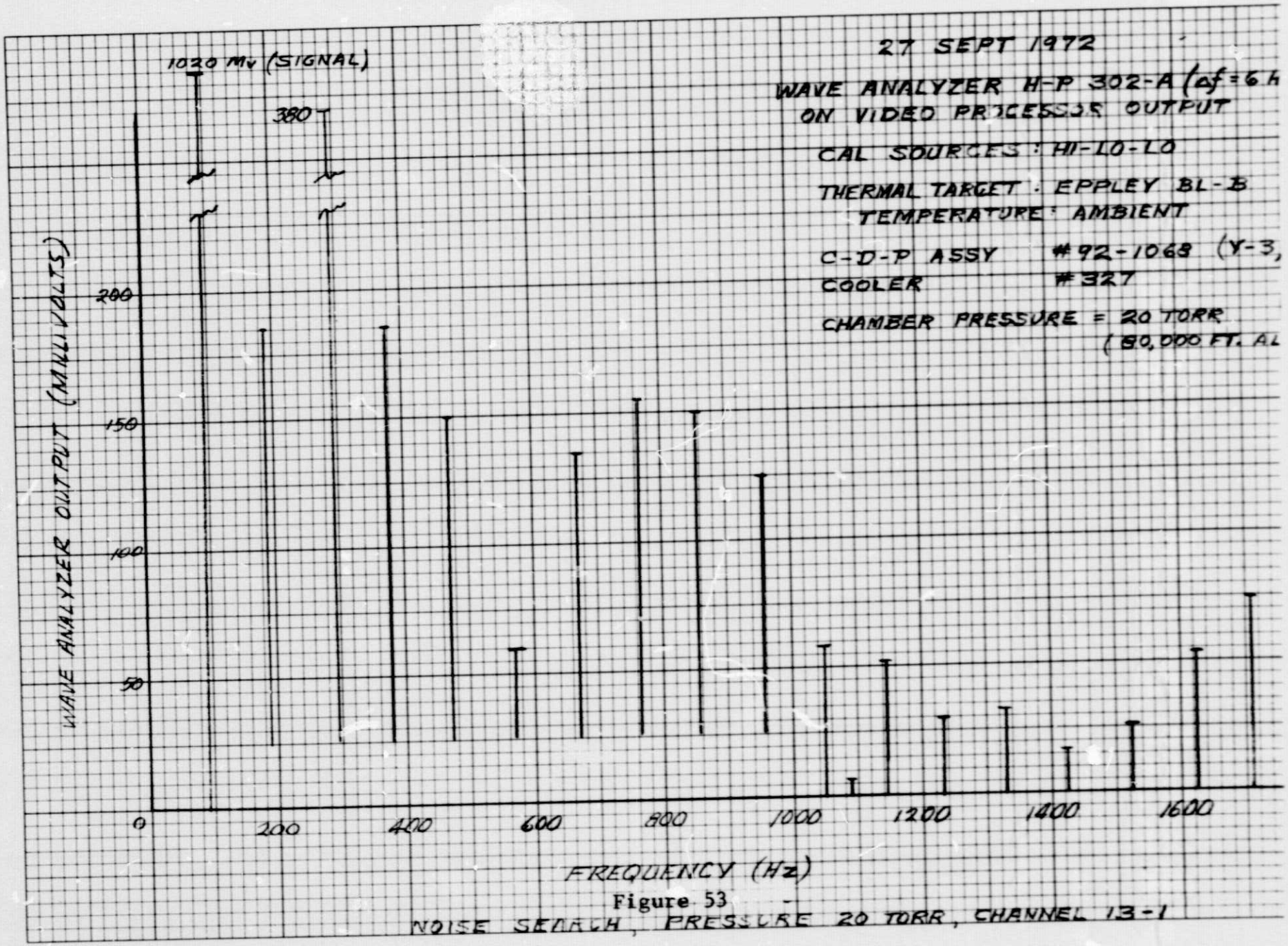

Figure 53
NOISE SIGNATURE, PRESSURE 20 TORR, CHANNEL 13-1

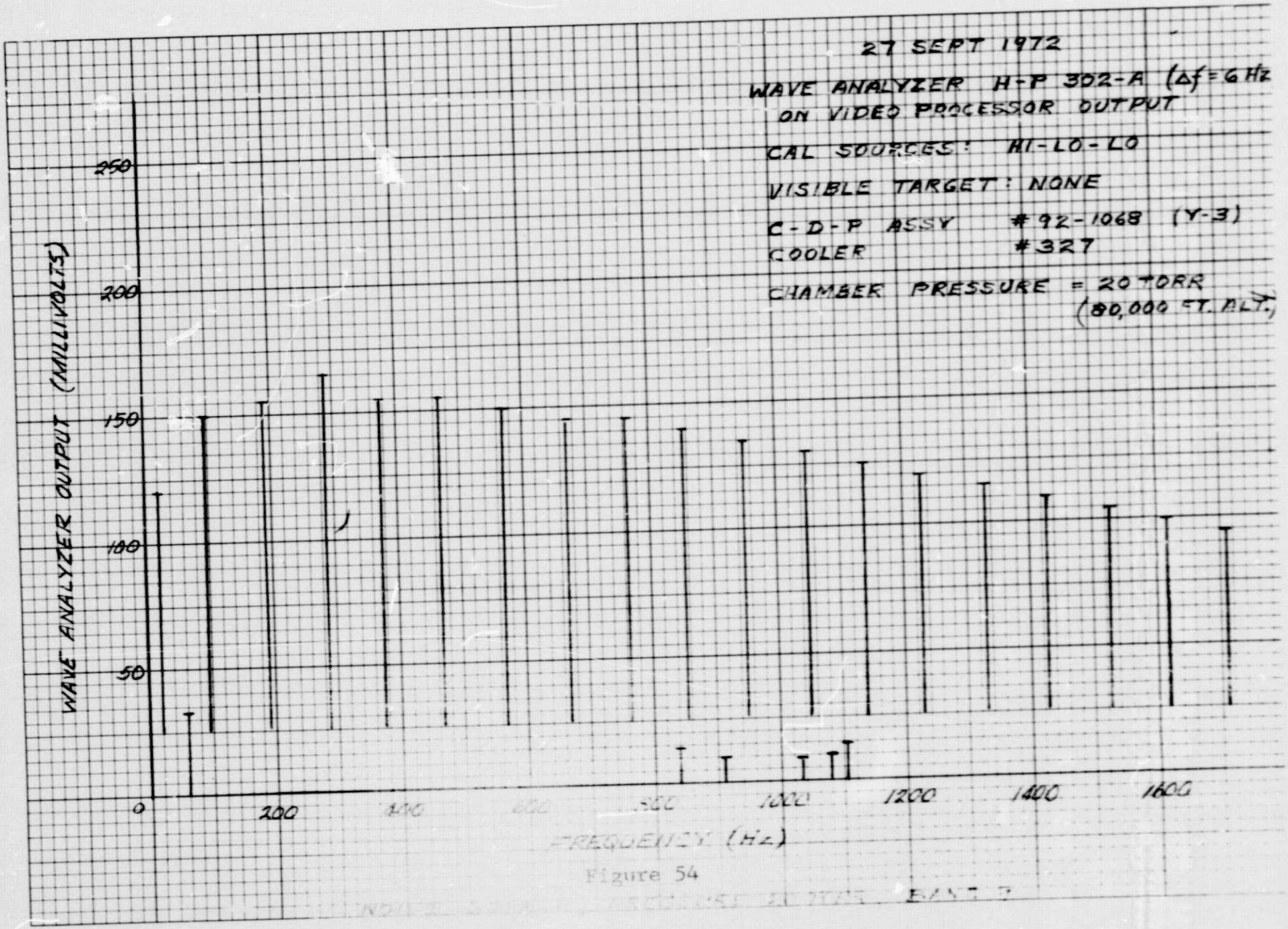
27 SEPT 1972
WAVE ANALYZER H-P 302-A (Δf = 6 Hz
ON VIDEO PROCESSOR OUTPUT
CAL SOURCES: HI-LO-LO
VISIBLE TARGET: NONE
C-D-P ASSY #92-1068 (Y-3)
COOLER #327
CHAMBER PRESSURE = 20 TORR
(80,000 FT. ALT.)
WAVE ANALYZER OUTPUT (MILLIVOLTS)
250
200
150
100
50
0
200
1000
1200
1400
1600
FREQUENCY (Hz)

Figure 54

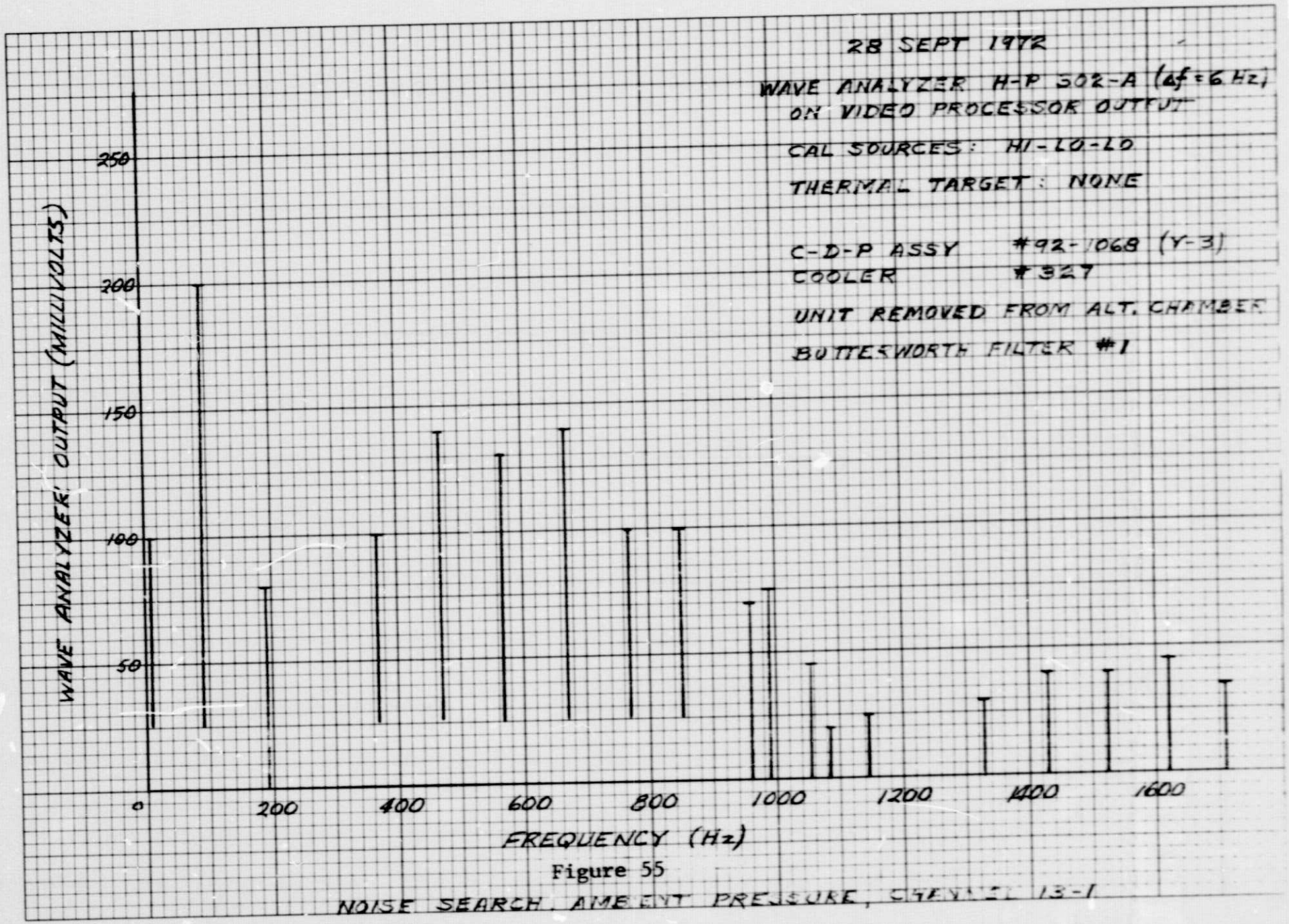

Figure 55

NOISE SEARCH. AMBIENT PRESSURE, CRYO # 13-1

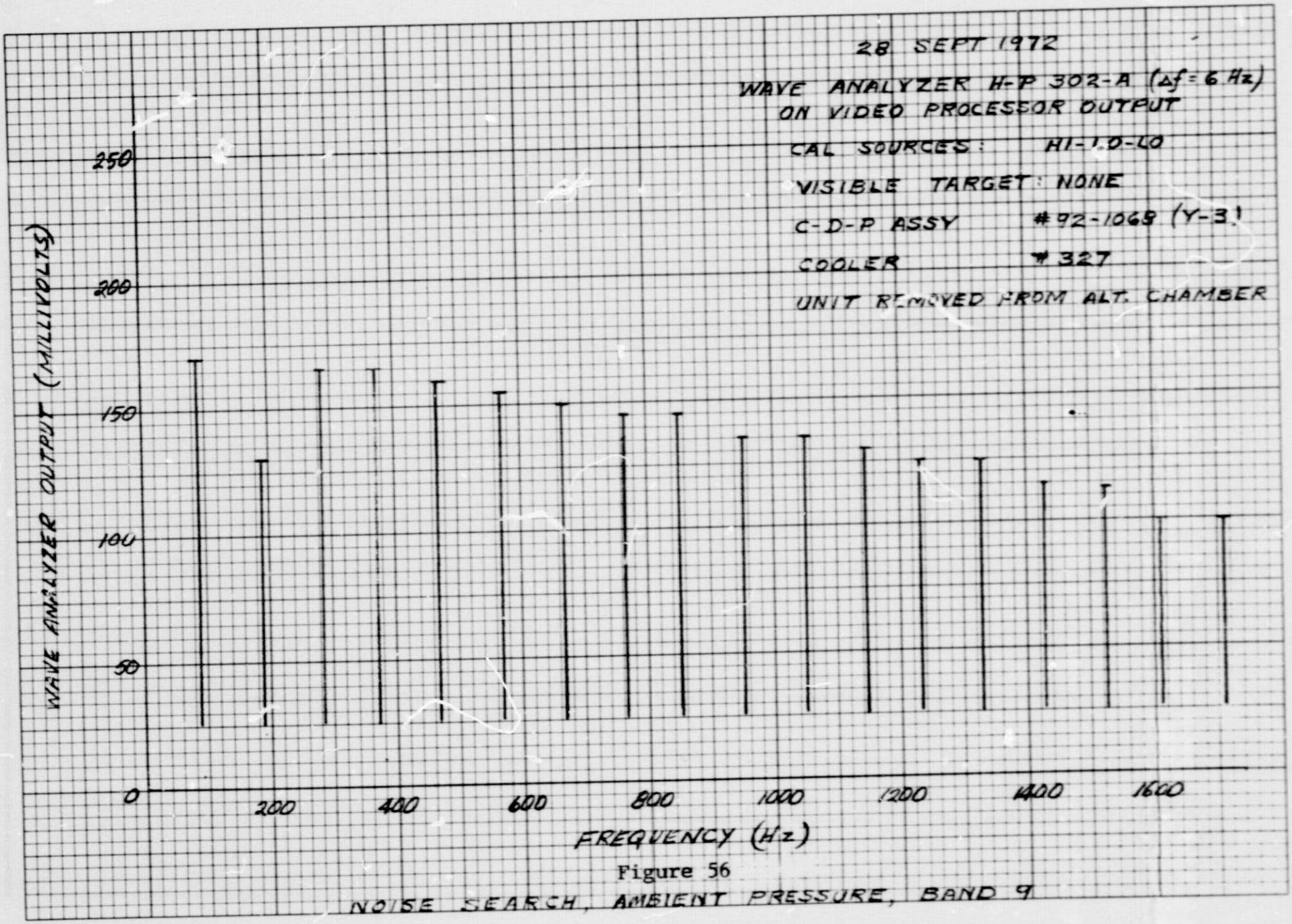

Figure 56

NOISE SEARCH, AMBIENT PRESSURE, BAND 9

frequency was correctly calibrated as 95 Hz. Note that Band 13 noise spik s were relatively less prominent than in Band 9 (Figure 55 response at 8 Hz is real, however). The noise generation around 1 kHz was still considered the most serious problem, leading to the next experiment.

5.5 MODULATIONS FROM COOLER MOTOR, JULY 1972

With the Scanner Assembly removed from the vacuum chamber, preamplifier outputs could be fed to the wave analyzer, giving a continuous-function monitoring of dark noise, uninterrupted by scanning sequences (dewar windows were blocked to exclude calibration sources and other changing radiation inputs). Figure 57 shows Band 13 noise contributions at 19, 985, 1000, and 1100 Hz, all linked to cooler motor operation. Band 9 showed only two significant peaks, at 118 and 240 Hz, but neither was influenced by either the cooler motor nor the GSE scan drive motor being turned off. No 20 or 50-Hz contributions were noted.

5.6 CHANGED NOISE COMPONENTS FROM A NEW COOLER, SEPTEMBER 1972

During an anomaly test run on 908072, the S192 Flight Hardware was run alone as part of the on-module Super-Systems Functional Interface Verification (SSFIV). The previous Malaker cooler No 327 in C-D-P No. 92-1068 had failed during the preceding test. Cooler No. 393 was installed. A change in noise components occurred, identified in FIAR S192-8199, written 9-12-72. No significant components around 1 kHz were found during that data analysis. Several SDO's showed 15 to 18-Hz noise components, however. This new cooler motor ran at lower voltage and at lower speed to achieve identical temperature regulation. The lower frequency noise identified is further indication that the

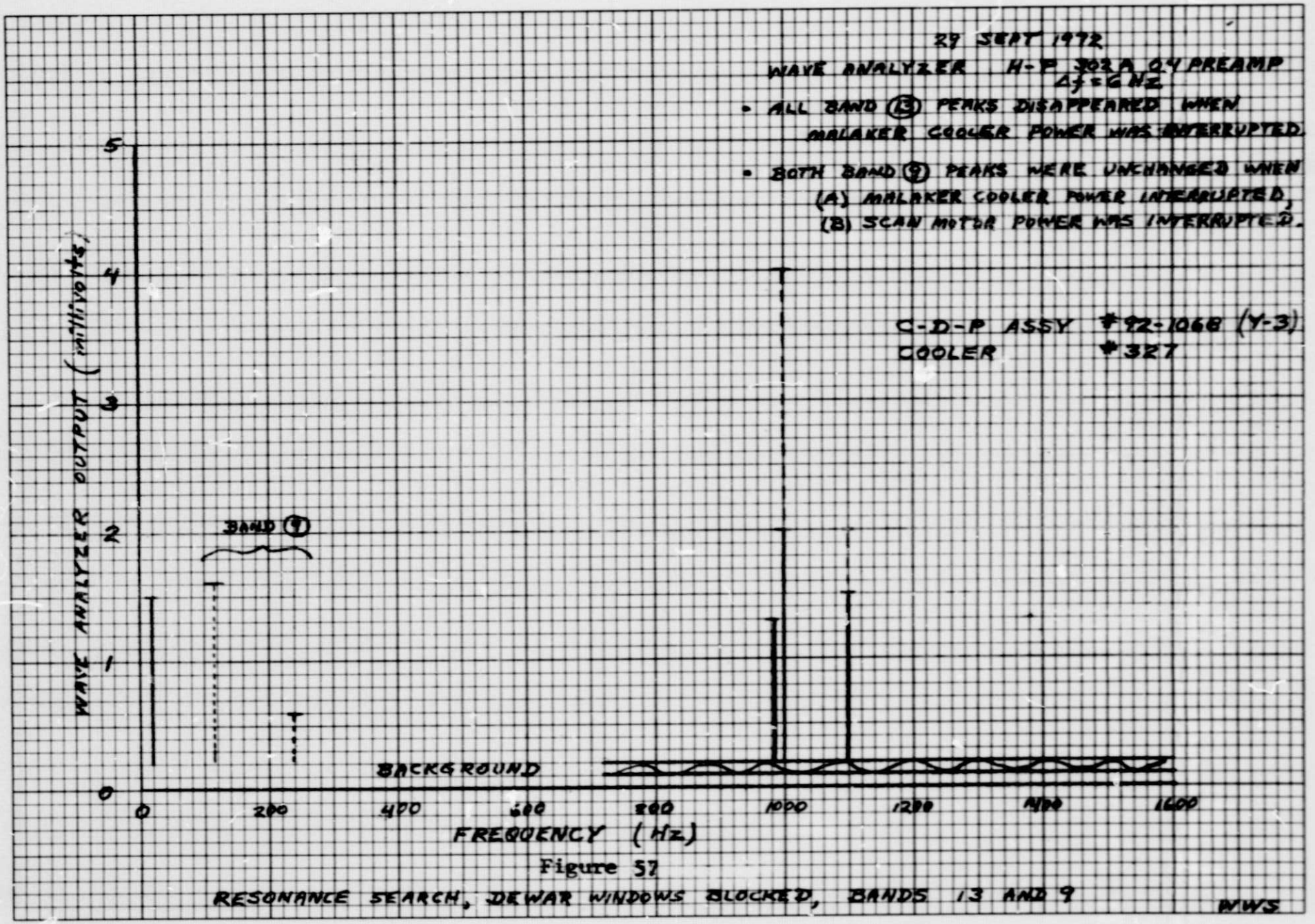

Figure 57

RESONANCE SEARCH, DEWAR WINDOWS BLOCKED, BANDS 13 AND 9

MWS

cooler was inducing noise in susceptible bands whose frequency was determined partly by cooler motor speed.

No further tests could be made until the Flight Hardware was set up on-module at KSC because of a structural failure accident to the External Scanner encoder mount.

In late September 1972 the corner frequency for all bands was changed from 0.04 Hz to 0.8 Hz by changing two resistors on each preamplifier board. The purpose was to reduce very low frequency oscillations (less than 1 Hz) primarily in Band 13.